CZECH TECHNICAL UNIVERSITY IN PRAGUE

Faculty of Civil Engineering

Department of Geotechnics

ANALYSIS OF TWO COMPUTER PROGRAMS FOR A PILE WALL DESIGN IN PRAGUE

A dissertation submitted by

Wenhao Zhu

in partial fulfilment of the requirements for the degree of *Master of Science*

Study programme: Civil Engineering

Branch of study: Building Structures

Supervisor: Ing. Jan Kos, CSc.

January 2021, Prague

[This page intentionally left blank]

CZECH TECHNICAL UNIVERSITY IN PRAGUE
Faculty of Civil Engineering
Thákurova 7, 166 29 Prague 6, Czech Republic

DIPLOMA THESIS ASSIGNMENT FORM

I. PERSONAL AND STUDY DATA

Surname: Zhu Name: Wenhao Personal number: 494861

Assigning Department: K135 - Department of Geotechnics

Study programme: Civil Engineering

Branch of study: Building Structures

II. DIPLOMA THESIS DATA

Diploma Thesis (DT) title: Analysis of two computer programs for a pile wall design in Prague

Diploma Thesis title in English: Analysis of two computer programs for a pile wall design in Prague

Instructions for writing the thesis:

The design of pile walls in Prague using two computer programs will be made. The first program will be based on the model of an elastic beam in the Winkler medium. The second will be the FEM program. The results will be compared, analyzed, and conclusions and suggestions will be made. Drawings of the resultant structures will be enclosed.

List of recommended literature:
Manuals of used computer programs
Eurocode EN 1997-1

Name of Diploma Thesis Supervisor: Ing. Jan Kos, CSc.

DT assignment date: 25.09.2020 DT submission date: 03.01.2021

DT Supervisor's signature Head of Department's signature

III. ASSIGNMENT RECEIPT

I declare that I am obliged to write the Diploma Thesis on my own, without anyone's assistance, except for provided consultations. The list of references, other sources and consultants' names must be stated in the Diploma Thesis and in referencing I must abide by the CTU methodological manual "How to Write University Final Theses" and the CTU methodological instruction "On the Observation of Ethical Principles in the Preparation of University Final Theses".

Assignment receipt date Student's name

Declaration of Authorship

I hereby declare that this master's thesis was written independently by myself under the guidance of the thesis supervisor Ing. Jan Kos, CSc. All sources and other materials used have been quoted in the list of references.

In Prague, on…… ……

Signature

ANALYSIS OF TWO COMPUTER PROGRAMS FOR A PILE WALL DESIGN IN PRAGUE

Abstract

Deep excavation designs deal with possible failures of retaining structures and soils. Multilevel tiebacks and/or props are often used, which makes the design more complex. It is significant to design by proper analysis approaches, providing reasonable results for the engineering suggestions on construction and risk reduction.

This thesis covers the retaining system design of a deep foundation pit in Prague based on Eurocodes, with the use of Sheeting Check and FEM programmes of the GEO5 software suite. The foundation pit to be excavated is quite adjacent to a tall building supported by a piled foundation, so the displacements of both the ground and the retaining structure are necessary to check. The behaviour of retaining structure in the staged excavation was analysed from the view of two methods concerning the soil-structure interaction (SSI) – subgrade reaction method (SRM) and finite element method (FEM).

The anchored pile wall was firstly designed with the necessary verifications. Subsequently, simulations for the excavation were done by the FEM, a few soil constitutive models with the yielding condition utilizing Mohr-coulomb failure criterion being introduced. A proper selection of constitutive models for the finite element analyses was done comprehensively, the results of which were discussed and compared with that from Sheeting Check programme. The final commentary, conclusions and the schema of the retaining structure were added.

Keywords: Deep Foundation Pit, Retaining Structures, SRM, FEM, SSI, GEO5.

Abstrakt

Projekty hlubokých jam se zabývají možnými poruchami pažicích konstrukcí a zemin. Často se používají víceúrovňová rozepření a/nebo kotvení, což činí návrh složitějším. Je důležité navrhovat pomocí správných analytických přístupů poskytujících přiměřené výsledky pro technické návrhy týkající se výstavby a snižování rizik.

Tato diplomová práce obsahuje návrh pažicího systému hluboké základové jámy v Praze dle Eurokódů, s využitím programů Pažení Posudek a FEM softwarového souboru GEO5. Základová jáma, která bude vyhloubena, zcela přiléhá k vysoké budově podporované pilotovým základem, takže je nutné zkontrolovat deformace základové půdy i pažicí konstrukce. Chování pažicí konstrukce během postupného hloubení bylo analyzováno z hlediska dvou metod zahrnujících interakci zeminy a konstrukce - metody závislých tlaků a metody konečných prvků (MKP).

Nejprve byla navržena kotvená pilotová stěna s nezbytnými kontrolami. Následně byly provedeny simulace výkopu pomocí MKP. Bylo zavedeno několik konstitutivních modelů zeminy s Mohr-Coulombovou podmínkou porušení. Správný výběr konstitutivních modelů pro analýzy konečnými prvky byl proveden komplexně. Jejich výsledky byly diskutovány a porovnány s těmi z programu Pažení Posudek. Přidány byly konečný komentář, závěry a schéma pažicí konstrukce.

Klíčová slova: Hluboká základová jáma, Pažicí konstrukce, Metoda závislých tlaků, MKP, Interakce, GEO5.

List of Contents

List of Figures

List of Tables

1. Introduction

1.1. Background

1.1.1. Development of the Analysis of Deep Excavation for Foundation Pit

As the fast urbanisation going on, land resources have become critical in the downtown area. On account of this, the utilisation of underground space has become an important topic in geotechnical engineering. Hence, deep excavation for creating more underground space has become commonplace in geotechnics.

Deep excavation for building foundation pit is often located in the clamouring downtown, encompassing complex excavation surroundings, such as a number of adjacent buildings, roads for transportations, intricate pipelines, as well as underground structures. Therefore, the design of retaining structures has to be considerate, ensuring the safety of excavation. The typical types of in-situ walls are summarized below[4] :

1. Braced walls, soldier pile and lagging walls;
2. Sheet-piling or sheet pile walls;
3. Pile walls (contiguous, secant);
4. Diaphragm walls or slurry trench walls;
5. Prefabricated diaphragm walls;
6. Reinforced concrete (cast-in-situ or prefabricated) retaining walls;
7. Soil nail walls;
8. Cofferdams;
9. Caissons;
10. Jet-grout and deep mixed walls.

1.1.2. Possible Failures in the Pit Engineering

There have been always massive uncertainties when it comes to the deep and large foundation pit excavation, which frequently results in quite a great deal of trouble during its design and construction process (see Figure 1.1).

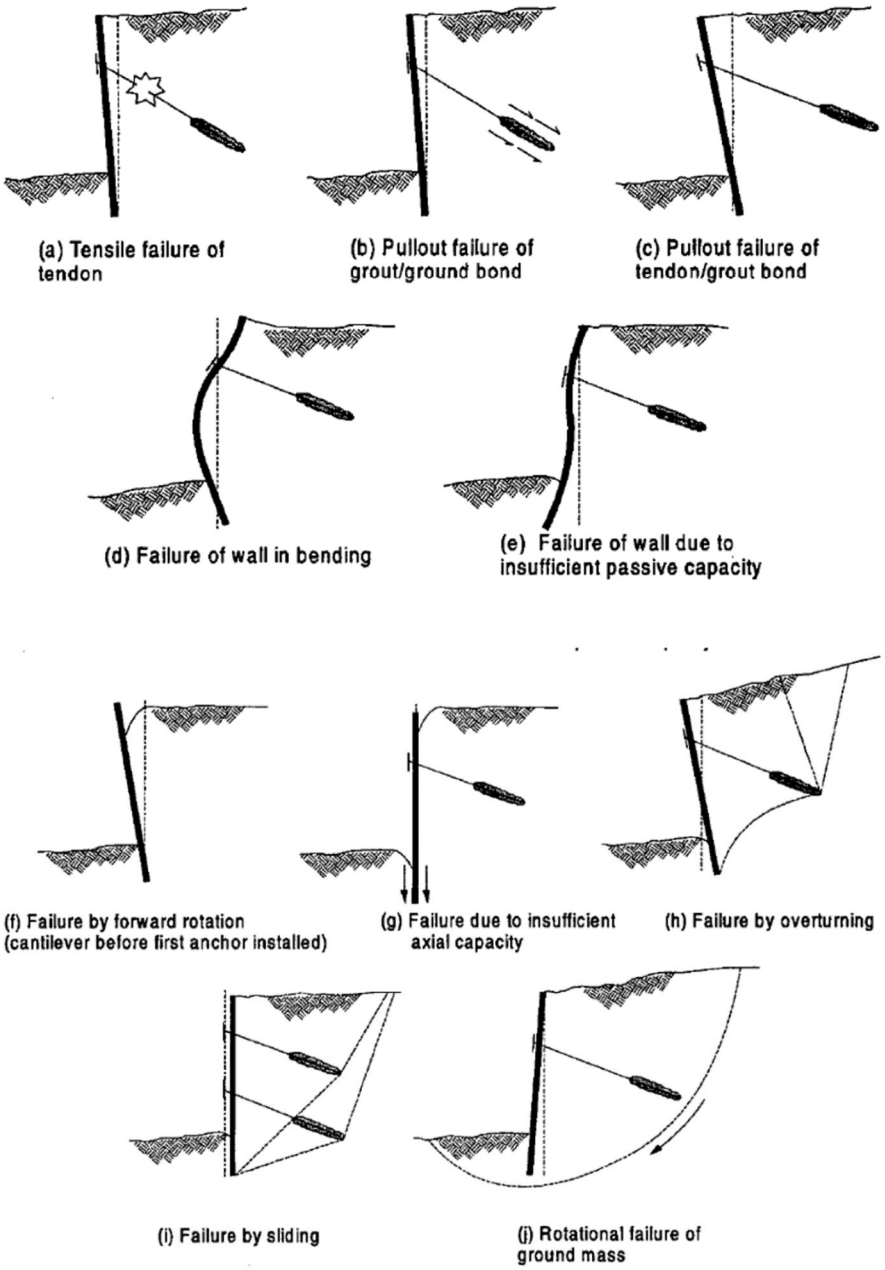

Figure 1.1 Potential failure conditions to be considered in the design of anchored walls[5]

1.1.3. Eurocode 7 – Geotechnical Design

As is mentioned in clause 2.4.7.1 of Ultimate Limit States in Eurocode 7-1, it shall be verified for the geotechnical design that the following limit states are not exceeded where relevant: [2]

- Loss of equilibrium of the structure or the ground, considered as a rigid body, in which the strengths of structural materials and the ground are insignificant in providing resistance (EQU);

- Internal failure or excessive deformation of the structure or structural elements, including e.g. footings, piles or basement walls, in which the strength of structural materials is significant in providing resistance (STR);
- Failure or excessive deformation of the ground, in which the strength of soil or rock is significant in providing resistance (GEO);
- Loss of equilibrium of the structure or the ground due to uplift by water pressure (buoyancy) or other vertical actions (UPL);
- Hydraulic heave, internal erosion and piping in the ground caused by hydraulic gradients (HYD).

1.2. Analysis Methodologies

A good geotechnical design must be able to meet all the requirements for limit state, to avoid possible failures. With the continuous development of calculation theories, the design and analysis theories of retaining structures in deep foundation pit engineering have also made considerable progress. Classical methods using the equilibrium limit state of the pressures (LEM) acting on the retaining walls was developed by introducing numerical methods: subgrade reaction method (SRM), finite difference method (FDM) or finite element method (FEM). For simple structures, stiff walls, limit equilibrium method can provide good results, but for more complex structures it is mandatory to take into the account of soil-structure interaction.[6]

1.2.1. Limit Equilibrium Method

LEM was developed in 1931 by Blum and in 1950 were performed tests on retaining wall in the US and UK.[9] This method assumes that the supporting structure is balanced under the action of the earth pressure and the lateral supporting force of the structure, and the embedded depth and anchoring force are obtained by using the balanced conditions of force and moment (see Figure 1.2). It is relatively simple for calculation, and it is the most used method in engineering practice. It's widely used with good results.

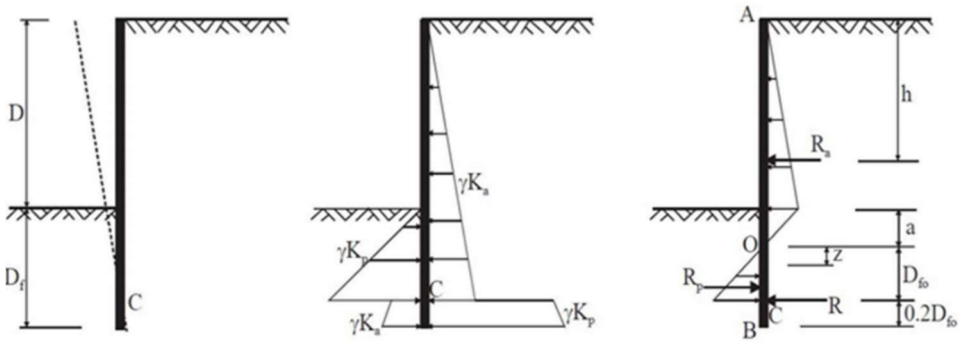

Figure 1.2 Design Principle of LEM

However, it is not recommended for walls with several levels of supports. After all, it is difficult to calculate the displacement of retaining structures by using this conventional method because it is based on soil shearing strength. Wall behaviour is tremendously important during the design process.

1.2.2. Subgrade Reaction Method

Subgrade Reaction Method (SRM) is based on the idealized model of soil medium proposed by Winkler (1867). Soil-structure interaction is a well-known one of the biggest challenges in geotechnical engineering. SRM calculation includes the consideration of soil-structure contact—it assumes that the lateral support is a set of independent elastic springs and the deflection of the soil medium at any point on the surface is directly proportional to the stress applied at the point and independent from other stresses applied at other locations.

$$p = ky \tag{1}$$

where,

p	Load acting on the interface between structure and soil;
k	Stiffness of the Winkler spring;
y	Translation of the structure into the subsoil.

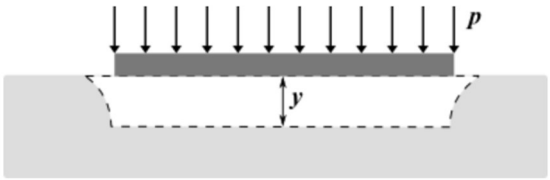

Figure 1.3 Winkler Model

The solutions for beams on elastic foundations usually include analytical methods, structural mechanics methods and finite element numerical methods. In the case of layered soil, the subgrade reaction of each soil layer is different, and more differential equations need to be established. Therefore, the solution is quite complicated. But with the use of computer programmes, this method is approachable and convenient.

1.2.3. Finite Element Method

The finite element method (FEM) allows us to determine the initial stresses and strains and their evolutions along the excavation sequence. It also considers the soil-structure interaction by bringing in contacts between the interfaces. The FEM replaces the original continuum including the retaining structure system and the ground with a finite number of discretized unit elements

connected by nodes, and then an approximate solution element mesh (the process of making the mesh is called mesh generation) is obtained. All the body and surface forces acting on the continuum can only be transferred between elements through the nodes connected them so that they are moved to the nodes to become the so-called *nodal forces* based on the equivalence principle. Generally, the basic principle of FEM is shown as below text.

After the discretization for the continuum, the element stiffness matrix and element force matrix are set up. The element stiffness matrix is given by:

$$[k]^e = \iiint [B]^T [D][B] dV, \tag{2}$$

where,

$[B]$ Transformation matrix, constant in each element;

$[D]$ Element stiffness matrix varied by the constitutive models of materials.

And the element force matrix is calculated from:

$$\{F\}^e = \iiint [B]^T [D][B] dV \{d\}^e = [k]^e \{d\}^e . \tag{3}$$

By the assembly of the equations of individual elements, the equation of the entire system is obtained, which is expressed as:

$$\{F\} = [K]\{d\} , \tag{4}$$

where,

$\{F\}$ Global nodal force vector, including boundary forces and the assembly of element body forces;

$[K]$ Global stiffness matrix, the assembly of all the element stiffness matrices.

With the boundary conditions, the equations can be solved and the nodal displacements $\{d\}^e$ are calculated. Then it is the last step of the finite element analysis (FEA) – postprocessing, that is, to determine the quantities of interest such as nodal stresses and strains. Nodal strains $\{\varepsilon\}^e$ are given by the following relationship with $\{d\}^e$:

$$\{\varepsilon\}^e = [B]^e \{d\}^e, \tag{5}$$

and then nodal stresses $\{\sigma\}^e$ given by the constitutive equation is as follows:

$$\{\sigma\}^e = [D]\{\varepsilon\}^e = [D][B]\{d\}^e . \tag{6}$$

The above text shows only the elastic condition. When the plastic behaviour is considered in the FEA, the yield surface must be indicated depending on the non-linear constitutive models and the total strain consists of two parts:

$$\{\varepsilon\}^{total} = \{\varepsilon\}^{el} + \{\varepsilon\}^{pl}. \tag{7}$$

The significant advantage of FEM in pit engineering is that soil properties can be simulated as elastoplastic and the interaction between the supporting structure and the soil can be considered. However, the procedure to set up the finite element is relatively much complicated because it is not an easy task to choose soil constitutive models, interfaces, premises to run the analysis of simulation as such. The computational FEM procedure is given in Figure 1.4. [32]

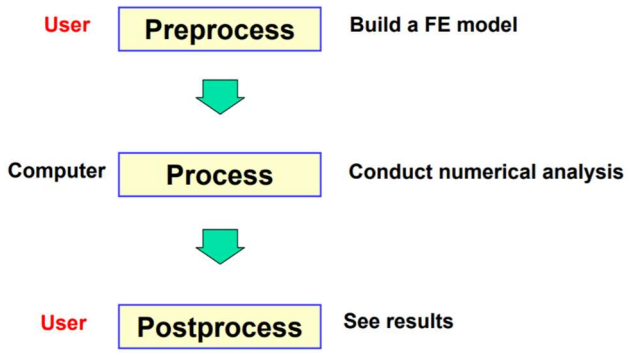

Figure 1.4 Typical FEA procedure by FEM commercial software

Though the FEM approach is generally regarded today as the "way to the future", in common practice the simple and well-known Subgrade Reaction Method (SRM) or "spring method", which is based on Winkler model, is still widely used and often preferred to more sophisticated FEM analyses, particularly in the early stage of design. The SRM permits to model even relatively complex cases simply and quickly, providing in general sufficiently reliable values of stresses in the wall and supports. On the other hand, the SRM has several drawbacks, deriving from the rough simplification assumed in simulating the response of the soil to wall movements.

One critical shortcoming is the difficulty in evaluating the coefficient of subgrade reaction k_h on a rational base. k_h is by no means an intrinsic property of the soil. Its value depends not only on soil stiffness but also on various "geometric-mechanical" factors (e.g. geometry and stiffness of wall/struts, excavation depth). Yet, the influence of the above factors on k_h is not clearly understood. Hence, indications for the selection of k_h values dependable for design may be helpful to many engineers who still rely on the "old" SRM for everyday practice.[20] The approaches to the calculation of k_h will be introduced in Chapter 2.

1.3. Typical Soil Constitutive Models

The selection of a material model suitable for the analysis of geotechnical structures adheres first of all to the character of the soil/rock environment. In the Finite Element Method-based process of comprehensive modelling of more complex problems, the selection of the numerical model represents an essential influence on specifying the input data and assessing the analysis results. In the following sections, some soil constitutive models based upon the Mohr-Coulomb failure criterion will be introduced and the discussions on the selection of soil models will be held.

Figure 1.5 represents the stresses point P in principal stress space. The hydrostatic line is a line in the principal stress space which is equally inclined to all the principal stress axes. Meridian Planes are the planes along the hydrostatic line. Deviatoric planes are perpendicular to the hydrostatic line. They are also called as an octahedral plane or π plane. Stress point in the deviatoric plane is represented by three parameters (ξ, r, θ). [48]

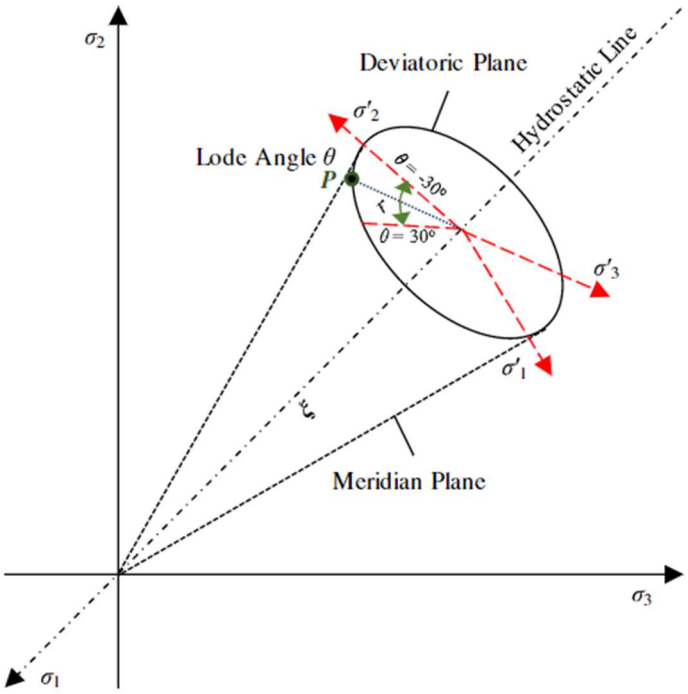

Figure 1.5 Typical representation of the failure envelope in principal stress space

1.3.1. Linear Models

Linear models provide a relatively fast but not very accurate assessment of the real material behaviour. They can be used in the cases where the analysis of stress or deformation of the groundmass is the priority, but not in the area and mode of the potential failure. They can also be used in cases, where only a local failure develops, having no fundamental influence on the

development of global failure, but which may result in premature termination of the analysis in the program.

Linear models are not used in the analyses of this paper because it is too simple and can't simulate the important non-linear elastoplastic property of soil. Soil-structure contact is not allowed in the FEA with linear soil constitutive models. Especially, it usually leads to larger deviations when it comes to deep excavation.

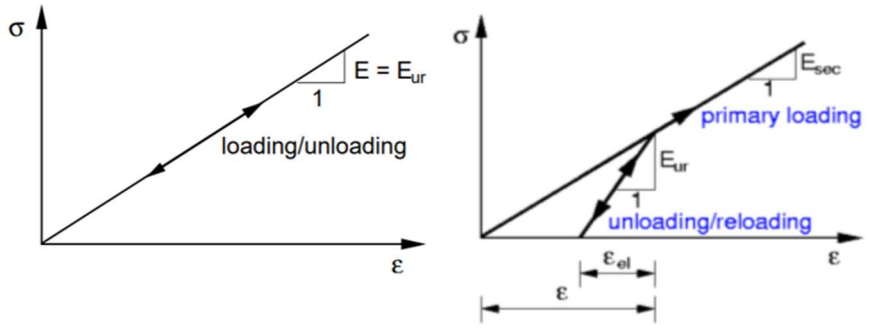

(a) Elastic model *(b) Modified elastic model*

Figure 1.6 Linear models: stress-strain relationship

1.3.2. Mohr-Coulomb Model

The Mohr-Coulomb (MC) model is an **elastic perfectly-plastic** model involving 5 parameters, which is essentially a combination of Hooke's law (Young's modulus, *E*, and the Poisson's ratio *v*) and the generalised form of Mohr-Coulomb's failure criterion (the angle of internal friction, *φ,* and cohesion, *c*). The Mohr-Coulomb's failure criterion is given by the equation that follows:

$$q = psin\,\varphi + ccos\,\varphi\ , \tag{8}$$

where,

c and *φ* are the shear strength parameters of material;

p and *q* are the maximum shear plane stresses, they are defined as:

$$q = \frac{\sigma_1 - \sigma_3}{2}, \tag{9}$$

$$p = \frac{\sigma_1 + \sigma_3}{2}. \tag{10}$$

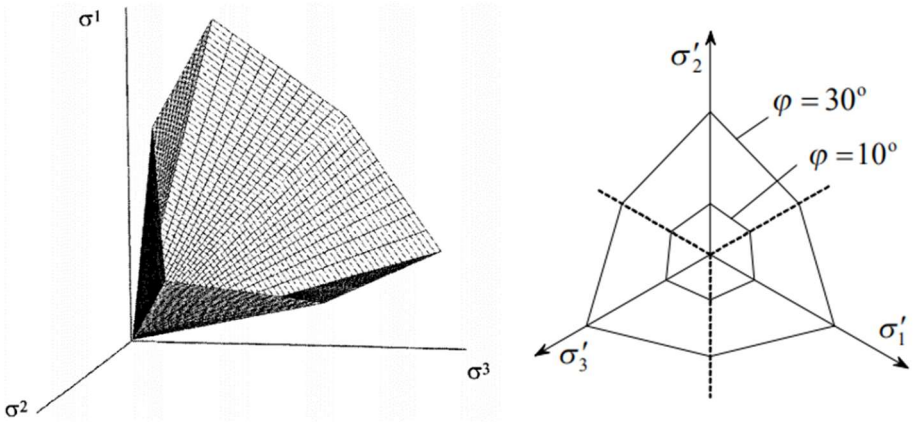

Figure 1.7 Failure contour of the Mohr-coulomb model in principal stress space and the π plane

The angle of dilation, ψ, must also be specified. The formulation of constitutive equations assumes effective parameters of the angle of internal friction φ_{eff} and cohesion c_{eff} in the GEO5 – FEM programme. By adopting the theory of elastoplasticity, it describes the plastic deformation of the soil reaching the yielding condition and reflects the failure behaviour of the soil. [13] [41]

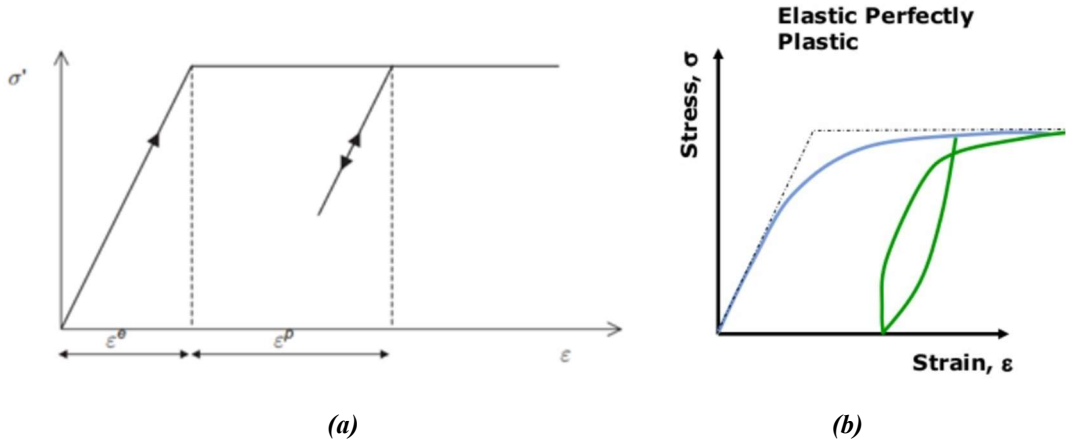

Figure 1.8 Stress-strain relationship of elastic perfectly plastic models

However, because the MC model is only a first-order model, the stress-strain relationship cannot be described well (see Figure 1.8 (a)). The comparison of stress-strain relationship of reality and elastic perfectly plastic models is given in Figure 1.8 (b). The stiffness below the failure contour is assumed to be linearly elastic, and the **nonlinear deformation behaviour** of soil and the influence of the **stress path** on soil mechanical properties cannot be considered. Nevertheless, the MC model could be used to get the first estimate of deformations order of magnitude, but the accuracy of more than 50% should not be expected (deformations may be a factor 2 off). [41]

Although the MC model has many shortcomings, it is widely used in geotechnical engineering for the initial design. With the accumulation of rich engineering experience, the failure

behaviour of soil can be better described. It is used in the analysis of the stability of foundation pits, slopes, etc. The MC yield surface can be defined in terms of three limit functions that plot as a non-uniform hexagonal cone in the principal stress space (see Figure 1.6). The MC yield function has corners, which may cause certain complications in the implementation of this model into the finite element method. The advantage on the other hand is the fact that the traditional soil mechanics and partially also the rock mechanics are based on this model.

1.3.3. Modified Mohr-Coulomb Model

Modified Mohr-Coulomb model (MMC) smoothens out the **corners** of the MC yield surface with the same input parameter as what MC required. Unlike the failure contour of Drucker-Prager model smoothening the MC's to be a cone, its projection of the yield surface into the deviatoric plane passes through all corners of the MC hexagon and as the MC yield function the MMC yield function depends on the **mean effective stress** σ_m and the **Lode angle** θ (see Figure 1.9). This results in a slightly stiffer response of the material and can be expected with the MMC plasticity model when compared to the MC model.

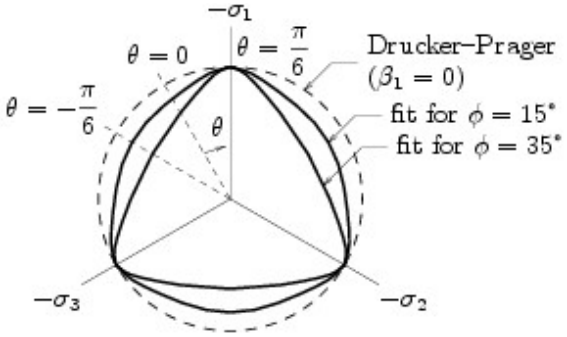

Figure 1.9 Modified Mohr-Coulomb failure contour in the deviatoric plane

Standard formulation Modified Mohr-Coulomb model assumes **elastic rigid-plastic** behaviour of the soil same as the MC model when the shear strength parameters of soil c and φ remain constant during the analysis. The enhanced version of the MMC model concerning hardening/softening (see Figure 1.10) in the GEO5 – FEM programme is available by activating "Advanced program options". It allows the evolution of these parameters as a function of the equivalent deviatoric plastic strain.

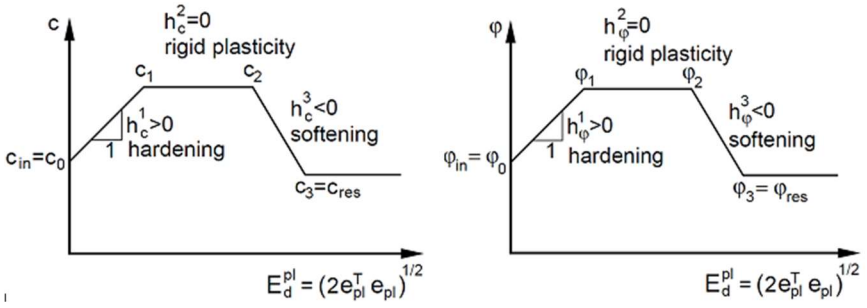

Figure 1.10 Hardening and softening of the MMC model

1.3.4. Hardening Soil Model

The Hardening Soil model is a true 2nd order model for soils in general (soft soils and harder types of soil), for any type of application. The model involves two aspects of hardening:

- friction hardening to model the plastic shear strain in deviatoric loading;
- cap hardening to model the plastic volumetric strain in primary compression.

Failure is also defined by means of the Mohr-Coulomb failure criterion. Due to the hardening, the model is much accurate for problems involving a reduction of **mean effective stress** and at the same time mobilisation of **shear strength**. Such situations occur in excavations, such as retaining structure problems. The input required for this model includes 10 parameters.

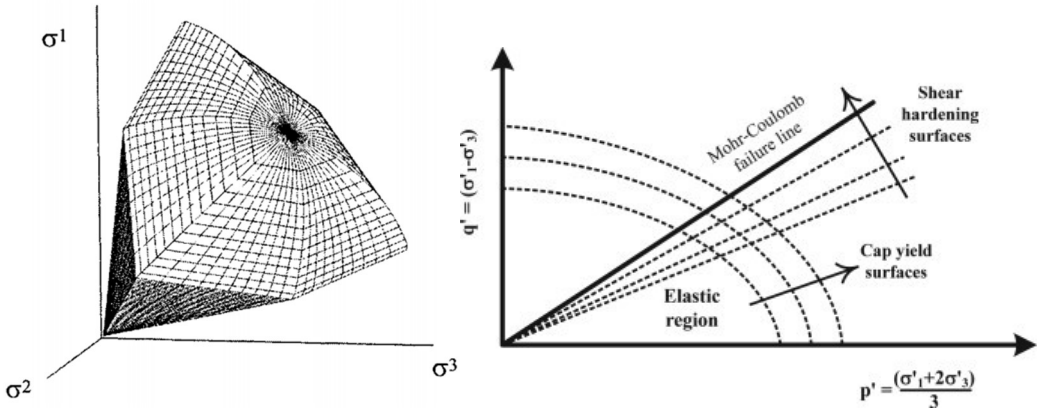

Figure 1.11 Yield contour of the HS model).[24]

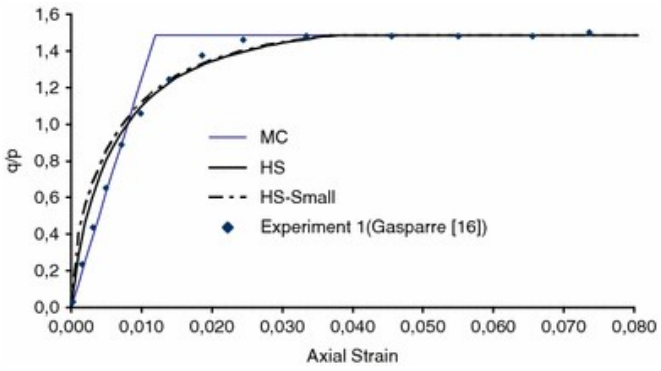

Figure 1.12 Comparison of the stress-strain curve of constitutive models and an experiment[25]

Figure 1.12 shows that before reaching the yield criterion, the stress-strain curve of MC has a certain deviation. Studies have proven that the FE simulation with HS soil model can well describe the displacement of retaining wall, the soil deformation around excavation pit. However, the HS model isn't available in the GEO5 – FEM programme.

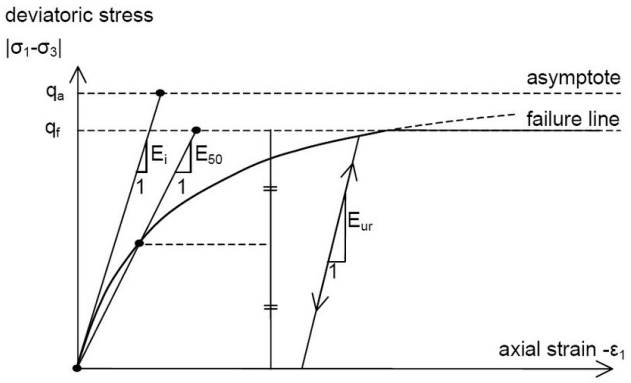

Figure 1.13 Hyperbolic stress-strain relation in primary loading for a standard drained triaxial test[28]

Though the Mohr-Coulomb model considers the variation of material strength with lateral compressive stress, it doesn't consider the variation of elastic modulus with lateral compressive stress and stress level. [55] This can't reflect the true characteristic of geological material. In this section, the elasticity modulus in the Mohr-Coulomb model was modified by employing the processing method of hardening soil nonlinear model.

In the HS model, deviatoric stress at failure, q_f, is adjusted based on the minor principal stress σ_3, the asymptotic value of deviator stress q_a being accordingly changed (see Eq. 11-12). It is the same for the stiffness moduli, which are adjusted from the reference stiffness values by multiplying a coefficient concerning the σ_3 value (see Eq. 13-14).

$$q_a = \frac{q_f}{R_f}, \tag{11}$$

$$q_f = (c \cdot \cot\varphi + \sigma_3) \cdot \frac{2\cdot\sin\varphi}{1-\sin} \tag{12}$$

$$E_{50} = E_{50}^{ref} \left(\frac{c\cdot\cot\varphi - \sigma_3'}{c\cdot\cot\varphi + p^{ref}} \right)^m \tag{13}$$

$$E_{ur} = E_{ur}^{ref} \left(\frac{c\cdot\cot\varphi - \sigma_3'}{c\cdot\cot\varphi + p^{ref}} \right)^m \tag{14}$$

where,

R_f Failure ratio (0.9 often is a suitable default setting);

m Stress dependency is given by power (usually a range of m values from 0.5 to 1 in different soil types with the values of 0.9–1 for the clay soils)[24] [48];

$E_{50}^{ref}, E_{ur}^{ref}$ Reference stiffness modulus (secant stiffness in standard drained triaxial test), reference stiffness modulus for unloading, corresponding to reference stress p_{ref} (p_{ref} = 100 kPa);

σ_3 Minor principal stress, which is the effective confining pressure in a triaxial test.

1.4. GEO5 Software

GEO5 is a software suite, developed by FINE company. It provides solutions for the majority of geotechnical tasks. Individual programs have the same user interface and communicate with each other, while each program verifies definite structure type.

1.4.1. GEO5 – Sheeting Check

This program is used to make an advanced design of embedded retaining walls using the method of elastoplastic non-linear analysis. It allows the user to model the real structure behaviour using stages of construction, to calculate the deformation and pressures acting upon the structure, to verify the internal anchor stability or to verify cross-sections (steel, RC, timber) and the bearing capacity of the anchors.

1.4.2. GEO5 – FEM

1.4.2.1. Introduction

This program, based on the principles of the finite element method, can simulate and analyse a wide scope of geotechnical engineering problems, including terrain settlement, retaining walls, slope stability, tunnels, excavation analysis, etc. It offers several material models for soils and a variety of structural elements such as walls, anchors, geotextiles or geogrids.

The GEO5 – FEM programme is used to compute displacements, internal forces in structural elements, stresses and strains and plastic zones in the soil and other quantities in every construction stage. Users can choose from a wide range of linear or nonlinear soil constitutive models to perform analysis of complex geotechnical problems like load carrying capacity, deformation and stress fields inside the layered soil body, solve stability, consolidation of saturated soils, plastic modelling of soils, modelling of structures, the interaction between the structures and the soil (anchors, rock bolts, sheeting piles), and excavation sequence.

1.4.2.2. Soil Constitutive Models

Soil constitutive models can be set either as linear or non-linear in the GEO5 – FEM programme. The linear models include Elastic and Elastic Modified models. Non-linear models show more advantages in the description of groundmass behaviour and distribution location of areas of potential failures.

Basic non-linear models can be again divided into two groups. The first group of models originates from the classical Coulomb failure condition, consisting of Drucker-Prager (DP), Mohr-Coulomb (MC), and Modified Mohr-Coulomb (MMC) models, etc. It is also possible to model hardening or softening of soils for the DP model and MMC model. A common feature of these models lies in the unlimited elastic deformation under the assumption of geostatic stress.

The second group of material models, which are based on the notion of the critical state of the soil, is represented by the Modified Cam-clay, Generalized Cam-clay, and Hypoplastic clay models. These models provide a significantly better picture of the non-linear response of soil to external loading. Individual material models differ not only in their parameters but also in the assumptions made.[16]

2. Design and Calculations with Sheeting Check Programme

2.1. Project Overview

This project concerns a foundation pit located in Prague, Czech Republic. The final depth of the excavation is 10.65m, which is for the basement of a 16-storey building to be constructed. The plane view of the pit excavation and its surroundings is given in Figure 2.1. The area circled by red lines is the pit to be excavated. To the south of it, there is a tall building quite adjacent, supported by piled foundations. Hence, compared with the surroundings in other parts, the south of the excavation is the most critical one. On account of this, the calculations and analysis of the deep excavation in this paper are bottomed on the south of the pit.

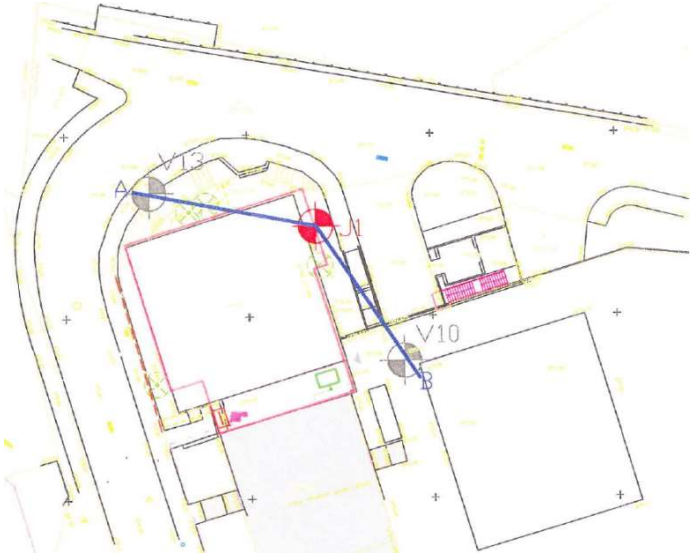

Figure 2.1 Project plane view

To simplify, the middle of the wall is considered for the analysis. The geological profile and geotechnical parameters of which are shown and listed in Figure 2.2 and Table 1, respectively.

Table 1. Soil geotechnical parameters

		GT1	GT4	GT5	GT6
Brief description		made-up ground	sandy clayey silt	weathered rock	partly weathered to unweathered rock
γ	$[kN/m^3]$	19.5	19.5	22	24
γ_{sat}	$[kN/m^3]$	-	-	23	25
c'	$[kPa]$	2	10	35	40
φ'	[°]	20	25	28	34
v	[-]	0.38	0.35	0.28	0.22
E_{def}	$[MPa]$	2-10	7-10	30-80	120-200

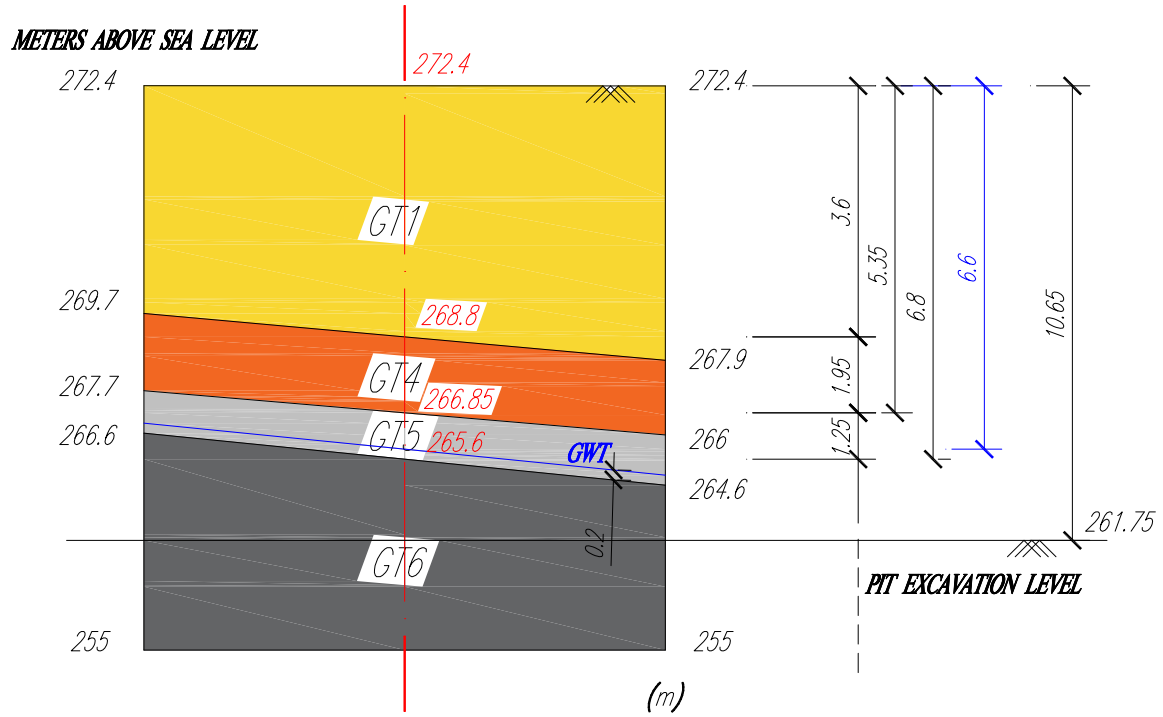

Figure 2.2 Geological Profile

The groundwater table is assumed to be 0.5 metres above the bottom of the soil layer GT5.

2.2. Calculation Assumptions for the Anchored Retaining Structure

2.2.1. Construction Sequence

To run Sheeting Check analysis, users can use GEO5 – Sheeting Design programme to determine the scheme of retaining structure preliminarily, such as the embedded length of the wall, anchorage and props. Assumptions with prescribed geometry of the retaining system are made as follows:

- Depth of the retaining wall: 12.6m;
- The pit is to be excavated stepwise. The designed construction sequence is listed in Table 3, the staged calculations sequence in the analysis by Sheeting Check programme being the same.
- Anchors: There are 3 rows of anchors considered between staged excavations. The depths of the anchor heads are assumed to be 0.3 metres above the excavation level (see Table 2).

Table 2. Depth of anchors

Anchor	No.	1	2	3
Depth	[*m*]	1.4	4.4	8.4

Table 3. Construction sequence

Stage	Excavation depth [m]	Anchorage and depth [m]	GWL in front of the wall [m]
1	-1.7	/	-6.6
2	-1.7	Anchor 1: -1.4	-6.6
3	-4.7	/	-6.6
4	-4.7	Anchor 2: -4.4	-6.6
5	-8.7	/	-9.2
6	-8.7	Anchor 3: -8.4	-9.2
7	-10.65	/	-11.2

Note that dewatering is used inside the pit in construction stage 5 and stage 7, which should be done before the excavation, and the groundwater table behind the wall remains the same during construction.

2.2.2. Surcharge

There are 2 critical piled foundations adjacent to the pit, transferring the loads from the walls of the 13-storey building to the underground. Each piled foundation is comprised of a single row of piles with a continuous beam as its cap on the top. The diameter of the piles is 1 metre and the distance between these two rows of piles is 6 m. The tips of piles are located on rock massif, GT5 or GT6.

Assumptions regarding surcharge considering more critical are made for the design and analyses:

- The first row of piles behind the pit (hereinafter called Pile Row 1) is assumed to be in contact with the retaining wall;
- The surcharge forces act at the level -6.5 metre on GT5;
- The loadings from the superstructure are resisted by the tips of the piles with no contribution from the side friction. Each pile in the Pile Row 1 bears the vertical normal force of 1029 *kN*, while the other row bears two times more, e.g. 2058 *kN*;
- For modelling convenience, the surcharge force is approximately taken as a concentrated force acting on a rectangular plate ($1 \times 1 m^2$), the schema of which is given by Figure 2.3.

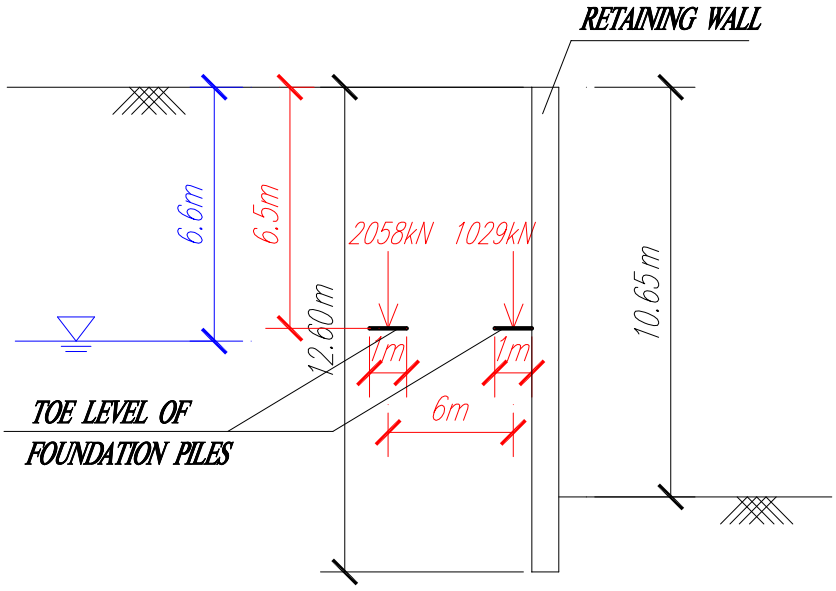

Figure 2.3 Schematic illustration of surcharge

2.2.3. Secant Pile Wall

Secant pile wall offers the most cost-effective and rapid solution where short-term water retention is required, the scheme of which is given in Figure 2.4. The wall consists of primary piles and secondary piles interlocking each other. Considering their firmness and the reinforcement, the secant pile wall can be divided into a few types. The soft-firm secant pile wall reinforced by rebars is introduced:

- Primary piles are constructed first using a 'soft' cement-bentonite mix (commonly 1 N/mm^2) or 'firm' concrete (commonly 10 N/mm^2).
- Secondary piles, formed in structural reinforced concrete, are then installed between the primary piles with a typical interlock of 150mm. These walls may need a reinforced concrete lining for permanent works applications, depending on the particular requirements of the project.

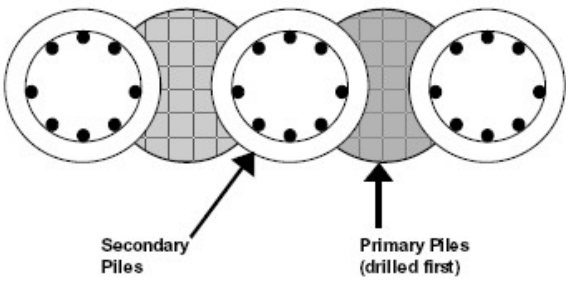

Figure 2.4 Secant pile wall[8]

Table 4. The main advantages and disadvantages of secant pile walls

Advantages	Disadvantages
➢ The flexibility of construction alignment. ➢ Enhancement of wall stiffness compared to sheet piles. ➢ Construction accessibility in the difficult ground (cobbles/boulders). ➢ Less noisy construction.	➢ Difficulty in the achievement of the verticality tolerances for deep piles. ➢ Difficulty in the total waterproofing in joints. ➢ Cost increment compared to sheet pile walls.

The soft primary piles are made of plain concrete with no enough capacity to resist the lateral transverse forces. On account of this, only the secondary reinforced piles are considered in the model for design and analyses. The geometry and material of the designed pile wall are summarised as follows:

- Primary piles: d = 0.75 m; plain concrete C25/30;
- Secondary piles: d = 0.75 m; reinforced concrete C25/30;
- The total length of the pile wall: 12.6 m;
- Secant length between primary and secondary piles: 0.25 m;
- The axial spacing between adjacent piles: 0.5 m;
- The axial spacing between piles with the same properties: 1.0 m;
- The anchor spacing is twice bigger than the spacing of reinforced piles: 2.0 m.

2.3. Design Methodologies

2.3.1. Design Approach

The design methodologies, approaches, factors of safety (FoS), etc are based upon Eurocodes. Eurocode 7 (EC 7) suggests three design approaches for verifications. Design approach 3 (DA 3) is applied in this paper, the core FoS values of which are generated by Sheeting Check programme automatically (see Figure 2.5).

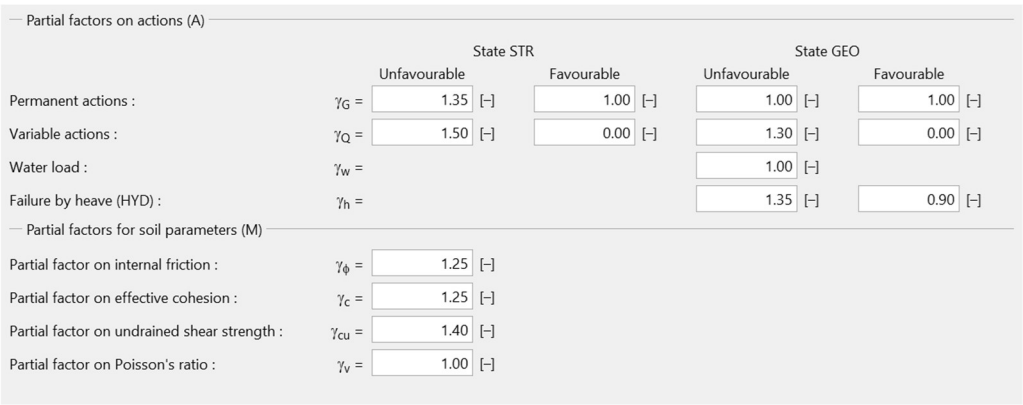

Figure 2.5 Summary of partial factors

2.3.2. Earth Pressure Calculation: Caquot-Kerisel Method

In 1948, Albert Caquot (1881–1976) and Jean Kerisel (1908–2005) developed an advanced theory that modified Muller-Breslau's equations to account for a non-planar rupture surface. They used a logarithmic spiral to represent the rupture surface instead. This modification is extremely important for **passive earth pressure** where there is soil-wall friction. [13] It properly considers the friction between soil and retaining structure.

Active and passive earth pressure is given by the following formula:

$$\sigma_a = \sigma_z K_a - 2c_{ef} K_{ac} \,, \tag{15}$$

$$\sigma_p = \sigma_z K_p \psi - 2c\sqrt{K_p \psi} \,, \tag{16}$$

where,

σ_z	Vertical geostatic stress;
c_{ef}	Effective cohesion of the soil;
K_a	Coefficient of active earth pressure, and passive earth pressure;
K_p	Coefficient of passive earth pressure (based on the table, K_p >1);
K_{ac}	Coefficient of active earth pressure due to cohesion;
ψ	Reduction coefficient (a table value, ψ⩽1).

The following analytical solution (Boussinesque, Caquot) is implemented to compute the coefficient of active earth pressure K_a:

$$K_a = \rho \, K_a^{Coulomb} \quad , \tag{17}$$

where,

K_a	Coefficient of active earth pressure due to Caquot;
$K_a^{Coulomb}$	Coefficient of active earth pressure due to Coulomb;
ρ	Conversion coefficient, which is calculated by:

$$\rho = [(1 - 0.9\lambda^2 - 0.1\lambda^4)(1 - 0.3\lambda^3)]^{-n} \,, \tag{18}$$

$$\lambda = \frac{\Delta+\beta-\Gamma}{4\varphi-2\pi(\Delta+\beta-\Gamma)} \,, \tag{19}$$

$$\Delta = 2tan^{-1}\left[\frac{|cot\delta|-\sqrt{cot^2\delta-cot^2\varphi}}{1+cosec\varphi}\right] \,, \tag{20}$$

$$\Gamma = sin^{-1}\left(\frac{sin\beta}{sin\varphi}\right) \,, \tag{21}$$

where,

β	Slope inclination behind the structure;
φ	Angle of internal friction of soil;
δ	Angle of friction between structure and soil.

The coefficient of active earth pressure due to cohesion, K_{ac}, is given by:

- when the backface inclination of the structure, $\alpha < {}^{\pi}/_{4}$,

$$K_{ac} = \frac{K_{ahc}}{\cos(\delta+\alpha)}\,, \tag{22}$$

where,

$$K_{ahc} = \frac{cos\varphi \cdot cos\beta \cdot \cos(\delta-\alpha)\cdot[1+tg(-\alpha)\cdot tg\beta]}{1+\mathrm{si}\ (\varphi+\delta-\alpha-\beta)}; \tag{23}$$

- when, $\alpha \geq {}^{\pi}/_{4}$,

$$K_{ac} = \sqrt{K_a}\,. \tag{24}$$

Hence, the horizontal (σ_x) and vertical (σ_z) components of the active earth pressure σ_a and passive earth pressure σ_p become:

$$\sigma_x = \sigma\cos(\alpha+\delta)\,, \tag{25}$$

$$\sigma_z = \sigma\sin(\alpha+\delta)\,. \tag{26}$$

2.3.3. Subgrade Reaction k_h

Chapter 1 introduces the basic principle of SRM method that is based on the Winkler model. The modulus of subgrade reaction k_h depends on parameters such as soil type, dimension, shape, embedment depth and type of foundation (Flexible or Rigid). In general, the methods of determination of k_h can be classified as ① Plate load test (the direct method to estimate the modulus of subgrade reaction k_h), ② Consolidation test, ③ Triaxial test, ④ CBR test, and ⑤ Empirical. Theoretical relations that are proposed by researchers (Bowles 1998; Elachachi et al. 2004). [26] [33] However, it is not possible to obtain all the subgrade reactions always.

The modulus of subgrade reaction, k_h, can be calculated by Schmitt method depending on the soil deformation modulus E_{def}. And it is given by the equation follows:

$$k_h = 2.1\left[\frac{{E_{oed}}^{\frac{4}{3}}}{(EI)^{\frac{1}{3}}}\right], \tag{27}$$

where,

EI	Bending stiffness of the structure [$MN{\cdot}m^2/m$];
E_{oed}	Oedometric modulus [MPa].

For safety reason, the lowest value of deformation modulus is used in the Sheeting Check programme. The relationship between E_{def} and E_{oed} is provided by:

$$E_{oed} = \frac{E_{def}}{\beta}, \tag{28}$$

$$\beta = 1 - \frac{2\upsilon^2}{1-\nu}. \tag{29}$$

2.3.4. Earth Pressures Analysis — Method of Dependent Pressures

The basic assumption of the method is that the soil or rock in the vicinity of the wall behaves as ideally elastic-plastic Winkler's material. This material is determined by the modulus of subgrade reaction k_h, which characterizes the deformation in the elastic region and by additional limiting deformations. When exceeding these deformations, the material behaves as ideally plastic. The following assumptions are used:

- The pressure acting on a wall may attain an arbitrary value between active and passive ones. But it cannot fall outside of these boundaries.
- The pressure at rest acts on an undeformed structure ($y = 0$).
- The pressure acting on a deformed structure is given by:

$$\sigma = \begin{cases} \sigma_r - k_h.y \\ \quad \sigma_a \quad \text{, for } \sigma < \sigma_a \\ \quad \sigma_p \quad \text{, for } \sigma > \sigma_p \end{cases}, \tag{30}$$

where,

σ_a, σ_p, σ_r	Active earth pressure, Passive earth pressure, Earth pressure at rest;
k_h	Modulus of subgrade reaction;
y	Deformation of structure.

The computational procedure of this method is as follows[7] [13]:

(1) The modulus of subgrade reaction k_h is assigned to all elements and the structure is loaded by the pressure at rest (see Figure 2.6(a));

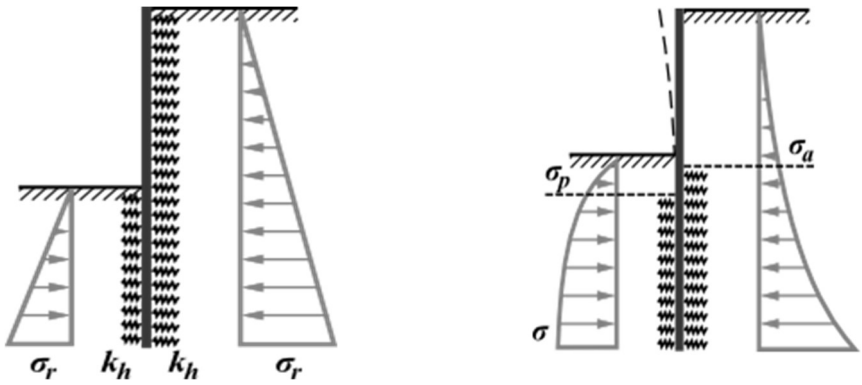

(a) Earth pressure at rest *(b) Active and passive earth pressures*

Figure 2.6 Scheme of Earth Pressures

(2) Scheme of the structure before the first iteration

The analysis is carried out and the condition for allowable magnitudes of pressures acting on the wall is checked. In locations at which these conditions are violated the program assigns the value of $k_h = 0$ and the wall is loaded by active or passive pressure, respectively (see Figure 2.6(b)).

(3) Scheme of the structure during the iteration process

The above iteration procedure continues until all required conditions are satisfied. In analyses of subsequent stages of construction, the program accounts for **plastic deformation** of the wall. This is also the reason for specifying individual stages of construction that comply with the actual construction process.

2.3.5. Method of Dependent Pressures in the Sheeting Check Programme

(1) Dependent pressures method is achieved by using the deformation variant of the FEM

The use of the **method of dependent pressures** requires the determination of subgrade reaction modulus k_h, which is assumed either linear or nonlinear. The actual analysis in the GEO5 – Sheeting Check programme is carried out by using the **deformation variant** of the finite element method. Displacements, internal forces, and the modulus of the subgrade reaction are evaluated at individual nodes.

(2) Discretization of the retaining structure

The following procedure for dividing the structure into finite elements is assumed:

- First, the nodes are inserted into all topological points of a structure (starting and endpoints, points of location of anchors, points of soil removal, points of changes of cross-sectional parameters).
- Based on selected subdivision the program computes the remaining nodes such that all elements attain approximately the same size.

(3) Assignment of k_h to each element

A value of the modulus of subgrade reaction is assigned to each element - it is considered as the Winkler spring of the elastic subsoil. Supports are placed onto already deformed structure - each support then represents a forced displacement applied to the structure.

(4) Anchor model

In the construction stage, where are introduced, prestressed anchors are modelled as a force. (see Figure 2.7 (b)). In other construction stages, the anchors are modelled as springs of stiffness k and force (Figure 2.7 (c)).

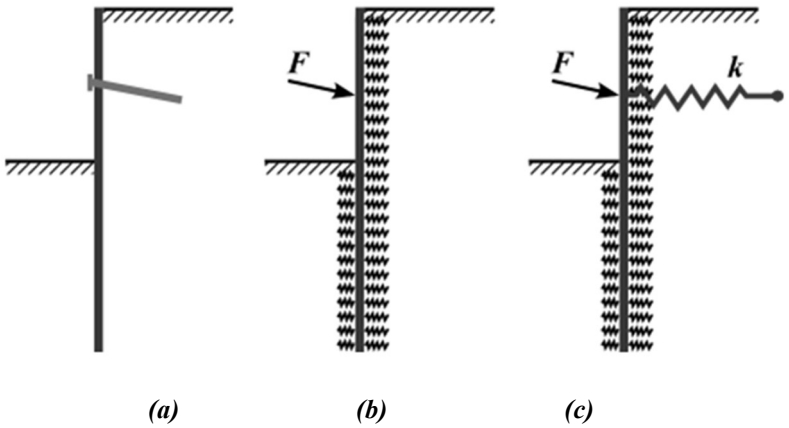

Figure 2.7 Calculation model of prestressed anchor

2.4. Design of Anchors

2.4.1. Calculation of Preliminary Assessment of Anchor Forces

The purpose of anchorage design is not only for the stabilization of the terrain behind the excavation but also the availability to counterbalance the pressures acting in the active zone.

(1) Minimum horizontal anchor force in total

LEM is used because it is fast and easy for the preliminary assessment of the approximate minimum total anchor force needed. The anchor forces per unit length along the retaining structure should at least counterbalance the remaining active earth pressure in each excavation:

$$\sum_{i=1}^{3} x_i = (E_a + E_q - E_p) \ [kN/m]. \quad (31)$$

(2) Earth Pressures from the soil self-weight

$$E_a = \sum \frac{1}{2} z_i (-2c_i \sqrt{K_{i,a,d}} + \sigma_Z K_{i,a,d}) \quad (32)$$

$$E_p = \sum \frac{1}{2} z_i (2c_i \sqrt{K_{i,p,d}} + \sigma_Z K_{i,p,d}). \quad (33)$$

where the vertical stress is given by:

$$\sigma_z = \sum \gamma_i z_i, \quad (34)$$

for the soil below the groundwater table (GTW), γ_{sat} is used instead.

(3) Earth Pressure from the surcharge

$$E_q = \sum K_{i,a,d} \frac{(q_{1,d}+q_{2,d})*1.35}{A} z_i / s \ , \quad (35)$$

where,

A is the loading area (A = $1m^2$);

$q_{1,d}$, $q_{2,d}$ are the designed values of the surcharge coming from foundation piles of the building adjacent to the excavation (γ_G = 1.35);

s is the spacing of the foundation piles (s = 2.3 m).

Table 5. Design values for the earth pressure calculations

	GT1	GT4	GT5	GT6
φ'_d [°]	16.23	20.46	23.04	28.35
c_d [kPa]	1.6	8	28	32
$K_{a,d}$	0.56	0.48	0.44	0.36
$K_{p,d}$	1.77	2.07	2.28	2.8

Table 6. Calculation of the minimum design values of horizontal total anchor force per unit length for the final excavation

	GT1	GT4	GT5 (dry)	GT5 (saturated)	GT6 (dry)	GT6 (saturated)	Summation
z (For E_a) [m]	3.60	1.95	0.75	0.50	0.00	5.80	/
z (For E_p) [m]	/	/	/	/	0.50	1.45	/
z (For E_q) [m]	/	/	/	/	/	6.10	/
E_a [kN/m]	66.73	39.97	6.55	8.44	/	179.34	301.03
E_p [kN/m]	/	/	/	/	102.04	175.68	277.72
E_q [kN/m]	/	/	/	/	/	644.56	644.56
r_x [kN/m]	/	/	/	/	/	/	667.87

Note: the passive earth pressure considers 0.5-metre dewatering below the final excavation, which is more critical.

When the final excavation is done which is after the installation of the 3rd row of anchor, there should be at least 667.87 *kN/m* that anchors provide horizontally (see Table 5 and Table 6). Given the spacing of anchors is 2.0 *m*, the minimum value of the horizontal designed anchor force in total is supposed to be 1335.74 *kN*.

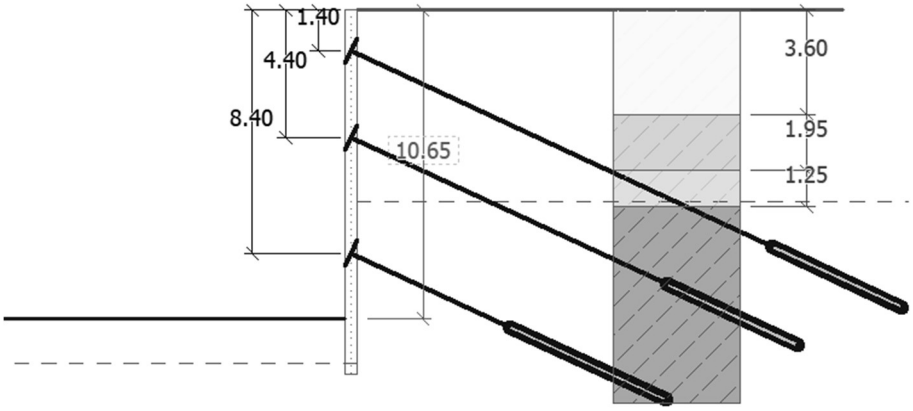

Figure 2.8 Schematic illustration of the anchored retaining wall after the final excavation

This calculation is also conducted for the anchor row 1 and row 2. The results of calculations show that the horizontal component of the total anchor force in the critical excavation after the 1st anchorage can be 0, and it should be at least 266.26 *kN/m* after the 2nd anchorage (see Appendix A).

2.4.2. Designed Anchorage

DYWIDAG temporary strand (0.62'', 15.7 *mm*, 1770 *MPa*) is used as the elements for anchorage. The main geometrical and mechanical properties of it are as follows:

1) Strand cross-sectional area (A): 150 mm^2;
2) Anchor root cross-sectional diameter: 250 *mm*;
3) Elasticity modulus (E): 195000 *MPa*;
4) Tensile strength (f_u): 1770 *MPa*.

Anchors are designed to be rooted in soil layers GT5 and GT6 are rocks in this design, the parameters of which are listed in Table 7. Detailed verifications of the design are given in the next few sections.

Table 7. Designed anchorage

Anchor No.	Spacing [m]	Dip Angle [°]	Free Length [m]	Root Length [m]	Number of Strands	Anchor Force [kN]
1	2.0	25	16	5	2	250
2	2.0	25	12	5	3	280
3	2.0	25	6	6	4	370

Note: The root diameters of anchors are all considered to be 250 mm; anchors are not post-stressed.

2.5. Design Verifications

2.5.1. Internal Stability

The internal stability of an anchorage system of sheeting is determined for each layer independently. The verification analysis determines the anchor force, which equilibrates the system of forces acting on a block of soil. The block is outlined by sheeting, terrain, line connecting the heel of sheeting with anchor root, and by a vertical line passing through the centre of anchor root and terrain.

The solution of the equilibrium problem for a given block requires writing down vertical and horizontal force equations of equilibrium. These represent a system of two equations to be solved for the unknown subgrade reaction and the maximum allowable magnitude of the anchor force. As a result, the program provides the maximum allowable anchor forces for each row of anchors. These are then compared with those prescribed in anchors.

Table 8. Verification of internal stability of anchors in the last stage

Anchor No.	Anchor force F_A [kN]	Max. allowable force in anchor F_{max} [kN]
1	258.34	4432.58
2	319.98	4707.12
3	442.37	5332.99

The anchor force that each row of anchors bears F_A doesn't exceed the allowable force F_{max}. Thus, the overall verification of internal stability is satisfactory.

2.5.2. Bearing Capacity of Anchors

The bearing capacity of anchors is checked by the frame of Anchor Verification in the GEO5 Sheeting Check programme. The maximum force acting on each anchor should not be greater than its bearing capacity.

$$min\left(\frac{R_t}{SF_t};\frac{R_e}{SF_e};\frac{R_c}{SF_c}\right) \geq P_{max} \tag{36}$$

where,

R_t, R_e, R_c Strength of anchor, Pull-out resistance from the soil, Pull-out resistance from grouting;

SF_i Safety factors for each strength.

Verifications of anchors are based on Limit State, where all the coefficients are 1.35. This is because the anchor is not a permanent load-bearing component.

The strength of anchor R_t is calculated by:

$$R_t = f_u A = f_u A_1 n \tag{37}$$

where the tensile strength of anchor in this design is f_u=1770 *MPa*; the cross-sectional area of each strand A_1=150 mm^2; n is the number of strands making up of the anchor.

R_e is the pull-out resistance from soil bonded with the anchor, which can be calculated from effective stress and bond strength when the resistance is unknown. If it is calculated from effective stress, it depends on the following 4 factors:

1) The diameter of the root;
2) Root length;
3) Geostatic stress (the deeper, the higher);
4) Soil internal friction angle.

However, with some trial calculations, the resistance obtained from this method is so small that the anchors have to be with long root length and deeply rooted. But this is not like the actual case, because all the anchors are rooted in stable rock layers—GT5 and GT6. Thus, it is much better to use the **bond strength method**. And it is given by the following equation:

$$R_e = \pi d l_k f \ , \tag{38}$$

where,

d Diameter of the root (in this design, d=250mm);

l_k Root length;

f Bond strength.

The bond strength between soil and anchor can be determined based on testing. There are some other tested micropiles rooted on GT5 and GT6, the bond resistance of which is 0.2-0.6 *MPa*.

Table 9 provides the suggested value of anchor-rock bond strength evaluated from the compressive strength of rock.[12] The compressive strength of GT5 (weathered shale) is 3-7 *MPa*. The compressive strength of GT6 (shale from partly weathered to non-weathered) is 14-20 *MPa*. Thus, the bond strength could be 0.3~1.0 *MPa*. With comprehensive considerations, the bond strength between soil and anchor is chosen as 0.4 *MPa* in this design.

Table 9. Recommended bond strength based on compressive strength [MPa]

Rock saturated uniaxial compressive strength	Suggested bond strength
>60	1.5~2.8
30~60	1~1.5
<30	0.3~1.0

R_c is the pull-out resistance from cement grouting. If neither the resistance per unit length nor the shear strength τ is known, it can be calculated based on EC2 by the equation follows:

$$R_c = \pi d_s l_k \tau = \pi d_s l_k \cdot 1.2\eta_1 f_{ctd} \,, \tag{39}$$

where,

d_s Strand diameter;

l_k Anchor root length;

η_1 Coefficient of cohesion (η_1 =1.0 for the good rooting ground condition of cohesion);

f_{ctd} Concrete strength in tension, which is calculated by:

$$f_{ctd} = \alpha_{ct} \cdot f_{ctk,005}/\gamma_c = \alpha_{ct} \cdot (0.7 f_{ctm})/\gamma_c = \alpha_{ct} \cdot \left[0.7 \cdot \left(0.3 f_{ck}\,\frac{2}{3}\right)\right]/\gamma_c \,, \tag{40}$$

$$R_c = \pi d_s l_k \times 1.2 \times 1.0 \times \alpha_{ct} \left[0.7 \times \left(0.3 f_{ck}\,\frac{2}{3}\right)\right]/\gamma_c \,, \tag{41}$$

where, α_{ct}=1.0, γ_c=1.5 (In the Czech Republic, the coefficients are not adjusted from standard values in EC2). In this design, the grouting substance used for anchor grouting is equivalent to C25/30 concrete, whose characteristic cylinder compressive strength f_{ck} = 25*MPa*.

Table 10. Verification of the bearing capacity of anchors in the last stage

Anchor No.	Depth z [m]	Maximum force F [kN]	Anchor strength R_t [kN]	Pull-out resistance (soil) R_e [kN]	Pull-out resistance (grouting) R_c [kN]	Utilization [%]
1	1.40	258.34	393.33	1163.55	326.64	79.04
2	4.40	319.98	590.00	1163.55	400.05	79.98
3	8.40	442.37	786.67	1396.26	554.33	79.80

Hence, the bearing capacities of anchors are satisfactory.

2.5.3. Overall Slope Stability

The two common and general methods of slope stability analysis are limit equilibrium and numerical methods in which the limit equilibrium method (LEM) considers the soil as a perfectly plastic and rigid material. The safety factor of limit equilibrium technique is calculated by Spencer method, Fellenius method, Morgenstern method, Janbu method, Bishop Method, etc.

The values of slope stability utilization of all those 5 methods do not exceed 100%, so it is acceptable in this design.

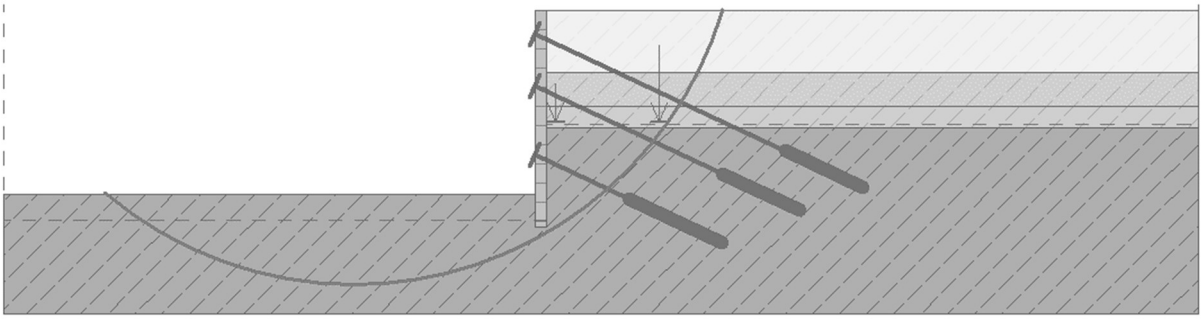

Figure 2.9 Possible slip surface in the last construction stage

2.5.4. Passive Pressure Utilization

Sheeting Check programme has the access to check the passive pressure utilization, which is to compare the maximum allowable and used passive resistance below the ditch bottom. Even if this verification is not standardly required, it can be useful for the optimization of the embedded length of the structure in the soil. Verification is done using a safety factor approach:

$$SF_p < \frac{R_{max}}{R_{mob}} . \tag{42}$$

The last excavation stage is the most critical one compared with others, where:

- Maximum passive pressure R_{max} = 472.98 *kN/m*;
- Mobilised passive pressure R_{mob} = 311.85 *kN/m*;
- Requested safety factor SF_p = 1.50 < 1.52.

Thus, the overall verification of passive pressure utilization is satisfactory. And it also verifies that the embedded length of the pile wall is designed fairly.

2.6. Results and Verifications

In this project, the hydraulic effects aren't essential, because the wall embedded deep inside the rock mass cutting off the possible hydraulic link inside and behind the retaining wall, and there is no confined aquifer existing. Hence, the verifications of UPL and HYD are negligible. The static equilibriums (EQU) and slope stability (a part of GEO) are checked in the above sections of the design. In this section, displacements of STR and GEO will be verified.

2.6.1. Internal Forces: the Constructibility

Table 11. Maximum internal forces in each construction stage

Stage No.	1	2	3	4	5	6	7
Max. shear force V_{max} $[kN/m]$	154.97	101.74	99.29	105.08	214.46	290.94	180.96
Max. bending moment M_{max} $[kN{\cdot}m/m]$	164.23	84.61	104.48	76.28	250.42	252.60	276.99

The maximum internal forces in each construction stage are listed in Table 11. For the whole construction sequence, the maximum shear force is 290.94 *kN/m*, and the maximum bending moment is 276.99 *kN·m/m*. Considering the 1-metre designed spacing of the reinforced pile, it can be inferred that this design is constructible. The distributions of internal forces of the first, intermediate, and last stages are given in Figure 2.10, Figure 2.11, Figure 2.12, respectively.

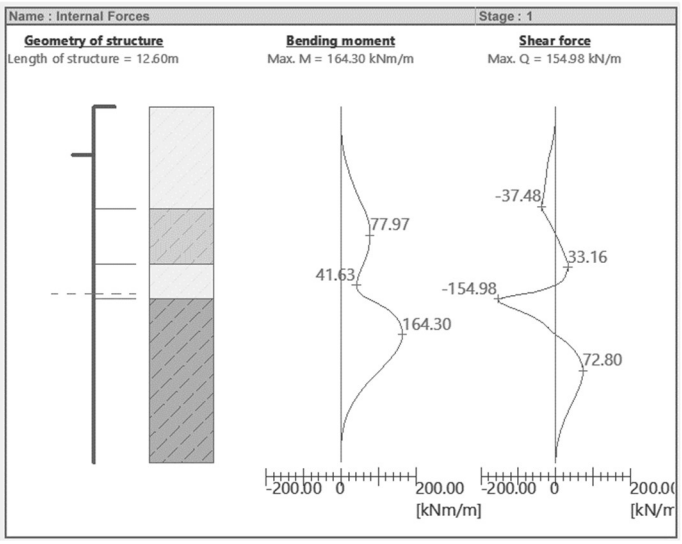

Figure 2.10 Internal Forces in the First Stage

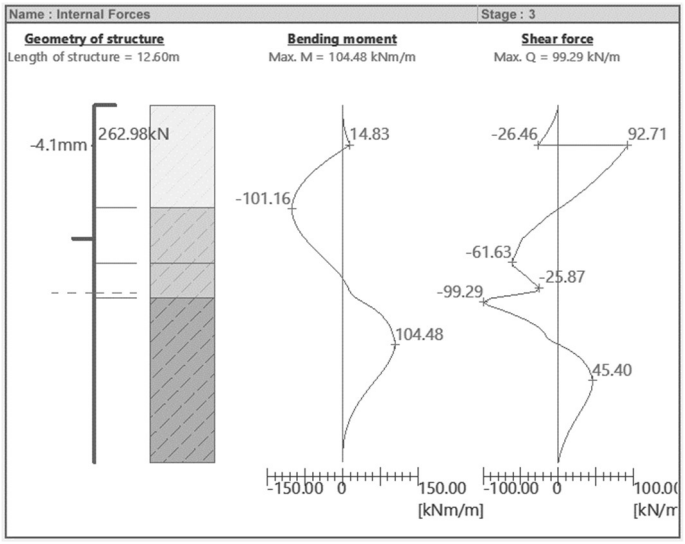

Figure 2.11 Internal Forces in the Intermediate Stage

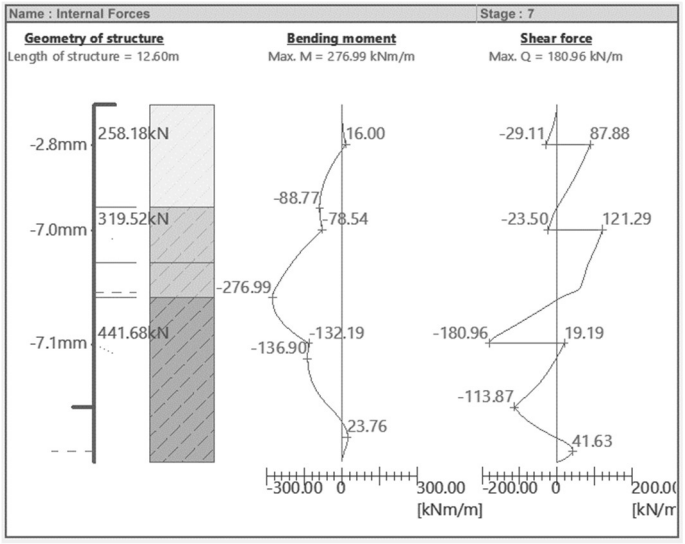

Figure 2.12 Internal Forces in the Final Stage

2.6.2. Results of Displacements

The displacements must also be checked manually as this is not automatically checked by the Sheeting Check program. Modulus of subgrade reaction k_h, earth pressure and flexural shape of the retaining wall in the first, intermediate and final stages are shown in Figure 2.13, 2.14, 2.15, respectively.

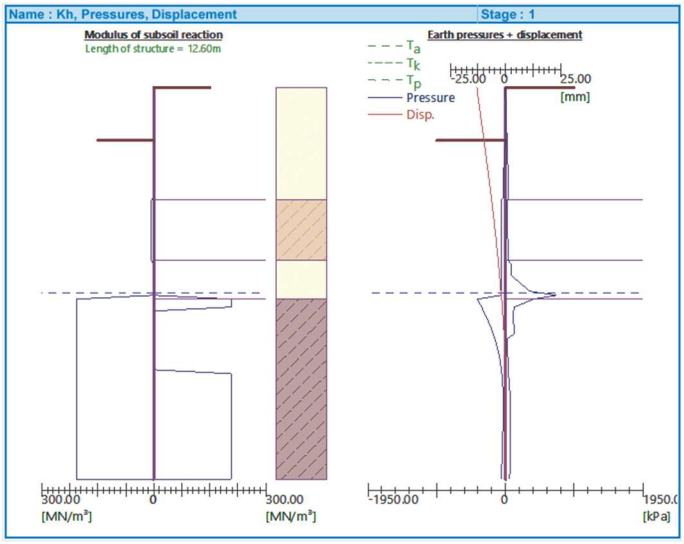

Figure 2.13 k_h, Earth Pressures and Displacements of the Wall in the First Stage

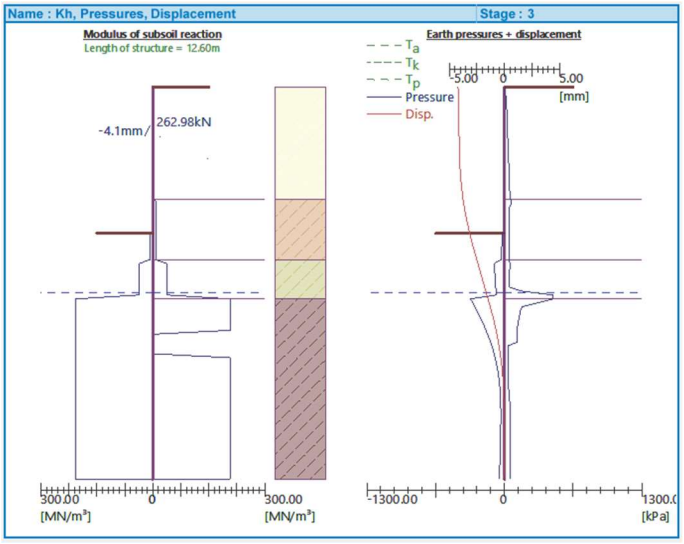

Figure 2.14 k_h, Earth Pressures and Displacements of the Wall in the Intermediate Stage

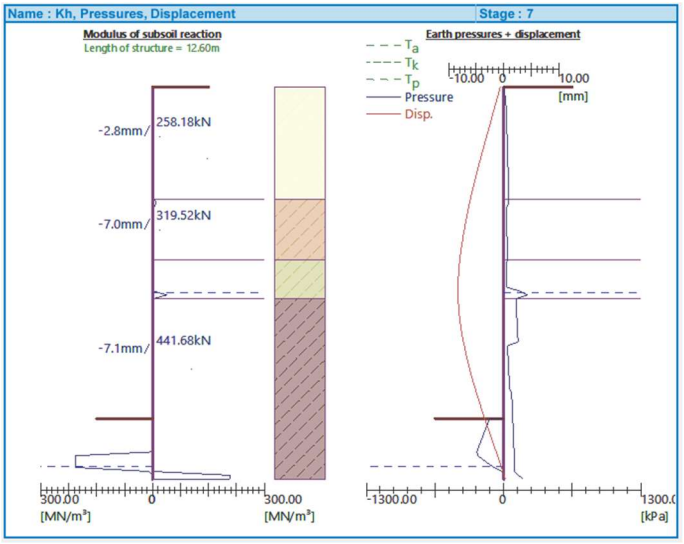

Figure 2.15 k_h, Earth Pressures and Displacements of the Wall in the Final Stage

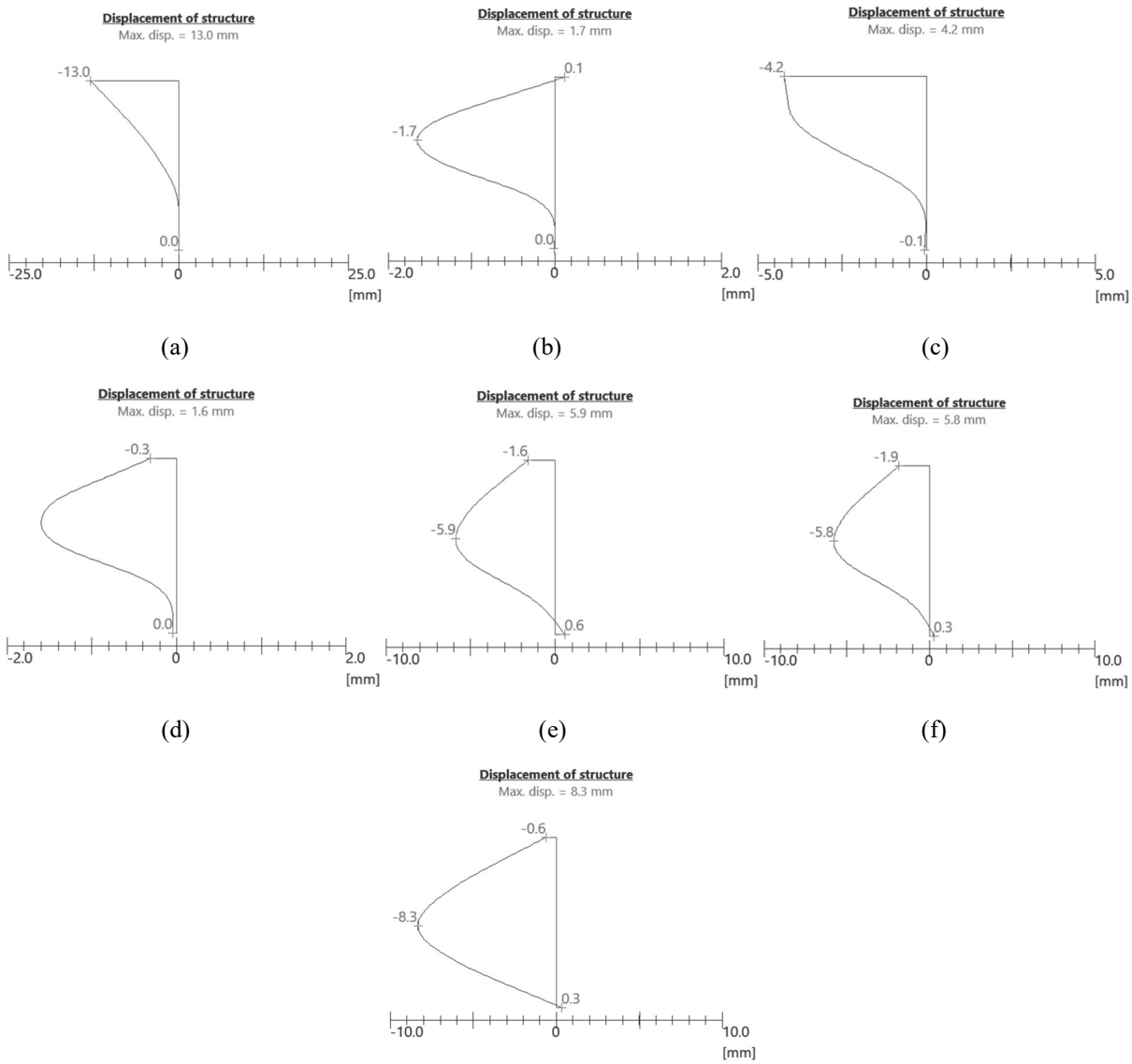

Figure 2.16 Displacement of structure in each construction stage

Table 12. Maximum structural displacement in each construction stage

Stage No.	1	2	3	4	5	6	7
Excavation Depth $H\,[\times 10^3\ mm]$	1.7	1.7	4.7	4.7	8.7	8.7	10.65
Max. Displacement $\delta_{max}\ [mm]$	-13.0	-1.7	-4.2	-1.6	-5.9	-5.8	-8.3

Note that the negative values denote the direction of the displacement is towards the excavation.

Sheeting Check programme provides terrain settlement calculation results from 3 methods—triangle, index and parabolic. But the results from those methods are quite distinct, which is not suitable for the evaluation of the ground settlement and decision on the accessibility of the design. The ground settlement is usually with great uncertainties.

When it comes to a project of pit engineering next to a building, the impact of excavations to it becomes a critical indicator to assess the design of retaining structures. Instead of considering the impact of the retaining structure by checking the ground settlement directly from those results provided by Sheeting Check programme, the assessment is held from the view of the maximum displacement δ_{max} and excavation depth H ratio.

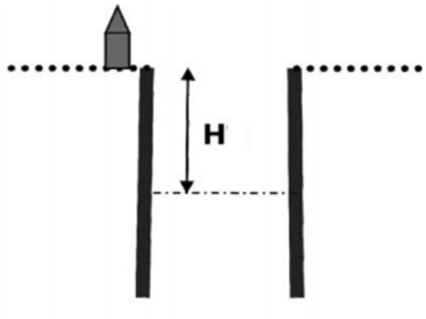

Figure 2.17 Example of an excavation next to the building [23]

Table 13. δ_{max} and H ratio in each construction stage

Stage No.	1	2	3	4	5	6	7
δ_{max}/H [%]	0.76	0.10	0.09	0.03	0.07	0.07	0.08

The displacements of retaining wall are important considerations in evaluating the impact to an adjacent structure, and allowable wall displacements depend on the ground condition, location of the adjacent building from the retaining wall, the existing condition and the foundation type of the building, etc. Hence, wall displacements should not be limited to an arbitrary value. A considered assessment on the adjacent buildings should be made to establish the limits on maximum wall displacements which can be higher or lower than 0.5%H that would not likely to cause damage to adjacent structures.[23]

The maximum displacement of the retaining structure is generally small enough, with the ratio to the excavation depth less than 0.5% (see Table 13). The δ_{max}/H ratio at the end of the first excavation (before the first anchorage) is 0.76%, which is in a way unacceptable. However, its excavation depth is 1.7 m which is unnecessary to reduce, because the anchors are to be constructed after, and on the other hand, Sheeting Check programme doesn't well include the overconsolidated soils, and the adjacent building is supported by deep piled foundations on rock massif. In this sense, simulation by the FEM could give an insight on this (introduced and discussed in Chapter 4 and 5).

3. Finite Element Simulation

3.1. General

The finite element analysis (FEA) is quite a different method, the general principle of which is introduced in section 1.2.3. This chapter covers the modelling methodology, discussions and theoretical background of FEM modelling settings including FEM mesh, materials, interface between distinct materials, soil constitutive models, the geo-static stress simulation, etc. The comparison of FEM and SRM in Chapter 4 correlate to the settings, calibrations and discussions in this chapter.

GEO5 – FEM program allows the simulations of various types of problems and analyses. The text below explains the basic terms and general procedures in a more detailed way. From the problem type aspect, it distinguishes two basic cases—plane strain and axial symmetry. From the type of analysis point of view, the program allows the following cases to be solved using individual modules, including stress, steady flow, unsteady flow, slope stability, and tunnels.[14]

3.2. FEM Mesh Generation

In the FEM, the weight functions and trial solutions are constructed by subdividing the domain of the problem into elements and constructing functions within each element. These functions have to be carefully chosen so that the FEM is convergent: The accuracy of a correctly developed FEM improves with mesh refinement, i.e. as element size, denoted by h, decreases, the solution tends to the correct solution. This property of the FEM is of great practical importance, as mesh refinement is used by practitioners to control the quality of the finite element solutions.[29]

Generally speaking, the mesh generation for the FEA is driven by two contending factors computational efficiency and accuracy. Therefore, a sufficient number of fine elements for mesh built in the prominent and critical regions are necessary. In this model, the mesh is refined in the wall and the surcharge region. The lower boundary limits both the horizontal and vertical displacement. The left and right boundaries limit the horizontal displacement, and the upper boundary is free from any constraint (see Figure 3.1).

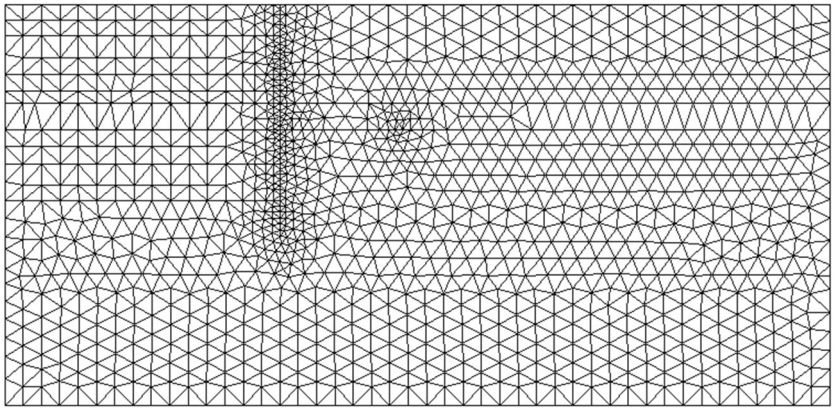

Figure 3.1 FEM Mesh

3.3. Initial Geostress – K_0 procedure

As we know, before the analysis for real construction sequence by FEM, it is necessary to generate run the initial phase calculation assumed without any soil displacement (see Figure 3.2). It provides the initial geo-stress for the analysis in the latter stages on the basis of the static equilibrium of the defined prescribed stresses. When adopting standard analysis, the initial stress is determined through the application of the finite element method. Nonlinear material models can be used to account for the evolution of possible failure surfaces already in the 1st calculation stage.

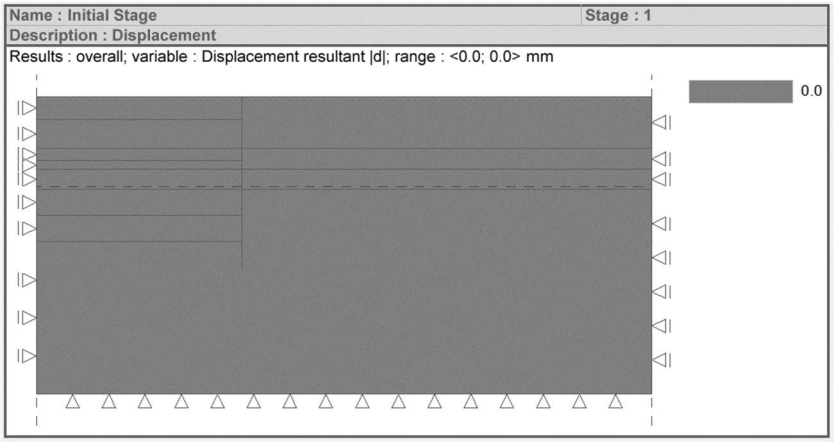

Figure 3.2 Ground displacement in the 1st stage

K_0 procedure is the method that allows for the calculation of geostatic stress in the 1st stage when a particular ratio between vertical and horizontal stress components is needed. For example, when dealing with overconsolidated soils the actual horizontal stress can attain much higher values than found in normally consolidated soils. The K_0 procedure generates only an elastic response. This analysis may lead to the evolution of plastic strains.

The calculation of the geostatic vertical stress is given by the following relationship:

$$\sigma_z = \sum_{i=1}^{n} \gamma_i \cdot h_i \tag{43}$$

where,

γ_i Unit weight of the i^{th} soil layer (if the soil is below the groundwater table, effective unit weight γ' is used);

h_i Thickness of the i^{th} soil layer.

The horizontal stress in the 1st stage is calculated as follows:

$$\sigma_x = K_0 \sigma_z \,, \tag{44}$$

where K_0 is the coefficient of horizontal pressure. It is assumed to be dependent on soil properties. If the K_0 parameter is not assigned manually, it can be derived from the relation with Poisson's ratio ν:

$$K_0 = \frac{\nu}{(1-\nu)} \,. \tag{45}$$

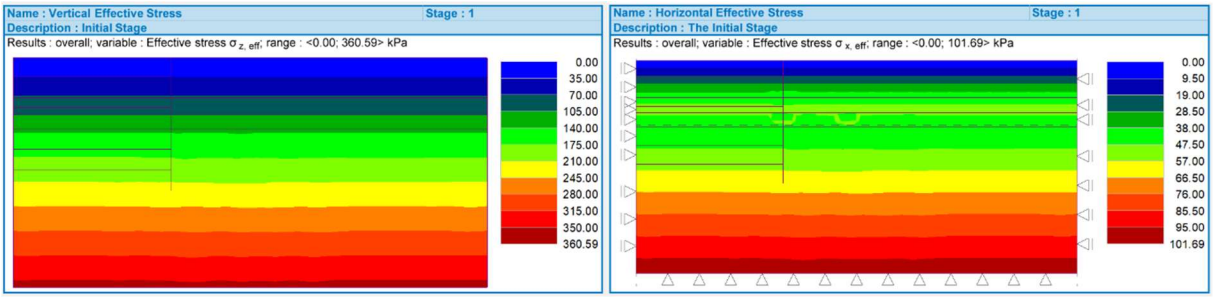

(a) ***(b)***

Figure 3.3 Effective stresses in the 1st stage: (a) σ_z (b) σ_h

The effective stresses adopting the K_0 procedure is given in Figure 3.3. The calculation phases performed in the FEA are listed in Table 14, where there are 3 more phases at the beginning of the calculation, compared to the designed construction sequence listed in Table 3 of section 2.2.1:

- Generation of initial geo-stress;
- Activation of surcharge coming from the existing piles of the adjacent building foundation, assumed as permanent actions;
- Construction of retaining wall.

Table 14. Calculation phases performed

Phase	Descriptions	Phase	Description
1	Initial stress	6	The 2nd excavation
2	Activation of the surcharge from the adjacent foundation piles	7	The 2nd anchorage
3	Pile wall construction (beam elements activation)	8	The 1st dewatering & the 3rd excavation
4	The 1st excavation	9	The 3rd anchorage
5	The 1st anchorage	10	The 2nd dewatering & the 4th excavation

3.4. Retaining Structure

3.4.1. Pile Wall

There are 3 types of constraint available for both endpoints of the beam elements in GEO5 – FEM programme:

- **Fixed**: the standard type;
- **Hinge**: usually acting as an internal hinge in between beams where no bending moment is allowed;
- **Foot:** a special type of a beam end-point support in the soil.

When the fixed type of connection is assumed, the beam and the soil element are connected at one point (a singular connection) often causing the evolution of plastic strains in the surrounding soil and loss of convergence. The foot support allows for a more realistic redistribution of contact stresses and prevents the beam from "penetrating" into the soil, consequently stabilizing the convergence process. On the other hand, a trial computational calculation with the only variable shows a larger horizontal displacement at the tip of the wall when the fixed support is used.[13]

Especially, in this project, the tip of the pile wall stands on a stable rock mass. It's less likely to see the wall penetrating to the ground. Thus, the retaining wall is set up with a "foot" support at the tip, the length of which is assumed to be equal to the width of the wall.

3.4.2. Soil-Structure Contact

Simulation of soil-structure interaction (SSI) plays an important role in the computation of most geotechnical problems. Generally speaking, there are two approaches to consider the SSI may be found in the studies. One is to treat the interface as a direct problem of compatibility (by means of Lagrangian multipliers, penalty formulation, etc.). The second approach makes use of the physical concept of an interface element. [52] In the GEO5 – FEM programme, the 2nd approach is available, that is, the interface element.

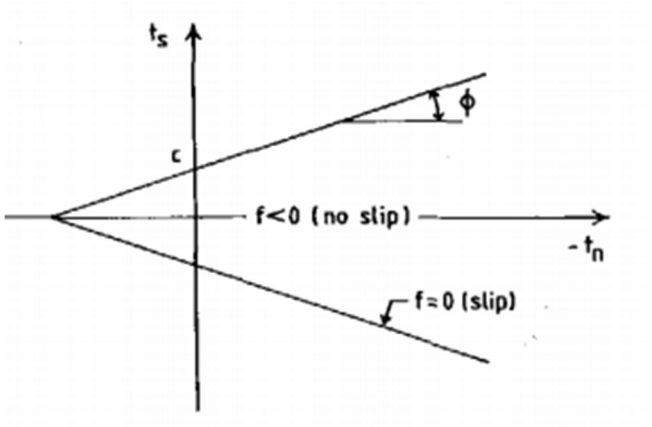

Figure 3.4 MC yield locus for a contact element [52]

The investigations showed that no additional constitutive relation for interface needs to be introduced when taken as a contact problem. The mechanical behaviours of the interfaces completely depend on the shear strength criterion of the interface and the properties of contact bodies, such as the Mohr-Coulomb law (see Section 1.3.2).[41] The contact elements in the finite element analysis will be based on the Mohr-Coulomb yield criterion (see Figure 3.4).

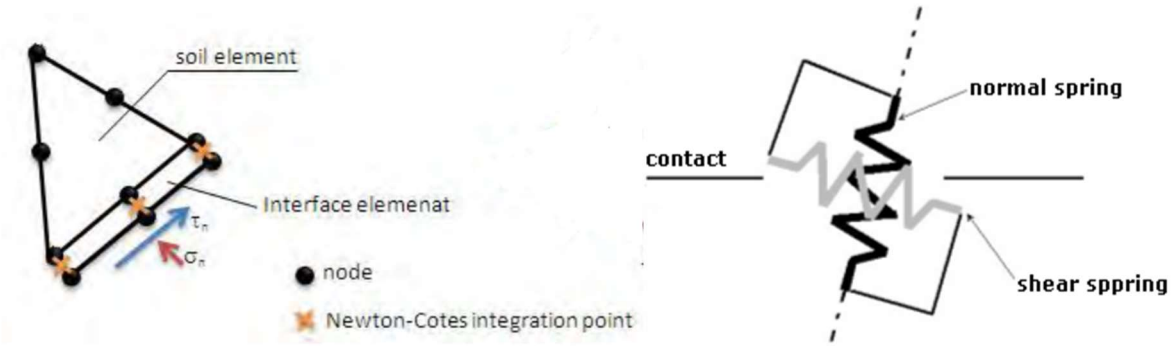

Figure 3.5 Contact element and elastic contact [15] [52]

The contact component acts with no thickness as to obtain the interfacial stress as a function of a relative displacement developed along with the interface. The elastic stiffness in the normal (k_n) and tangential (k_s) directions can be imagined as spring stiffness along with a given interface (see Figure 3.5).[15] Although in the case of **fully plastic behaviour**, the selection of

parameters k_n and k_s is not essential, the values assigned to these parameters are decisive for the success of the solution of a given nonlinear problem.

In the case of distinct materials (E_1, E_2, G_1, G_2), the lower values of k_n and k_s are to be used. A reliable selection of the values of these parameters is not an easy task and is usually dependent on the problem. Providing these values are too large (above 100000 kN/m^3), the iteration process may oscillate. On the other hand, setting the values of k_s and k_n too low (below 10000 kN/m^3) leads to non-realistic deformations of structure.[13] However, considering possible unrealistic structural deformations, the values are to be adjusted where they are too low. The determination of contacts may relate these two stiffness values to the material parameters of the soil adjacent to the contact, which is given by:

$$k_n = {}^{E}/_{t}\,, \tag{46}$$

$$k_s = {}^{G}/_{t}\,, \tag{47}$$

where,

t	Assumed thickness of fictitious contact layer;
G	Shear modulus of elasticity, $G = {}^{E}/_{2((1+\nu))}$;
E	Elastic modulus.

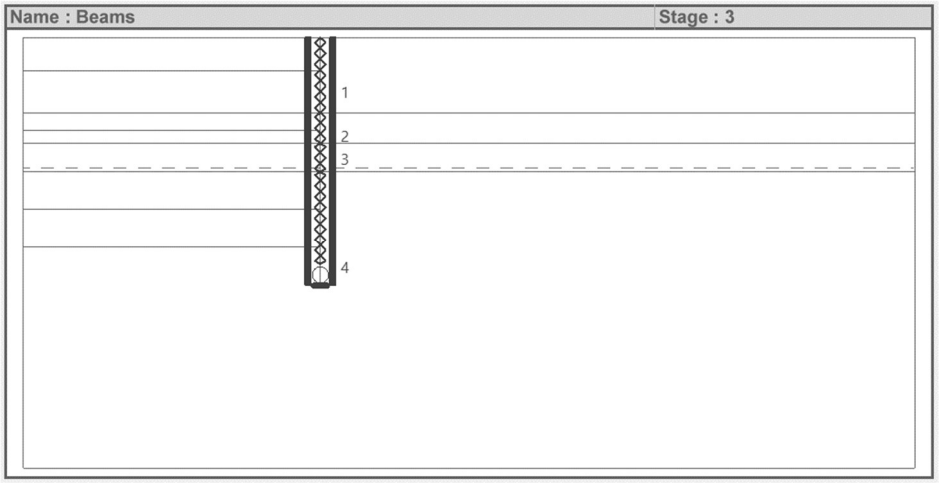

Figure 3.6 Beam elements

To achieve assigning individual contact between the retaining wall and each soil layer, the whole wall is comprised of a few numbers of beam elements connected fixedly with different contact types in the finite element model, correlating with different soil layers (see Figure 3.6).

A 0.1-metre thickness of the contact layer is the usually assumed default setting.[49][51] But to avoid unrealistic behaviour and calculation oscillation due to too low or too high stiffness, and to make sure the contact stiffnesses with respect to each soil layer are approximately in proportion, it is assumed that the contact thickness is 0.3 *m* in this simulation.

The reduction parameters c and μ can be specified also indirectly by reducing the strength parameters c and $tan(\varphi)$ of the soil adjacent to the contact. In general, this reduction is greater for cohesionless soils, and the reduction parameters should be less than 1.[14][15] It is assumed that the reductions for the contact by the first sandy layer, GT1, are set to be 0.7; while the reductions for GT4, GT5, GT6, are given as 0.5, 0.3, 0.3, respectively. The values of contact springs' stiffnesses and the reduction factors for each contact are summarised in Table 15.

Table 15. Summary of the parameters of contact elements between soils and the retaining structure

Contact No.	Corresponding soil layer	k_n $[kN/m^3]$	k_s $[kN/m^3]$	δ_c	δ_μ
1	GT1	12480	10000	0.7	0.7
2	GT4	37449	13870	0.5	0.5
3	GT5	233333	91146	0.3	0.3
4	GT6	616667	252732	0.3	0.3

Note that the calculated stiffness values not greater than 10000 kN/m³ are adjusted to this value.

3.4.3. Anchorage

Origin		Length and inclination / end		Anchor spacing	Diameter / area	Elastic modulus	Tensile strength	Active	Force
x [m]	z [m]	l [m] / x [m]	α [°] / z [m]	b [m]	d [mm] / A [mm²]	E [MPa]	F_c [kN]	in compress.	F [kN]
0.00	-1.40	l = 21.00	α = 25.00	2.00	d = 250.0	195000.00	531.00	☐	250.00
0.00	-4.40	l = 17.00	α = 25.00	2.00	d = 250.0	195000.00	796.50	☐	280.00
0.00	-8.40	l = 12.00	α = 25.00	2.00	d = 250.0	195000.00	1062.00	☐	370.00

Figure 3.7 Anchorage settings in the FEM

The settings for the anchorage in the FEM are listed in the table of Figure 3.7, and the schema of the anchored retaining wall when the pit is excavated to its designed level is as is depicted in Figure 3.8.

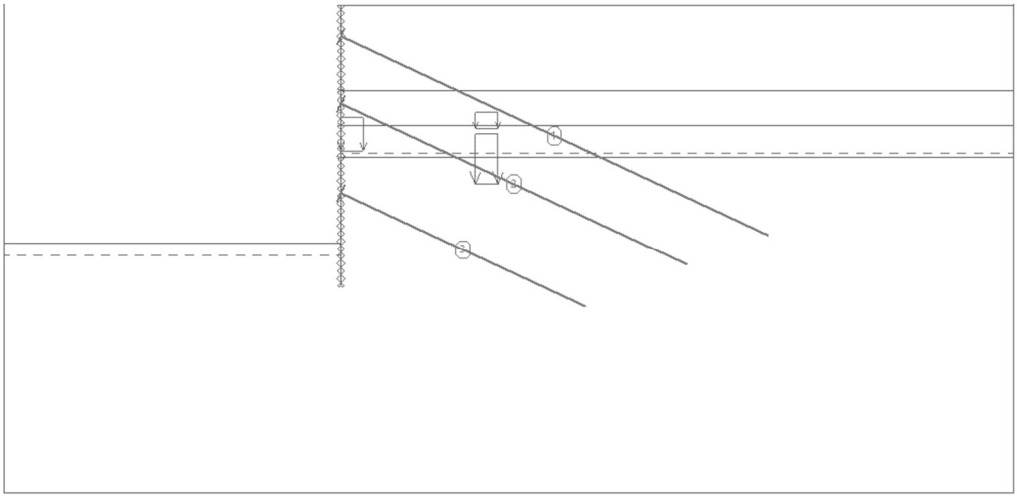

Figure 3.8 The anchored retaining wall after the final excavation

3.5. Selection of Soil Constitutive Model

The accuracy of a finite element calculation in geotechnical engineering is principally related to both the mechanical parameters obtained from field tests and laboratory tests, as well as the constitutive models utilising the parameters for computational simulation. Because of the high **nonlinearity and discreteness** of soil, there is a certain deviation from those two factors. Hence, a comprehensive consideration of the soil constitutive selection is the key.

The selection of soil constitutive models is not a simple task; on the other hand, the parameters of a model may not be easily attained although they are described with clear physical meanings. There are 2 constitutive models in terms of the Mohr-Coulomb failure criterion analysed and discussed by the FEM in this paper:

- Mohr-Coulomb (MC);
- Modified Mohr-Coulomb (MMC).

This is because the number of parameters for the MC model is less, and it can better simulate the failure characteristics of soil (Mohr-Coulomb yield criterion). It is very convenient to apply and is widely used in geotechnical engineering calculation and analysis in various fields.

However, the model cannot express the nonlinear characteristics of the soil before yielding and cannot distinguish the loading and unloading stress paths. Many studies have compared FEA results with the constitutive models with the monitored results, indicating that there are large deviations in the calculation of some problems in the actual engineering analysis (such as the rebound of the bottom of the pit during excavation).

MMC model is adopted as it has the advantage of an automatic consideration of hardening and softening of soil shear strength parameters where necessary (see Section 1.3.3). And the inputs of it are the same as that of the MC model. So, it could provide another perspective for the simulation analysis.

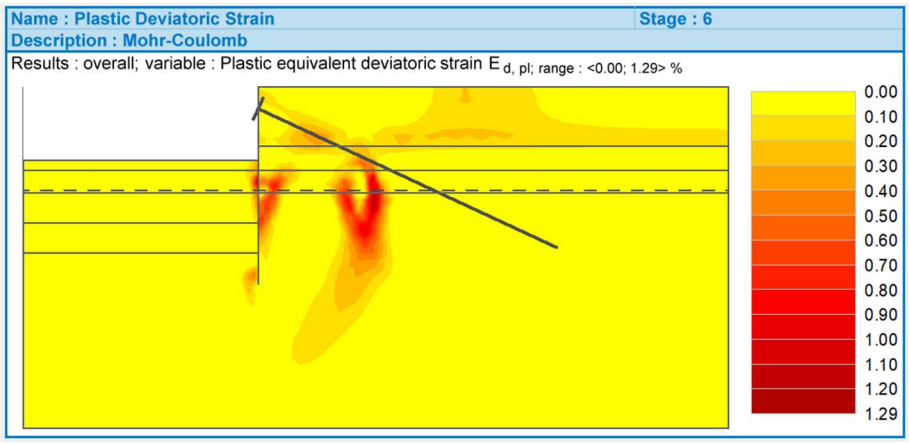

(a)

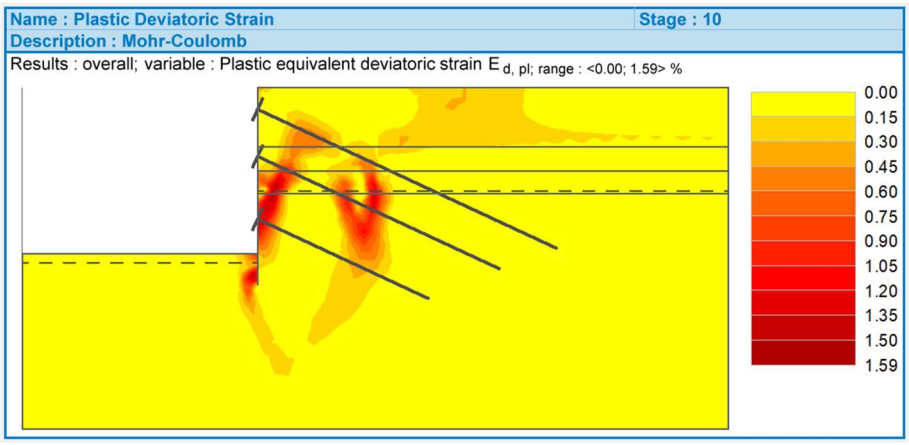

(b)

Figure 3.9 Plastic equivalent deviatoric strain in (a) the intermediate and (b) the final stage

When the pit excavation is simulated with the MC constitutive model, the soils inside the excavation barely reach the MC yield surface in the intermediate and the final stages(see Figure 3.9). This results in the linear stress-strain condition, yet soil appears to be elastoplastic property. So, the MC model in this project would ultimately turn out to be more unrealistic if the elastic modulus is not selected and calibrated well.

3.6. *The Calibration of the FEM Model*

Assumptions are made in the previous structural deformation analysis using SRM using Sheeting Check programme in Chapter 2:

- It is considered that there is no side friction around the adjacent foundation piles resisting the external loading. That is to say, the surcharge is only from the tip of the foundation piles;
- The adjacent foundation piles all stand on the level 0.5 m above GT6;
- The lowest deformation modulus of soils is selected so that the stiffness of subgrade reaction is low.

These assumptions result in the most critical deformation of the retaining wall. Nevertheless, in the finite element non-linear analysis, a reasonable judgement on the elastic modulus is crucial. By inputting the lowest soil moduli and unfavourable surcharge condition in the non-linear FEA, the settlement of the 2nd row of piles appears to be unrealistically large (see Figure 3.10). This is because of the adoption of the lowest modulus and the assumption that the total loading is only resisted by the tip of piles (see Figure 3.10), which is an impossible case for designed piled foundations. Thus, it's necessary to adjust the surcharge and the selected deformation modulus for the finite element analysis.

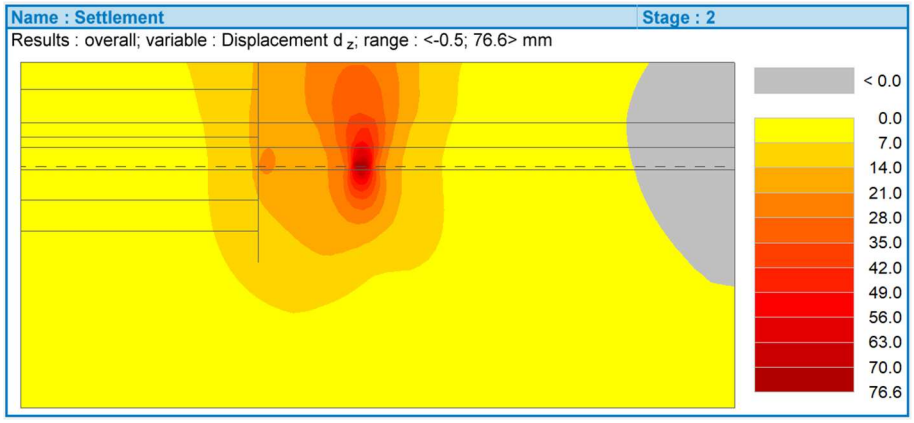

Figure 3.10 Ground settlement results in the 2nd stage with MC soil constitutive model when the FEM model is not calibrated

3.6.1. *Elastic Modulus Calibration*

Usually, the selection of the appropriate value of elastic modulus for the MC model depends on the stress path of the in-situ application.[56] The elastic modulus for the MC model can also be easily calibrated if the E_{50} (the secant modulus when the deviatoric stress is 50% of that when the soil yields) and the corresponding minor principal stress σ_3 for the load test is known. If not, there are numerous candidate secant moduli to select from, as is shown in Figure 3.11. Lower

elastic modulus selected can result in unrealistically large displacement when the deviatoric stress is the same.

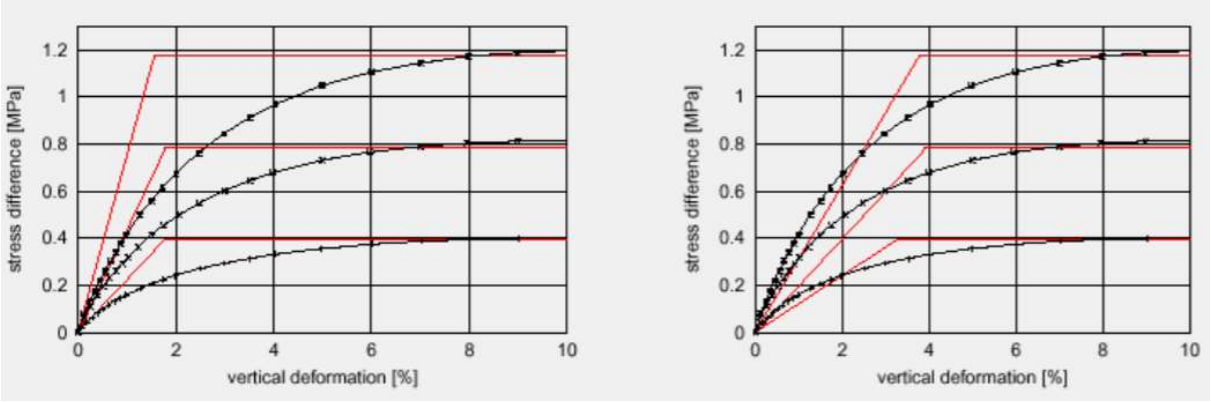

Figure 3.11 Calibrations of elastic modulus for the Mohr-Coulomb model[53]

The soil parameters for the MC model were not measured experimentally but instead pulled from the available database on the basis of the classification according to the Czech standards.[44] The soil deformation modulus is given ranging in a certain interval in this project, and the lower deformation modulus contains the deformation from plasticity.

To calibrate with the reasonable range of settlement of foundation piles which is about 25-40 *mm* with input parameters concerning the FoS, a larger value of the elastic modulus for is selected the MC model of GT5 and GT6. Besides, it is assumed that the elastic modulus equals to the relevant oedometric modulus for GT1 and GT4. The ratio of modulus of unloading/reloading E_{ur} to the elastic modulus E and is usually selected as 3 or so and can range from 2 to 5 approximately. [13] [22] [53] Considering the properties of each soil layer, this ratio is considered as 3.5(GT1), 4(GT4), 2.8(GT5), 2.5(GT6). The soil moduli for the FEA are listed in Table 16.

Table 16. Summary of soil moduli

Soil layer	Range of E_{def} [*MPa*]	E [*MPa*]	Ratio of E_{ur}/E [-]	E_{ur} [*MPa*]
GT1	2-10	3.74	3.50	13.10
GT4	7-10	11.23	4.00	44.94
GT5	30-80	70	2.80	196.00
GT6	120-200	185	2.50	462.50

Note that for the layers of rock massif, GT5 and GT6, a 0.5-MPa/m increment of elastic modulus is considered.

3.6.2. *Surcharge*

To calibrate to a reasonable pile settlement, the second row of the adjacent foundation piles is adjusted to be 2 loads (q_1 = 500 kN/m^2, q_2 = 1558 kN/m^2). q_1 is cautiously chosen to represent all the side frictions along the foundation pile located on the upper part of GT5; while q_2 denoting the bearing pressure of the soil below the pile is subsequently diminished and located deeper.

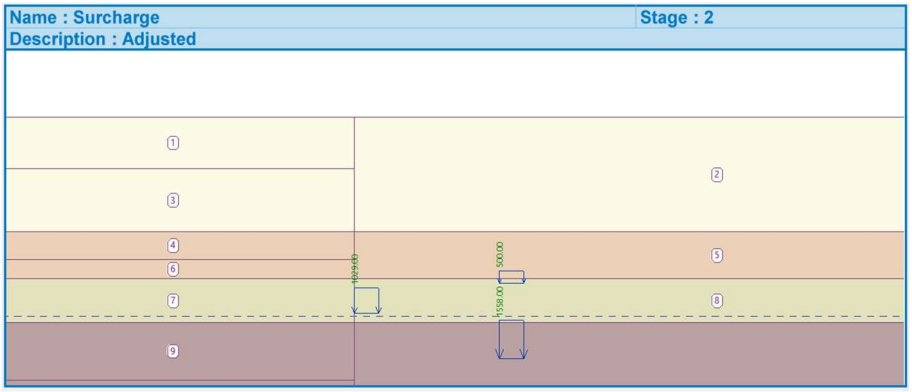

Figure 3.12 Schematic illustration of the modified surcharge

Based on the above-mentioned changes of the elastic modulus and surcharge, the maximum ground settlement in the 2nd stage when there is only the surcharge activated has become 26.8 *mm* (see Figure 3.13).

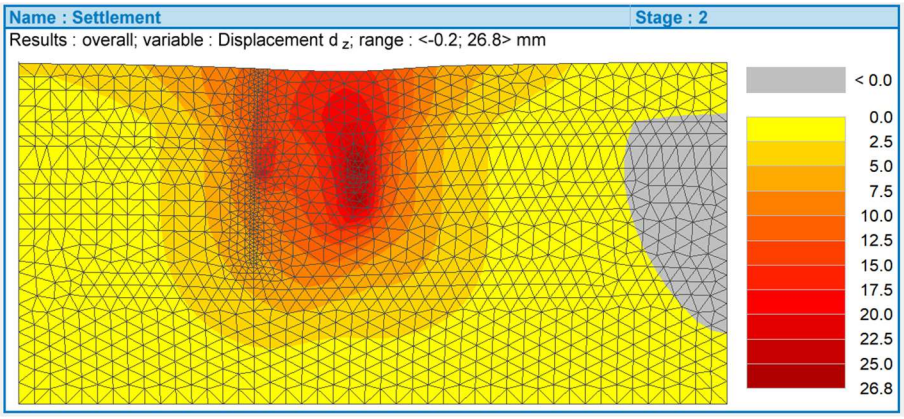

Figure 3.13 Ground settlement in the 2nd stage with MC model when the FEM model is calibrated

3.6.3. *Discussions on the Stress Path and Overconsolidation*

The strength and deformation properties of soil are not only about the stress state it is in but also relevant to the change of the stress state, that is, **stress-path dependent**. An excavation is a progressive process of unloading (see Figure 3.14). And this becomes more important when it comes to the deep excavation which deals with a great deal of unloading.

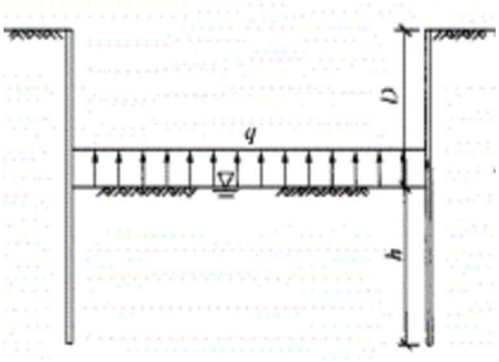

Figure 3.14 Excavation unloading[59]

In general, the stress path of soil can be divided into 3 zones with different features of the stress path for the excavation in foundation pit engineering (see Figure 3.15).[18] Studies have proven that the structural and ground displacements in the FEA with hyperbolic constitutive models match better with the monitored results. However, the MC model with the stress-strain relationship being elastic-perfectly plastic does not consider the stress path of soil, which shows greater advantages. [18][44]

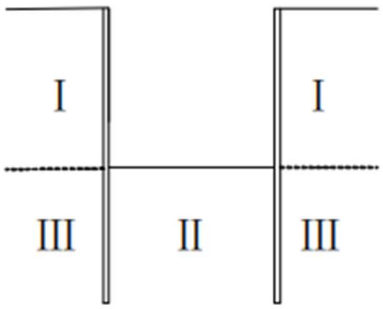

Figure 3.15 Stress path divisions for pit excavation

Hence, simply applying the parameters from load tests or table values easily result in unrealistic results. The main features of the above-mentioned 3 zones for foundation pit excavations are stated below, including the change of stresses and the stress path: [18]

- ***Zone Ⅰ:***

$\Delta\sigma_h < 0, \Delta\sigma_v \approx 0$, stress path: P-B.

- ***Zone Ⅱ:***

$\Delta\sigma_v < 0, \Delta\sigma_h \approx 0$, stress path: P-C-D.

- ***Zone Ⅲ:***

$\Delta\sigma_v < 0, \Delta\sigma_h < 0$, stress path: between P-B and P-C.

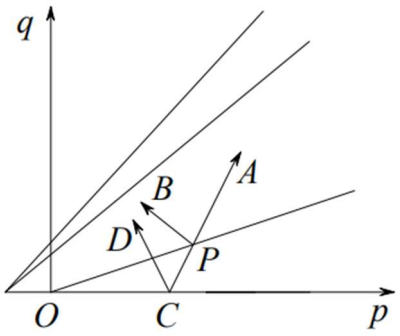

Figure 3.16 Stress path in the p-q plane[22]

As the MC model is not able to consider the stress path, horizontal stress σ_h of the soil in ***Zone II*** decreases as the excavation goes deeper. But this is not the reality according to the stress path divisions. σ_h in ***Zone II*** acts as passive earth pressure, so there can be greater lateral displacement of retaining wall if it is not calibrated.

Plenty of studies have shown that the relationship between σ_z and σ_x (or σ_1 and σ_3) is linear for a normally consolidated soil, e.g.,

$$\sigma_x / \sigma_z = K_{0,n}\,. \tag{48}$$

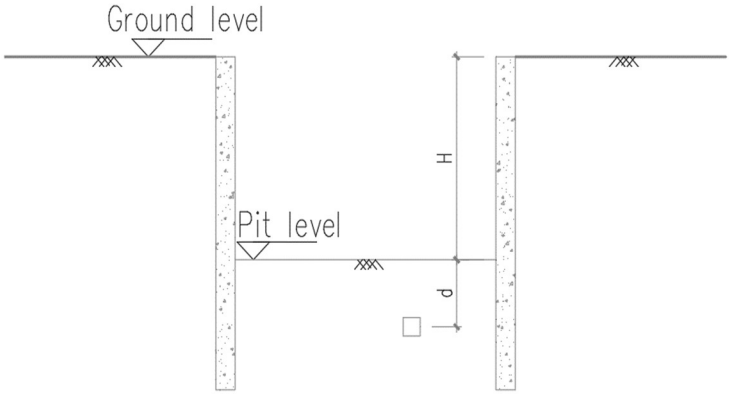

Figure 3.17 Schema for the stress state illustration

However, this simple linear relationship is false when it comes to the soils below the pit (***Zone II***) which have become overconsolidated as the unloading going on during excavation. Assuming that there is only one type of homogeneous soil, the stress state of a point below the pit (see Figure 3.17) before excavation is:

$$\sigma_z = \gamma(H + d)\,; \tag{49}$$

$$\sigma_x = K_{0,n} \cdot \gamma(H + d). \tag{50}$$

The stress state of a point below the pit after excavation with a depth of H is as follows:

$$\sigma_z' = \gamma d \ ; \tag{51}$$

$$\sigma_x' = K_0 \cdot \gamma d \ ; \tag{52}$$

where, $K_{0,n}$ and K_0 denote the coefficient of horizontal pressure of normally consolidated soil and overconsolidated soil, respectively.

Thus, the overconsolidation ratio is given by:

$$OCR = {\sigma_z}/{\sigma_z'} = {\gamma(H+d)}/{\gamma d} \ . \tag{53}$$

Because soil is elastoplastic, there is always residual stress remained when coming across unloading. In other words, the horizontal stress doesn't decline proportionally as the vertical stress declines, because by considering the overconsolidation caused by unloading there is always $K_0 > K_{0,n}$.[57] The relationship between K_0 and $K_{0,n}$ can be expressed as:

$$K_0 = K_{0,n} \cdot OCR^m = {\sigma_x}/{\sigma_z} \left({\sigma_z}/{\sigma_z'}\right)^m ; \tag{54}$$

where m is an experience value. The most common alternative for this exponent is $m = \sin\varphi$, or 0.5. Some studies have indicated m $\approx$ 1.0.[57] [58]

Hence, the variation quantity of horizontal stress is deducted as follows:

$$\Delta\sigma_h = K_0\sigma_z' - K_{0,n}\sigma_z = K_{0,n}OCR^m \cdot \sigma_z' - K_{0,n} \cdot \sigma_z' \, OCR = K_{0,n}\gamma d(OCR^m - OCR). \tag{55}$$

According to equation (55), and considering equation (45), the relationship between $\Delta\sigma_h$ and ν is given as follows:

$$\Delta\sigma_h = {1}\Big/{\left(\frac{1}{\nu} - 1\right)} \left(OCR^m - OCR\right) \Delta\sigma_z \ ; \tag{56}$$

where, $\Delta\sigma_z = \gamma d$.

It can be judged from equation (56) that $\Delta\sigma_h$ is positively correlated to the Poisson's ratio ν. Because $m <$ (or $\approx$) 1, $OCR - OCR^m <$ (or $\approx$) 0, the equation is expressed as follows when the absolute values are considered:

$$|\Delta\sigma_h| = {1}\Big/{\left(\frac{1}{\nu} - 1\right)} \left(OCR - OCR^m\right) \Delta\sigma_z \ . \tag{57}$$

For a certain excavation, the reloading pressure, $\Delta\sigma_z$, is constant. So is the coefficient of horizontal pressure for normally consolidated soil, $K_{0,n}$. Therefore, it is the value of $OCR - OCR^m$ (hereinafter, called OCR-coefficient) of a soil during unloading that determines the decreased value of the horizontal stress, $|\Delta\sigma_h|$. As the range of the exponent, m, is known, the OCR-coefficient is in a positive correlation with OCR.

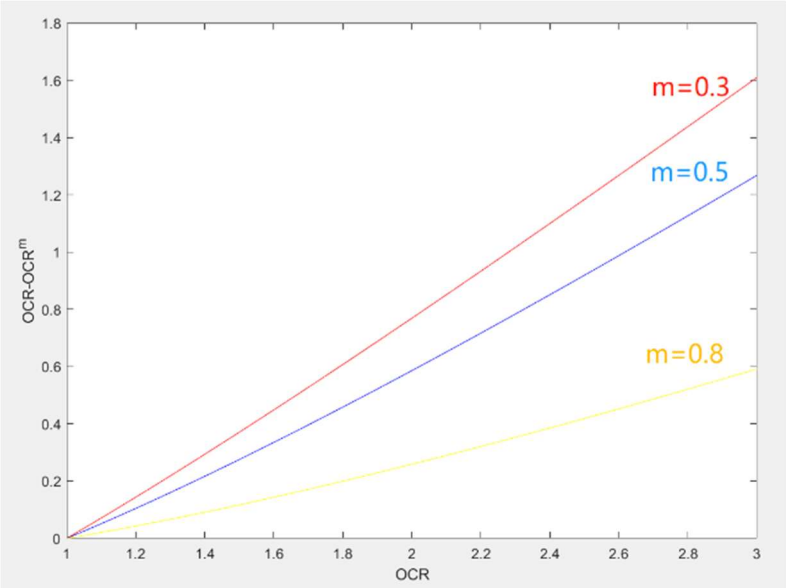

Figure 3.18 Relationship between OCR and OCR-coefficient

Hence, if the soil is close to the excavation level, $|\Delta\sigma_h|$ can be bigger because the OCR-coefficient is higher. Whereas, on the other hand, if the soil is deep, $|\Delta\sigma_h|$ approaches zero.

However, K_0 can't be updated stagewise for excavation unloading in GEO5 – FEM. The horizontal stress in GEO5 – FEM can be calculated by the K_0 manually or input automatically calculated from the Poisson's ratio:

- If this is manually input, K_0 can be calculated by Eq. 54. In this case, the coefficient K_0 is increased so that the decrease of the vertical stress is compensated;
- If it is automatically calculated from ν using the eq. 45. The coefficient K_0 is calculated from a smaller value of ν, the decrease of horizontal stress $\Delta\sigma_h$ is controlled.

Here, the latter approach to keep lower decreases of the horizontal stress is to be used. For the initial geostatic stress (K_0 procedure), the Poisson's ratio, ν, remains the same as the previous. And from the 4th calculation stage when the excavation commences, ν of the soils in ***Zone II*** is to be changed as follows:

- The Poisson's ratio of the soils closest to the excavation level is decreased as is listed in Table 17;

- The Poisson's ratio of other deeper soil is assumed to be 0.01 (it can't be zero because ν is a denominator in Eq. 45 for the calculation of K_0).

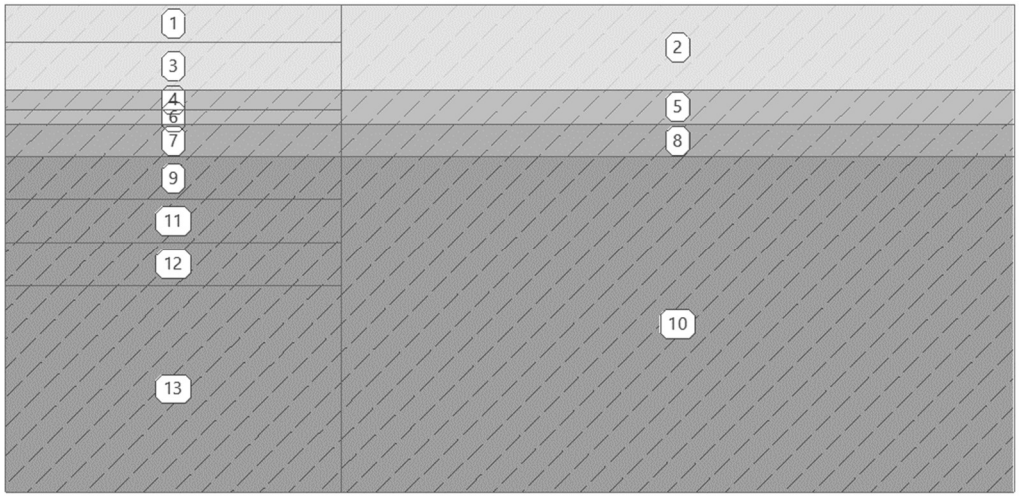

Figure 3.19 Schematic illustration of soil blocks for adjusting Poisson's ratio

Table 17. Adjusted Poisson's ratio

Soil block	Excavation of activation	previous ν (for the initial stage)	new ν (for the relevant new excavation)
GT1-③	1st Excavation	0.38	0.25
GT4-⑥	2nd Excavation	0.35	0.22
GT5-⑦	2nd Excavation	0.28	0.15
GT6-⑪	3rd Excavation	0.22	0.1
GT6-⑫	4th Excavation	0.22	0.1

The horizontal stress of a few points in different depth is monitored in the 3rd stage (before excavation) and 4th stage (the 1st excavation) as an example (see Figure 3.20). There are fewer decreases in horizontal stress when the model Poisson's ratios of soils are calibrated.

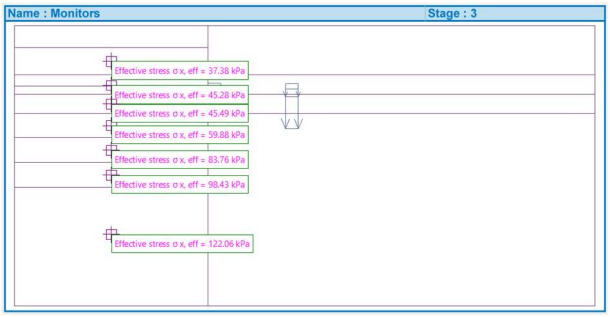

(a)

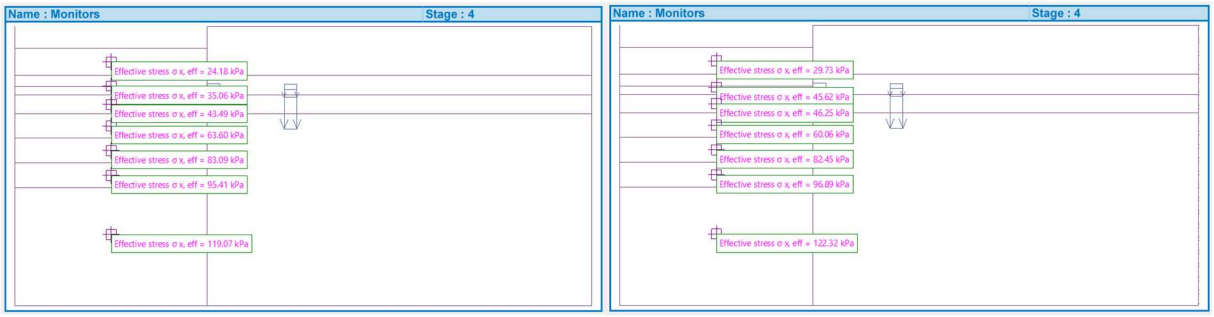

(b) *(c)*

Figure 3.20 Horizontal stress monitoring: (a) the 3rd stage, (b) the 4th stage with ν not calibrated, (c) the 4th stage with ν calibrated

The comparison of structural displacement is given in Figure 3.21. When the Poisson's ratio is calibrated concerning over-consolidation, the horizontal stress inside the pit does not decrease so that the retaining structure does not deform as much as it is when the value of ν is not calibrated**.**

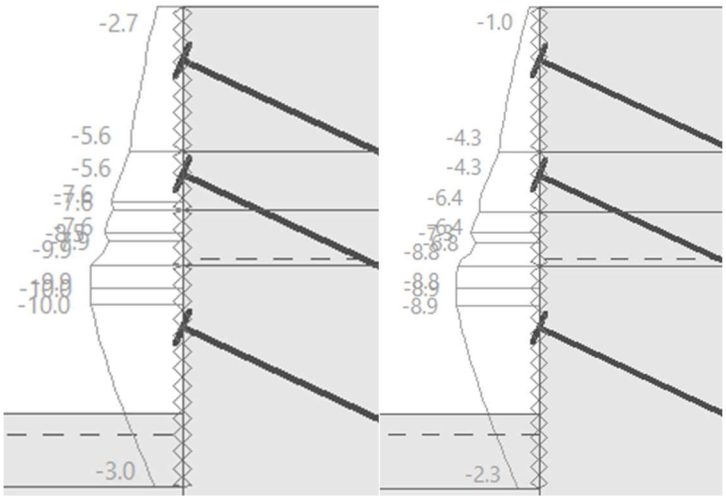

(a) *(b)*

Figure 3.21 Lateral displacement of the retaining structure in the final stage with ν: (a) not calibrated, (b) calibrated

4. Discussions on the Results of Sheeting Check and FEM

4.1. Chapter Introduction

To compare the results obtained from the different calculations, not only the final stage of construction but also an intermediate stage is considered. Hereinafter, the discussions will be held in the following two stages:

- **Intermediate stage**: the end of 2nd excavation;
- **Final stage**: the end of the 4th excavation (e.g. the last excavation to the pit level).

Consequently, the intermediate stage and the final stages are the 6th and 10th calculation step in the FEM programme, respectively; 3rd and 7th in the Sheeting Check programme.

The staged construction sequence in Sheeting Check and FEM are different because the initial geostatic condition is simulated in the FEM. The comparisons of the results from these two programmes are given in the next few sections, in which the Stage No. 0 (the 3rd calculation stage in the FEM) denotes the construction stage when the pile wall is inserted into the ground. This is only valid in the FEA, not the analysis by the Sheeting Check programme. Other construction stages correlate to each other.

4.2. Results and Comparisons of Ground Movement

4.2.1. FEM Programme

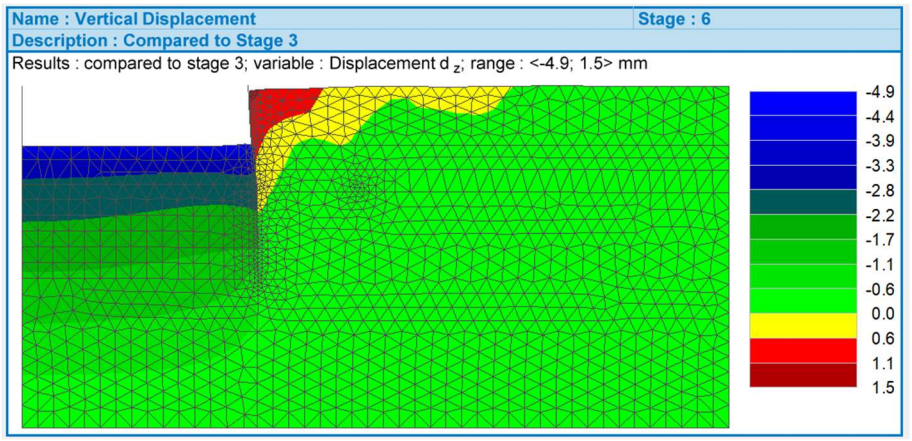

(a) MC

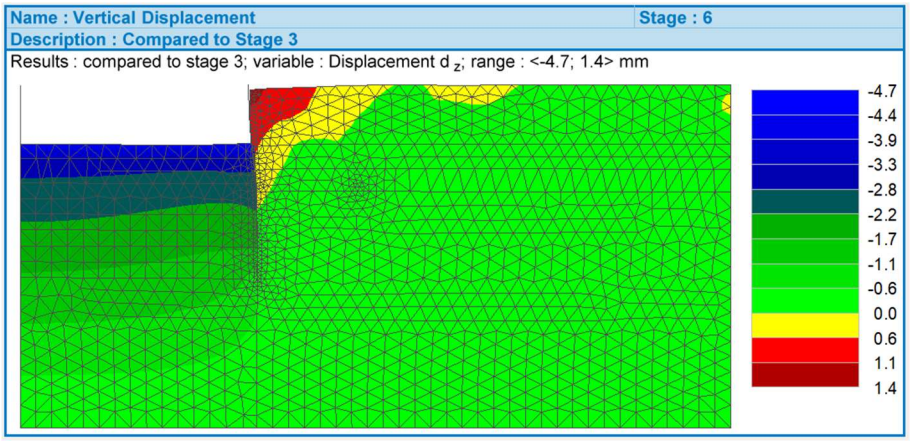

(b) MMC

Figure 4.1 FEM – Comparison of ground settlement between the beginning of excavation and the intermediate stage

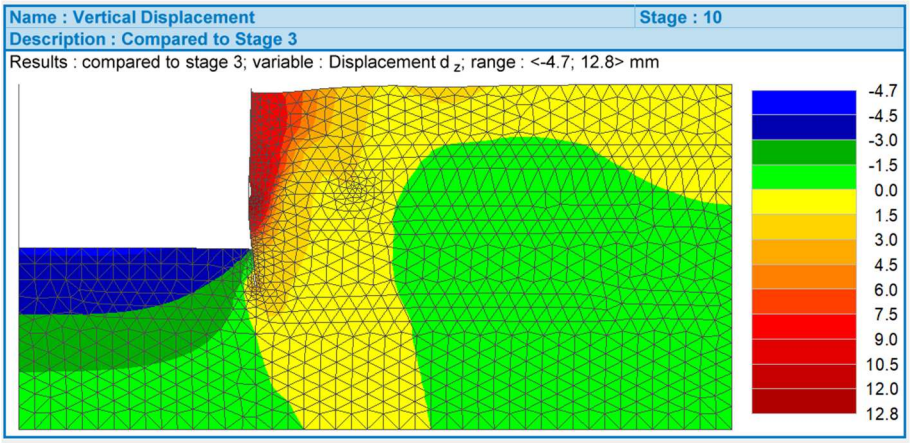

(a) MC

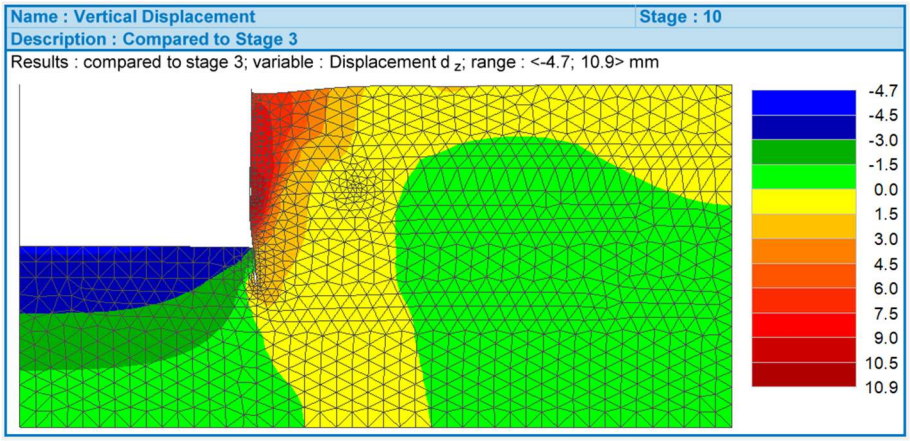

(b) MMC

Figure 4.2 FEM – Comparison of ground settlement between the beginning of excavation and the final stage

The ground vertical displacement is given in Figure 4.2. The magnitude of ground rebound inside the pit does not have big different; whereas, the MC model shows relatively greater values in the terrain settlement behind the pit.

4.2.2. Sheeting Check Programme without FoS

In the Sheeting Check programme, the ground rebound cannot be calculated, but the terrain settlement behind the retaining structure. The approach to the calculation includes the triangle method, index method, parabolic method, etc. The index method is adopted for discussions (see Figure 4.3).

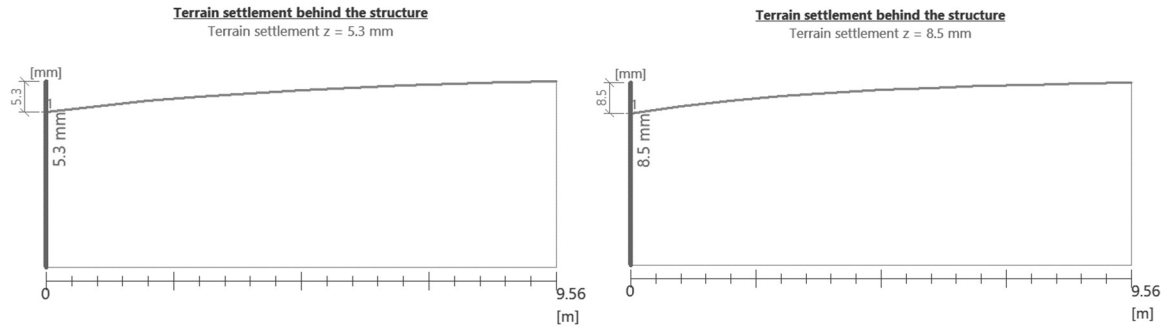

(a) *(b)*

Figure 4.3 Sheeting Check – Terrain Settlement in (a) the intermediate stage (b) the final stage

4.2.3. Comparison of Ground Movement

The finite element analysis with the Mohr-Coulomb model appears to be most critical in the terrain settlement (see Table 18). In the intermediate stage, the terrain settlement calculated by the index method is about 4 times higher than the results by the finite element method; whereas, in the final stage, the value of terrain settlement in the FEM is higher.

Table 18. Comparison of the extreme value of terrain settlement behind the pit [mm]

	Intermediate stage	Final stage
Sheeting Check (without FoS)	5.3	8.5
FEM – MC	1.5	12.8
FEM – MMC	1.4	10.9

4.3. Results and Comparisons of Structural Displacement

4.3.1. FEM Programme

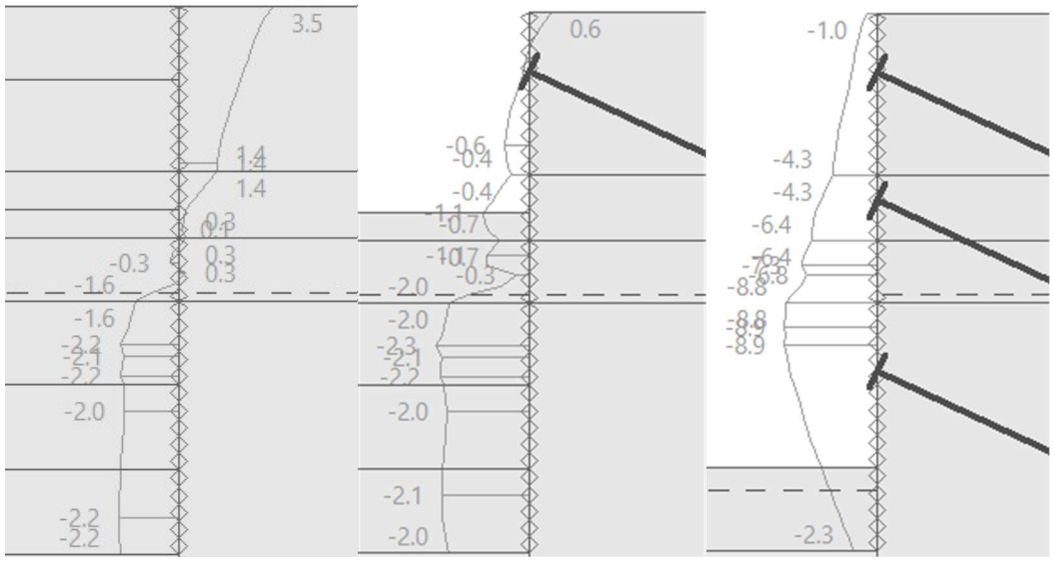

(a) *(b)* *(c)*

Figure 4.4 Lateral displacements of the retaining wall with the use of the MC model in the: (a) beginning of excavation; (b) intermediate stage; (c) final stage

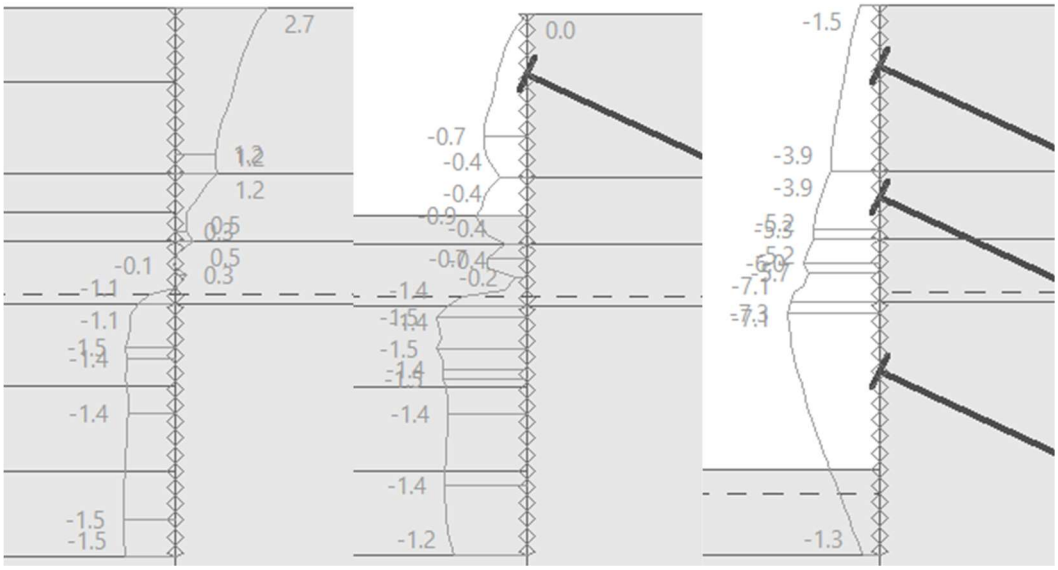

(a) *(b)* *(c)*

Figure 4.5 FEM – Lateral displacements of the retaining wall with the use of the MMC model in (a) the beginning of excavation; (b) the intermediate stage; (c) the final stage

4.3.2. SRM by Sheeting Check Programme with no FoS

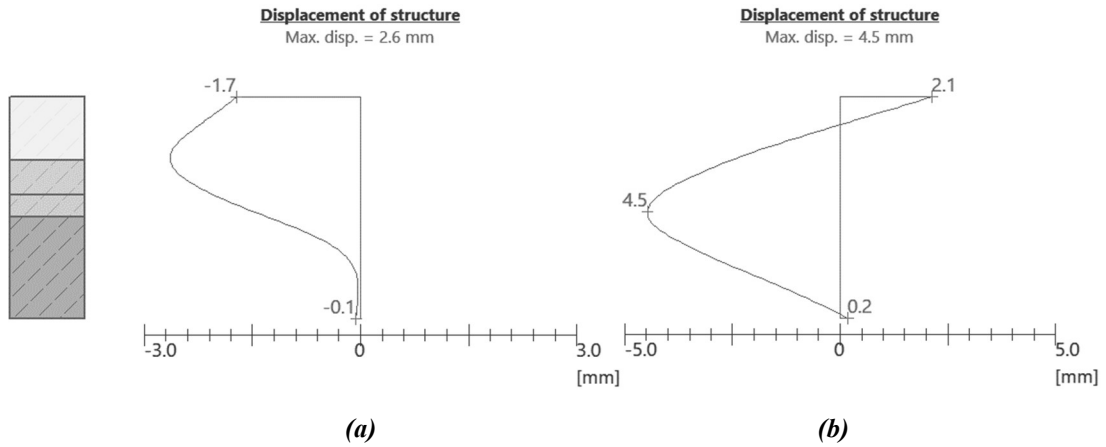

Figure 4.6 Displacement of the structure in (a) the intermediate stage (b) the final stage

Table 19. Extreme structural displacements in each construction stage Sheeting Check

Stage No.	Negative extreme displacement [mm]	Positive extreme displacement [mm]
1	-10.6	0
2	-1.2	1.9
3	-2.6	-
4	-1.1	2.1
5	-3.8	1.1
6	-3.7	0.9
7	-4.5	2.1

Note: the negative values denote displacements in the direction to the excavation; the positive values denote displacements towards the terrain behind the retaining wall.

4.3.3. Comparison of Structural Displacement

Table 20. Comparison of maximum structural displacement in each construction stage [mm]

Stage No.	0	1	2	3	4	5	6	7
Sheeting Check (with FoS)	/	-13	-1.6	-4.2	-1.6	-5.9	-5.9	-8.4
Sheeting Check (without FoS)	/	-10.6	1.9	-2.6	2.1	-3.8	-3.7	-4.5
FEM (MC)	3.5	-2.4	-2.4	-2.3	-2.2	-6.6	-6.5	-8.9
FEM (MMC)	2.7	-1.5	-1.5	-1.5	-1.5	-5.2	-5.2	-7.3

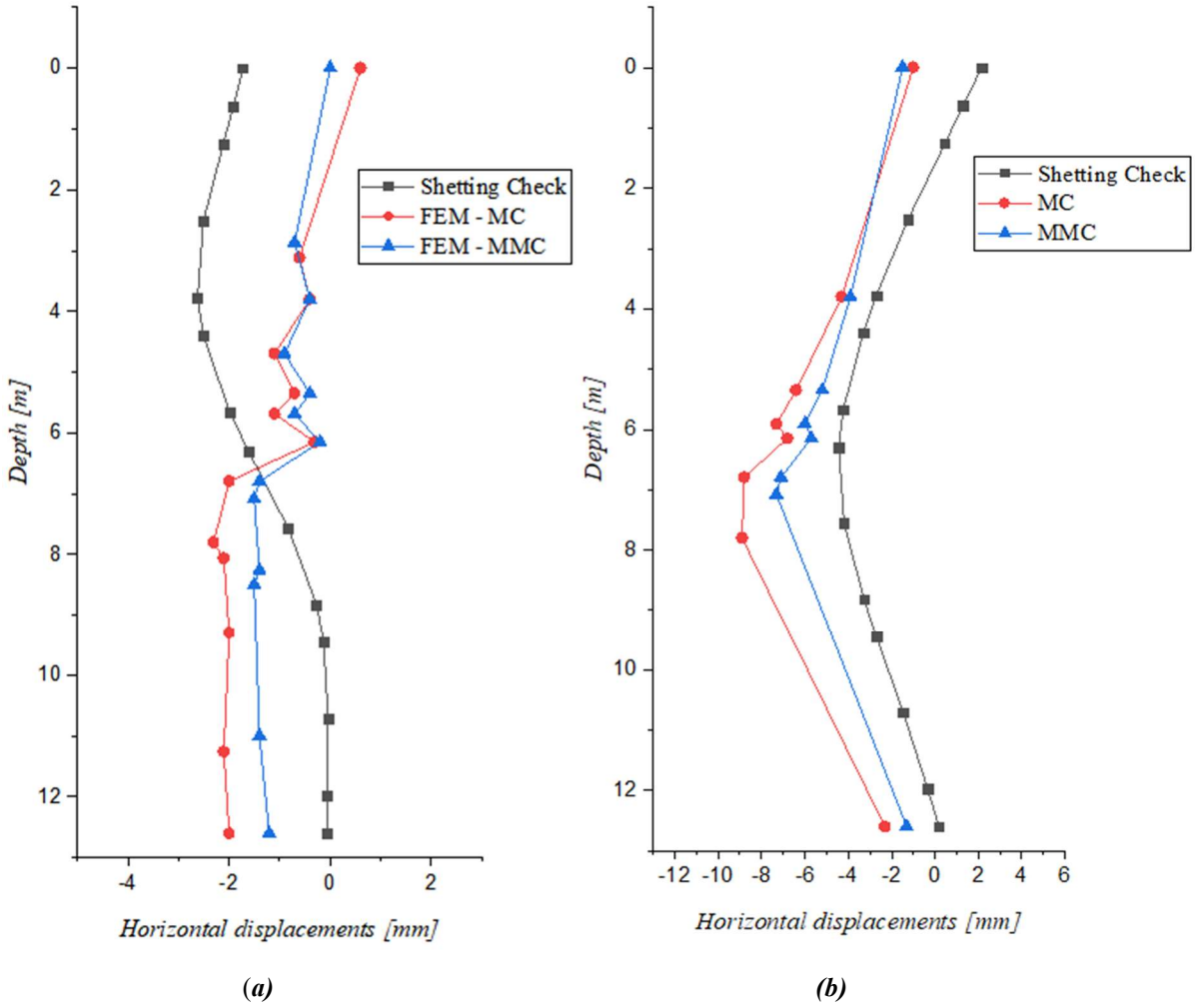

Figure 4.7 Comparison of the overall displacement of the wall by various approaches in (a) the intermediate stage (b) the final stage

The maximum displacement of the retaining structure is summarised stepwise in Table 20 and the comparison of its flexural shape in the intermediate and final stages is given in Figure 4.7. Discussions regarding it is as follows:

- As the Poisson's ratio of soils are calibrated regarding the OCR in the FEM, the part of the retaining structure above the places where the loadings act does not flexure much, which is different from the result of Sheeting Check.
- **Displacement at the tip of the pile wall**
  Sheeting Check programme tends to make the tip of the pile fixed. On the contrary, the displacement at the tip of the pile in all stages doesn't change much in the FEA, which is within the interval from -3 to -1 *mm* approximately. Considering the initial displacement of the wall in the 3rd stage when the pile wall is activated, it is generally fixed at rock massif, GT6, which is reasonable;

- **Maximum displacement**

  Before the pit is excavated below the surcharge level, the maximum lateral displacement of the structure is somewhere a bit above the excavation; while it moves to the level of surcharge when the excavation goes deeper. The most critical part is always the place at the level where the foundation piles stand on in the FEA.

- **Different consideration of anchor's prestressing force**

  As is introduced in Section 2.3.5, the method of dependent pressures is utilised in the Sheeting Check programme, where the prestressing anchors are assumed to be a concentrated force applied in the passive zone of the retaining wall supported by a spring. Directly assuming the prestressing force acting on the wall tends to be conservative. That's why the wall bends towards the terrain behind the pit after anchorage. This effect outstands much at the top of the wall especially. However, in the FEM, the lateral displacement of the retaining wall diminishes only a little due to the discretisation of the ground continuum.

4.4. Results and Comparisons of Internal Forces

Table 21. Comparison of overall maximum shear force in each construction stage [kN/m]

Stage No.	0	1	2	3	4	5	6	7
Sheeting Check (with FoS)	/	154.97	101.69	99.35	105.10	214.96	291.51	181.15
Sheeting Check (without FoS)	/	153.34	117.73	112.67	123.98	214.41	283.14	172.92
FEM (MC)	44.3	33.7	33.7	60.5	49.8	262.1	247.1	217.7
FEM (MMC)	45.9	34.6	34.6	60.4	45.1	248.8	233.7	207.6

Table 22. Comparison of maximum bending moment in each construction stage [kN·m/m]

Stage No.	0	1	2	3	4	5	6	7
Sheeting Check (with FoS)	/	164.27	84.59	104.57	76.15	251.55	253.91	278.47
Sheeting Check (without FoS)	/	143.59	93.47	108.92	111.47	236.50	236.47	222.39
FEM (MC)	54.3	54.7	54.5	74.2	55	299.7	293.2	301.9
FEM (MMC)	62.8	63.1	62.9	76.3	64.9	249.2	244.5	260.4

The comparisons of shear force and bending moment are given in Table 21 and Table 22. In the Sheeting Check programme, the surcharges coming from adjacent foundation piles are both assumed as a concentrated force acting at the level of -6.5 m. But in the FEM, due to the calibration, the surcharge from the 2nd row of foundation piles is assumed to be comprised of 2 concentrated forces, one of which is above -6.5 m. And this component of surcharge increases horizontal active earth pressure acting on the wall from its level to -6.5m, resulting in greater

internal forces at the level of -6.5 m than the results of Sheeting Check. So, even if the selection of parameters of soil in the Sheeting Check programme is more conservative. Therefore, when it comes to the design of reinforcements, it is still necessary to leave room for the neglected loadings that come from the side of foundation piles.

5. Conclusions and Discussions

5.1. Conclusions

The main task of this dissertation is to design a secant pile wall for a deep excavated foundation pit located in Prague, Czech Republic. This was defined as a preliminary design owing to the fact that the soil parameters were given by table values based on their classifications. Yet, it was not simple to determine parameters to analyse the ground and retaining wall. Two perspectives of design and analyses are given in Chapter 2 and 3.

Chapter 1 introduced the general design methodologies retaining structures, typically the subgrade reaction method as well as the finite element method with a few soil constitutive models, which the analyses by GEO5 – Sheeting Check and FEM programmes are based upon.

In Chapter 2, the analysis was held by GEO5 – Sheeting Check programme. Assumptions regarding the settings of the model as well as material properties were made at first. Analyses including the retaining wall and prestressing anchors were based upon the Winkler medium subsequently.

In Chapter 3, the finite element non-linear analysis was done by GEO5 – FEM programme, which was based on the Mohr-Coulomb failure criterion for both soil constitutive models and contact elements. Studies have proven that the MC model is good for preliminary designs, but simply adopting soil parameters is irresponsible. To diminish its deficiencies and to obtain more realistic results, the calibrations were made in the aspects of initial ground settlement, and the change of horizontal stress below the excavation level. The whole model was adjusted to calibrate reasonable facts, including the settlement of the adjacent foundation piles, overconsolidation of the highly stress-path dependent soils below the pit. In this way, the surcharge, elastic modulus, and Poisson's ratio were modified where necessary. The calibrations of the overall model and soil parameters for the MC constitutive model play an important role in the finite element analysis: the elastic modulus of soils for FEA was calibrated reasonably instead of using a random or critical value; the considerations of stress path and OCR helped to decrease the exaggerated lateral displacements of the retaining wall, which was also discussed mathematically.

The results of above-mentioned analyses in two distinct aspects of methodologies were compared in Chapter 4, including displacements of the ground and retaining wall, internal

forces. The models in both computer programmes consider the soil-structure interaction (SSI) but in different manners. The SSI is embodied in the Sheeting Check programme by means of the SRM with Winkler medium as well as the earth pressures are calculated by Caquot-Kerisel method, where the friction angle between soil and structure is taken into account. As for the FEM, the SSI is given by the soil-structure contact elements, where elastic springs with respect to the adjacent soils are introduced.

5.2. Deficiencies and Expectations

The Mohr-Coulomb constitutive model, being linearly elastic–perfectly plastic, cannot reflect the elastoplastic property of soils. Compared with the hyperbolic stress-strain relationship (see Figure 1.13), it shows fewer advantages when the soil does not reach the yield criterion. But as its input is less, it is good for judgements if the necessary parameters are calibrated. Although the modified Mohr-Coulomb model can consider 'hardening and softening', it still may result in deviation.

Although the finite element analysis in this paper did not reflect the elastoplastic property well, the parameters of soils were cautiously selected with proper calibrations. The elastic modulus was calibrated in this paper, but the shear strength of soils is not considered to be calibrated which appears to be non-linear in reality.

But the MC model can be modified to achieve the variation of elastic modulus if the soil parameters and loading condition are given, especially E_{50}^{ref} and σ_3, where the constant elastic modulus of soil in the MC model is assumed to be equal to E_{50}^{ref}=E_{oed}^{ref} for both oedometer and triaxial tests.[56] A study from Song, et al. (2011) indicates that by approximately considering the variation of the elastic modulus of the soils inside the excavation is considered as the stress path of it changes for the MC model can result in more realistic the lateral displacement of retaining walls. This is achieved by adjusting the E_{50} of each layered soil by using Eq. 13-14 in section 1.3.4 of the hardening soil model, which mainly depends on the minor effective principal stress and initial reference modulus and stress.[18] [22] Although this adjustment for the MC model is not perfect, which neglects the shear strength and cap hardening, simulated compared with the pure MC model which is linearly elastic before yielding, the displacement of retaining wall has proven to be more realistic although the deviation could still exist.

References

[1] EN 1990. Eurocode basis of structural design. CEN Comité Européen de Normalization, Brussels.

[2] EN 1997-1. Geotechnical design: Part 1: General rules. CEN Comité Européen de Normalization, Brussels.

[3] EN 1992-1-1. Design of concrete structures: General rules and rules for buildings. CEN Comité Européen de Normalization, Brussels.

[4] M. Ufuk Ergun, 2008, 'Deep Excavations', *Electronic Journal of Geotechnical Engineering*, available at: www.ejge.com/Bouquet08/UfukErgun_ppr.pdf.

[5] Ralph W. Strom & Robert M. Ebeling 2002, 'Methods Used in Tieback Wall Design and Construction to Prevent Local Anchor Failure, Progressive Anchorage Failure, and Ground Mass Stability Failure', Information Technology Laboratory (U.S.), Engineer Research and Development Center (U.S.).

[6] Ilies, N-M. 2014, 'Design optimization of diaphragm walls', *Procedia Technology*, 8th International Conference Interdisciplinarity in Engineering, INTER-ENG 2014, 9-10 October 2014, Tirgu-Mures, Romania.

[7] Pruska, J., Kopecny, J. 2010, 'Design of Sheet Piling for the Prague Metro Operation System IV.C 2nd Phase Using GEO5 Software. Prague 2010', *Transport and City Tunnels - Proceedings of the 11th International Conference Underground Constructions Prague 2010*, Prague, CZECH REPUBLIC, 14-16 June 2010, pp. 783-788.

[8] https://www.deepexcavation.com/en/secant-pile-walls.

[9] Varghese P. Foundation Engineering, New Delhi: PHI Learning Private Limited, 2005.

[10] S. S. Konnur, A. M. Hulagabali 2016, 'Numerical Analysis of MSE wall using Finite Element and Limit Equilibrium Methods', *Indian Geotechnical Conference IGC*, 15-17 December 2016, IIT Madras, Chennai, India.

[11] Zhang, W., et al. 2020, 'Effects of jet grouting slabs on responses for deep braced excavations', *Underground Space*, DOI: https://doi.org/10.1016/j.undsp.2020.02.002.

[12] Han, J., Chen, Q., Liu, Y.-K., 2005, 'Bond strength between anchor grout and rock or soil masses', *Chinese Journal of Rock Mechanics and Engineering*, vol. 2, No.19, pp. 3482.

[13] Fine Ltd. 2014, 'GEO5 - User's Guide (Version 19)', http://www.geo5.com.br/wp-content/uploads/2015/01/geo_5_user_guide_en.pdf.

[14] Fine Ltd. 2009, 'GEO5 Engineering Manuals', https://www.finesoftware.eu/engineering-manuals/.

[15] Fine Ltd. 2009, 'Engineering Manuals for GEO5 programs – Part 3', www.finesoftware.eu.

[16] Fine Ltd. 2009, 'GEO FEM - Theoretical manual', https://data.fine.cz/handbooks-chapter-pdf/geo5_fem_theoretical_guide.pdf.

[17] Fine Ltd. 2020, 'Finite Element Method (FEM) – Introduction', https://data.fine.cz/handbooks-chapter-pdf/em20_en.pdf.

[18] Ahmed Z. et al. 2020, 'Variability effect of strength and geometric parameters on the stability factor of failure surfaces of rock slope by numerical analysis', *Arabian Journal of Geosciences*, vol. 13, No.21, pp. 1112.

[19] Jiang, H. & Xie, Y. 2011, 'A note on the Mohr–Coulomb and Drucker–Prager strength criter', *Mechanics Research Communications*, vol.38, No.4, pp. 309-314.

[20] Josifovski, J., Susinov, B., and I. Markov 2015, 'Analysis of soldier pile wall with jet-grouting as retaining system for deep excavation', *Proceedings of the XVI ECSMGE Geotechnical Engineering for Infrastructure and Development*, DOI: 10.13140/RG.2.1.1421.8722.

[21] Monaco, P., Marchetti, S., 'Evaluation of the Coefficient of Subgrade Reaction for Design of Multi-propped Diaphragm Walls From DMT Moduli', *Proceedings of the 2nd International Conference on Communication, Devices and Computing*, Haldia Institute of Technology, March 14–15, 2019, pp. 993-1002.

[22] Song Guang, Song Er-xiang 2014, 'SELECTION OF SOIL CONSTITUTIVE MODELS FOR NUMERICAL SIMULATION OF FOUNDATION PIT EXCAVATION', *Engineering Mechanics*, vol. 31, No.5, pp. 86-94.

[23] Paul Fok et al., 2012, 'Limiting values of retaining wall displacements and impact to the adjacent structures', *The IES Journal Part A: Civil & Structural Engineering*, vol. 5, No. 3, pp. 134–139.

[24] Surarak, C., et al. 2012, 'Stiffness and strength parameters for hardening soil model of soft and stiff Bangkok clays', *Soils and Foundations*, vol. 52, No, 4, pp. 682–697.

[25] Hejazi, Y., et al., 2008, 'Impact of constitutive models on the numerical analysis of underground constructions', Acta Geotech. 3, pp. 251–258, https://doi.org/10.1007/s11440-008-0056-1.

[26] Wang, SD, et al. 2020, 'Comparative investigation on deformation monitoring and numerical simulation of the deepest excavation in Beijing', *Bulletin of Engineering Geology and the Enviro,* DOI: 10.1007/s10064-020-02019-y.

[27] Ziaie-Moayed, R. and Janbaz, M. 2009, 'Effective Parameters on Modulus of Subgrade Reaction in Clayey Soils', *Journal of Applied Sciences*, vol. 9, pp. 4006-4012.

[28] Reza Saeedzadeh et al. 2011, 'USE OF GRANULAR DRAINS IN UPLIFT REDUCTION OF BURIED PIPELINES IN SATURATED SAND DEPOSIT', Conference: *6th International Conference on Seismology and Earthquake Engineering,* Tehran, Iran.

[29] Pruska, J 2003, 'Comparison of geotechnic softwares - Geo FEM, Plaxis, Z-Soil', *Proceedings of XIIIth conference ECSMGE*, vol.2, pp. 819-824.

[30] Fish, J. and Belytschko 2007, T., *A First Course in Finite Elements*, John Wiley & Sons, Ltd,

[31] Daryl L. Logan 2000, *A First Course in Finite Elements*, Thomson, ISBN: 978-0-470-03580-1.

[32] GOUW Tjie-Liong 2014, 'Common Mistakes on the Application of Plaxis 2D in Analyzing Excavation Problems', *International Journal of Applied Engineering Research*, vol. 9, pp. 8291-8311.

[33] Olivier de Weck & Il Yong Kim 2004, Finite Element Method, Massachusetts Institute of Technology, http://web.mit.edu/16.810/www/16.810_L4_CAE.pdf.

[34] Sadrekarimi, J. 2009, ' Comparative study of methods of determination of coefficient of subgrade reaction', *Electronic Journal of Geotechnical Engineering*, vol. 14.

[35] Bowles, J. E. 1998, *Foundation Analysis and Design*, 6th ed., McGrow-Hill International press.

[36] Elachachi, S. M., D. Breysse and L. Houy 2004 "Longitudinal Variability of Soils and Structural Response of Sewer Networks," *Computers and Geotechnics*, 31(8): 625-641.

[37] Miguel Ángel Vivas Mefle 2014, *Study of the Accuracy of Limit State: Geo and Compliance with Eurocode 7 in Slope Stability Analysis*, MSc thesis. University of Birmingham.

[38] Craig, R. F. 2004, *Craig's Soil Mechanics*, 7th ed., Spon Press, New York.

[39] Ismail, M. K. A. et al. 2020, 'Contact Stiffness Parameters of Soil Particles Model for Discrete Element Modeling using Static Packing Pressure Test', *AIP Conference Proceedings*, 2020:1. https://aip.scitation.org/toc/apc/2020/1.

[40] POPA, H., BATALI, L. 2010, 'Using Finite Element Method in geotechnical design. Soil constitutive laws and calibration of the parameters. Retaining wall case study', *WSEAS Transactions on Applied and Theoretical Mechanics*, vol. 5, pp.177-186.

[41] Mao, Jq. 2005, 'A finite element approach to solve contact problems in geotechnical engineering', *International Journal for Numerical and Analytical Methods in Geomechanics*, vol.29, No. 5, pp.525-550.

[42] Brinkgreve, R., 2005, 'Selection of Soil Models and Parameters for Geotechnical Engineering Application', Geo-Frontiers Congress, pp. 69-98, January 24-26, 2005, Austin, Texas, United States *https://doi.org/10.1061/40771(169)4.*

[43] Z Soil.PC, 2018, 'THE HARDENING SOIL MODEL - A PRACTICAL GUIDEBOOK', *http://www.zsoil.com/zsoil_manual_2018/Rep-HS-model.pdf.*

[44] Kadlicek, T, et al. 2016, 'APPLYING HYPOPLASTIC MODEL FOR SOFT SOILS TO THE ANALYSIS OF ANCHORED SHEETING WALL', *ACTA GEODYNAMICA ET GEOMATERIALIA*, vol.12, No.2 (182), pp. 125-136.

[45] Qian, J. et al. 2020, 'Calibration of soil parameters based on intelligent algorithm using efficient sampling method', *Underground Space*, *https://doi.org/10.1016/j.undsp.2020.04.002*.

[46] DING, K. & WANG X. 2016, 'Analysis of Excavation with Numerical Simulation and Monitoring Data Has Effect on Surface Subsidence', *International Conference on Applied Mechanics, Mechanical and Materials Engineering*, ISBN: 978-1-60595-409.

[47] Shu, J., et al. 2019, 'Sequential Measurement and Analysis of Large Underground Retaining Structures by Diaphragm Wall Anchor for the Spring Area', *Advances in Civil Engineering*, https://doi.org/10.1155/2019/5291420.

[48] Singh, A., et al. 2019, 'Study on Mohr–Coulomb-based three-dimensional strength criteriaand its application in the stability analysis of vertical borehole', *Arabian Journal of Geoscience*, 12, 578 (2019). https://doi.org/10.1007/s12517-019-4752-y.

[49] Fu, Y., et al., 2020, 'Parameter Analysis on Hardening Soil Model of Soft Soil for Foundation Pits Based on Shear Rates in Shenzhen Bay, China', *Advances in Materials Science and Engineering*, vol. 2020, Article ID 7810918, 11 pages, 2020. https://doi.org/10.1155/2020/7810918

[50] Soos von, P., 2001, 'Properties of Soil and Rock' (in German), *Grundbautaschenbuch*, vol. 1, 6th Ed., Ernst and Son, Berlin, pp. 117–201.

[51] Adis Skejic, 2012, 'Interface Formulation Problem in Geotechnical Finite Element Software', *Electronic Journal of Geotechnical Engineering*, vol. 17, pp. 2035-2047.

[52] Van Langen, H. 1991, Numerical Analysis of Soil Structure Interaction, PhD thesis, Delft University.

[53] Wojciech Sołowski, 2018, 'Geo-E2010 Advanced Soil Mechanics L'(lecture), Aalto University, School of Engineering.

[54] Trung Ngo-Duc, 2019, Determination of Unloading -Reloading Modulus and Exponent Parameters (m) for Hardening Soil Model from Drained Triaxial Test of Soft Soil in Ho Chi Minh City', *Modern Environmental Science and Engineering*, vol. 5, No. 1, pp. 677-683.

[55] CUI, X. Z., et al. 2016. 'Mohr-Coulomb Model Considering Variation of Elastic Modulus and Its Application', *Key Engineering Materials*, Vols. 306-308, pp.1445-1448.

[56] Vakili, K. N., et al. 2013, 'A PRACTICAL APPROACH TO CONSTITUTIVE MODELS FOR THE ANALYSIS OF GEOTECHNICAL PROBLEMS', *The Third International Symposium on Computational Geomechanics (ComGeo III)*, Krakow, Poland, Volume: 1.

[57] Cheng, Y., 1999, 'Study on the change lateral stress in the soil below foundation pits' (in Chinese), *Low Temperature Architecture Technology*, No. 4 (78), pp. 39-41.

[58] Boháč, J., et al. 2013, 'Methods of determination of K0 in overconsolidated clay', Proceedings of the 18th International Conference on Soil Mechanics and Geotechnical Engineering, Paris. Available at: https://web.natur.cuni.cz/uhigug/masin/download/BMMNR_Paris13.pdf.

[59] Wei, G. & Zheng, J., 2006, 'Calculated method of passive earth pressure in deep pit engineering considering excavation effect' (in Chinese), *Chinese Journal of Geotechnical Engineering*, vol. 28, Supp., pp.1493-1496.

Appendix A. *Preliminary Calculations of Anchor Force after the 1st and 2nd Anchorage*

1. The 2nd excavation after the 1st Anchorage

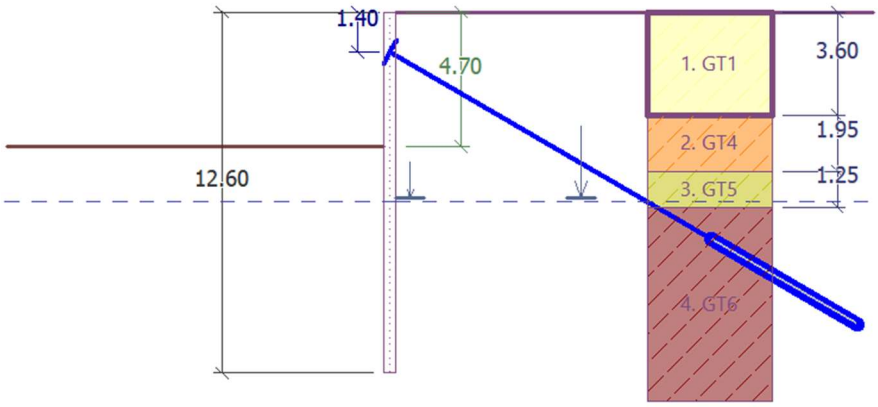

Figure A.1 Schematic illustration of the calculations for anchorage (1)

Table 23. Calculation of the minimum design values of horizontal total anchor force per unit length for the 1st excavation

	GT1	GT4	GT5 (dry)	GT5 (saturated)	GT6 (dry)	GT6 (saturated)	sum
z *(For* E_a*)* $[m]$	3.6	1.95	0.75	0.5	/	5.8	/
z *(For* E_p*)* $[m]$	/	0.85	0.75	0.5	/	5.8	/
z *(For* E_q*)* $[m]$	/	/	/	/	/	6.1	/
$E_a\,[kN/m]$	66.73	39.97	6.55	5.62	/	179.34	298.22
$E_p\,[kN/m]$	0.00	24.37	60.01	46.57	/	1851.04	1981.99
$E_q\,[kN/m]$	0.00	0.00	0.00	/	/	644.56	644.56
Required r_x $(\geqslant 0)$	/	/	/	/	/	/	**0**

$$\boldsymbol{E_p > E_a + E_q}$$

Required total anchor force $r_x \geq 0$.

2. The 3rd excavation after the 2nd Anchorage

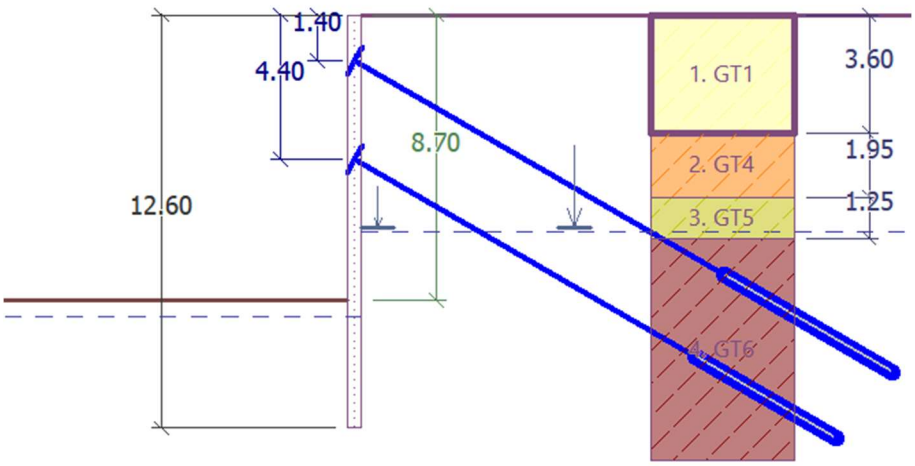

Figure A.2 Schematic illustration of the calculations for anchorage (2)

Table 24. Calculation of the minimum design values of horizontal total anchor force per unit length for the 3rd excavation

	GT1	GT4	GT5 (dry)	GT5 (saturated)	GT6 (dry)	GT6 (saturated)	sum
z (For E_a) [m]	3.6	1.95	0.75	0.5	/	5.8	/
z (For E_p) [m]	/	/	/	/	0.5	3.4	/
z (For E_q) [m]	/	/	/	/	/	6.1	/
E_a *[kN/m]*	66.73	39.97	6.55	8.44	/	179.34	301.03
E_p *[kN/m]*	/	/	/	/	35.19	644.14	679.33
E_q *[kN/m]*	/	/	/	/	/	644.56	644.56
Required min. r_x *[kN/m]*	/	/	/	/	/	/	**266.26**

$$\boldsymbol{E_p < E_a + E_q}$$

Required total anchor force $r_x \geq 266.26$ *kN/m*.

Appendix B. *Sheeting Check Programme without FoS: Lateral Displacements of the Retaining Wall*

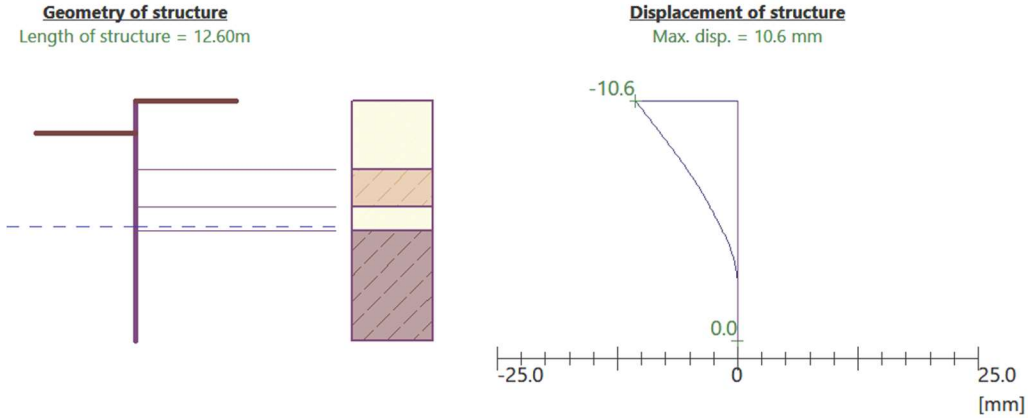

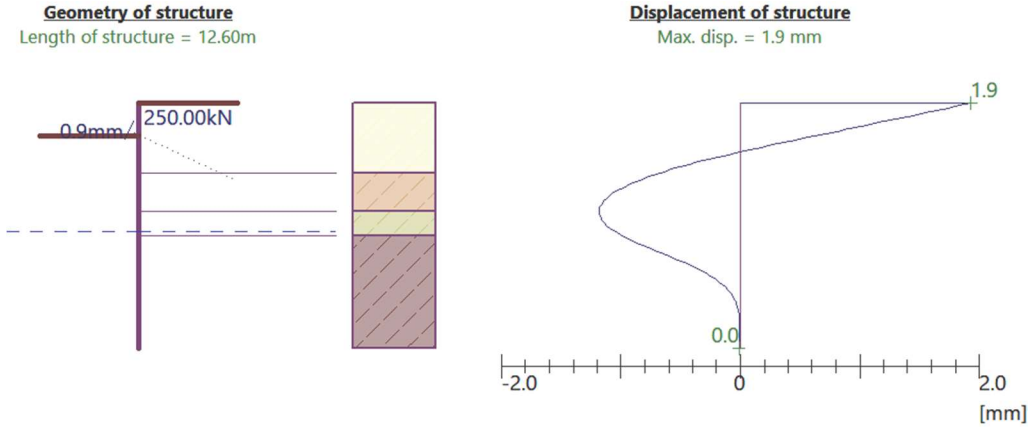

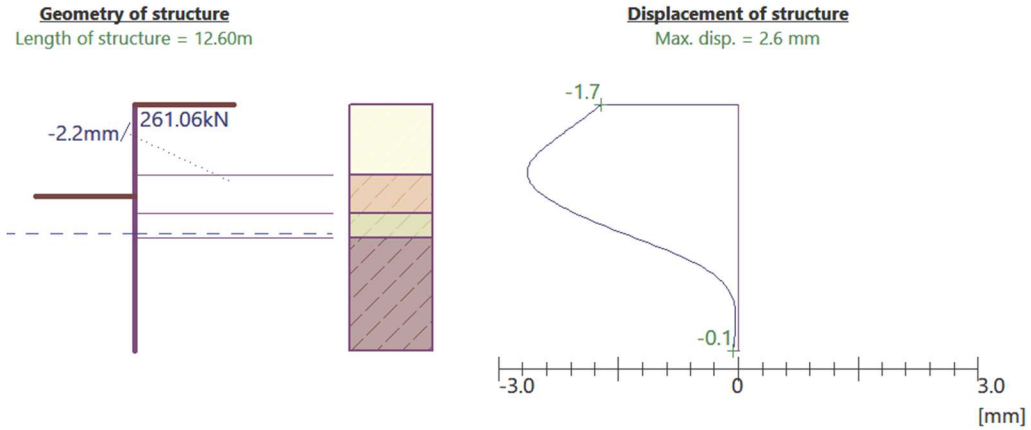

Appendix B. Sheeting Check Programme without FoS: Lateral Displacements of the Retaining Wall

Geometry of structure
Length of structure = 12.60m

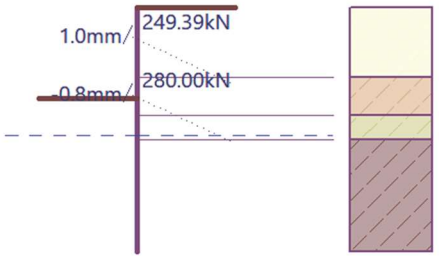

Displacement of structure
Max. disp. = 2.1 mm

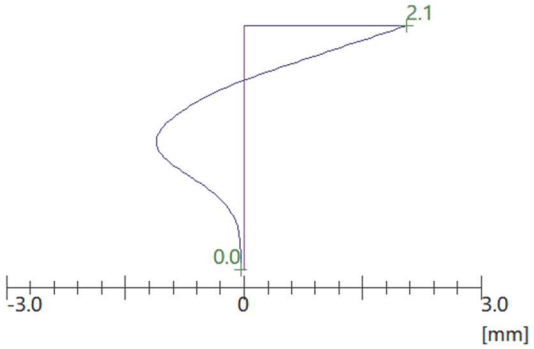

Geometry of structure
Length of structure = 12.60m

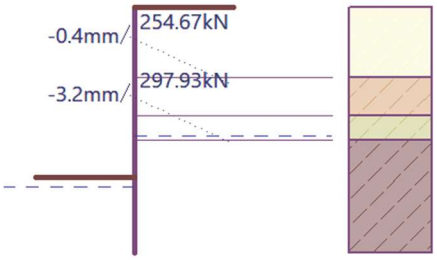

Displacement of structure
Max. disp. = 3.8 mm

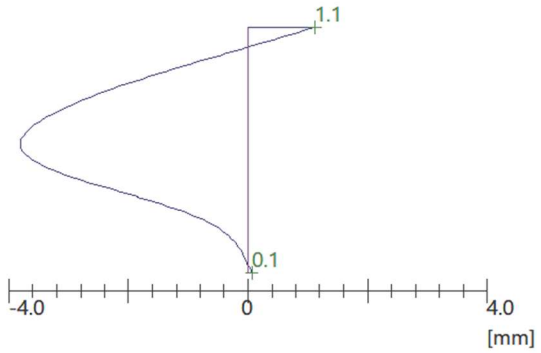

Geometry of structure
Length of structure = 12.60m

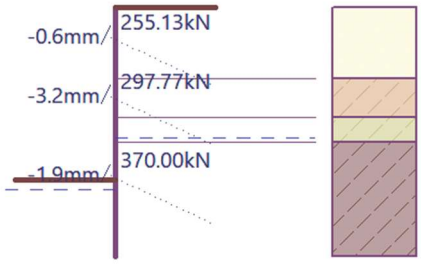

Displacement of structure
Max. disp. = 3.7 mm

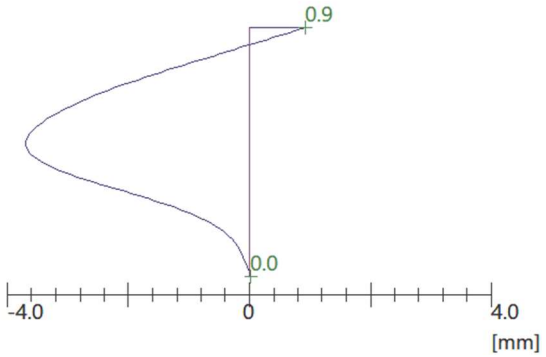

Geometry of structure
Length of structure = 12.60m

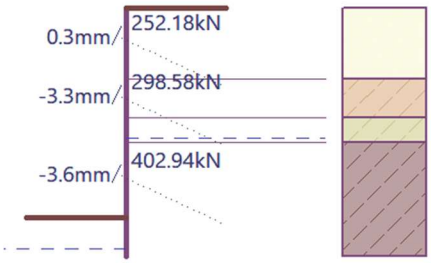

Displacement of structure
Max. disp. = 4.5 mm

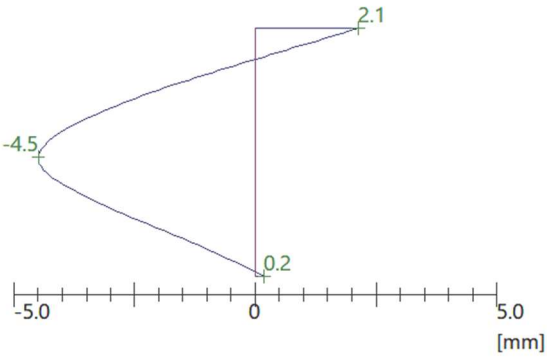

Appendix C. *FEM: Lateral Displacements of the Retaining Wall*

(1) Mohr-Coulomb

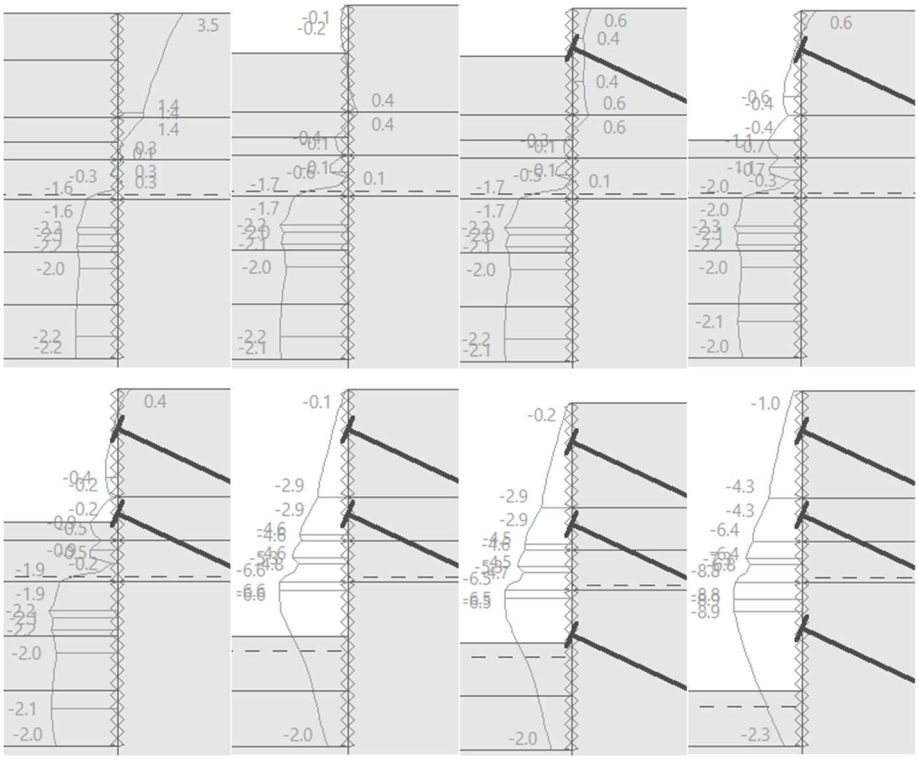

(2) Modified Mohr-Coulomb

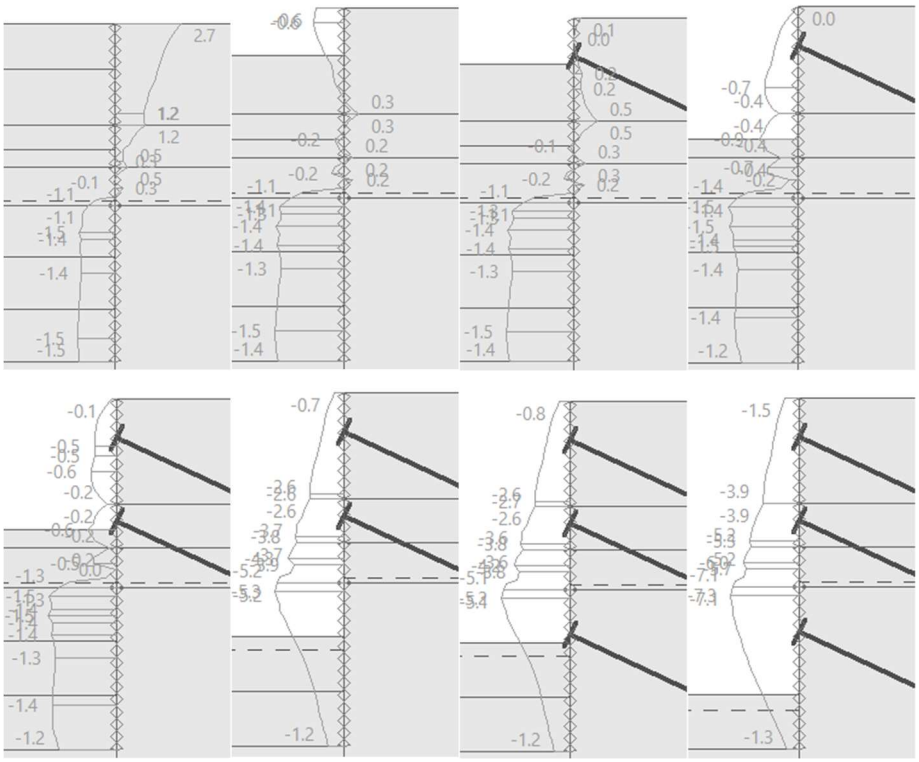

Appendix D. *Data for the Comparison of Structural Displacements*

Table 25. Comparison data of structural horizontal displacements in the intermediate stage

Sheeting Check		FEM - MC		FEM - MMC	
Depth	Horizontal displacements	Depth	Horizontal displacements	Depth	Horizontal displacements
[*m*]	[*mm*]	[*m*]	[*mm*]	[*m*]	[*mm*]
0	-1.72	0	0.6	0	0
0.63	-1.92	3.115	-0.6	2.868	-0.7
1.26	-2.13	3.8	-0.4	3.8	-0.4
2.52	-2.52	4.7	-1.1	4.7	-0.9
3.78	-2.63	5.35	-0.7	5.35	-0.4
4.4	-2.51	5.685	-1.1	5.685	-0.7
5.67	-1.98	6.15	-0.3	6.15	-0.2
6.3	-1.62	6.8	-2	6.8	-1.4
7.56	-0.83	7.8	-2.3	7.08	-1.5
8.82	-0.27	8.065	-2.1	8.255	-1.4
9.45	-0.13	9.3	-2	8.5	-1.5
10.71	-0.04	11.26	-2.1	11	-1.4
11.97	-0.05	12.6	-2	12.6	-1.2
12.6	-0.06	8.65			
		8.3			
		12.6			

Table 26. Comparison data of structural horizontal displacements in the final stage

Sheeting Check		FEM - MC		FEM - MMC	
Depth	Horizontal displacements	Depth	Horizontal displacements	Depth	Horizontal displacements
[*m*]	[*mm*]	[*m*]	[*mm*]	[*m*]	[*mm*]
0	2.14	0	-1	0	-1.5
0.63	1.59	3.8	-4.3	3.8	-3.9
1.26	1.12	5.35	-6.4	5.35	-5.2
2.52	0.19	5.913	-7.3	5.91	-6
3.78	-0.53	6.152	-6.8	6.15	-5.7
4.4	-0.78	6.8	-8.8	6.8	-7.1
5.67	-1.09	7.8	-8.9	7.08	-7.3
6.3	-1.09	12.6	-2.3	12.6	-1.3
7.56	-0.72				
8.82	-0.18				
9.45	-0.03				
10.71	0.03				
11.97	-0.01				
12.6	0.18				

Appendix E. *Envelope of Internal Forces and Designed Reinforcement*

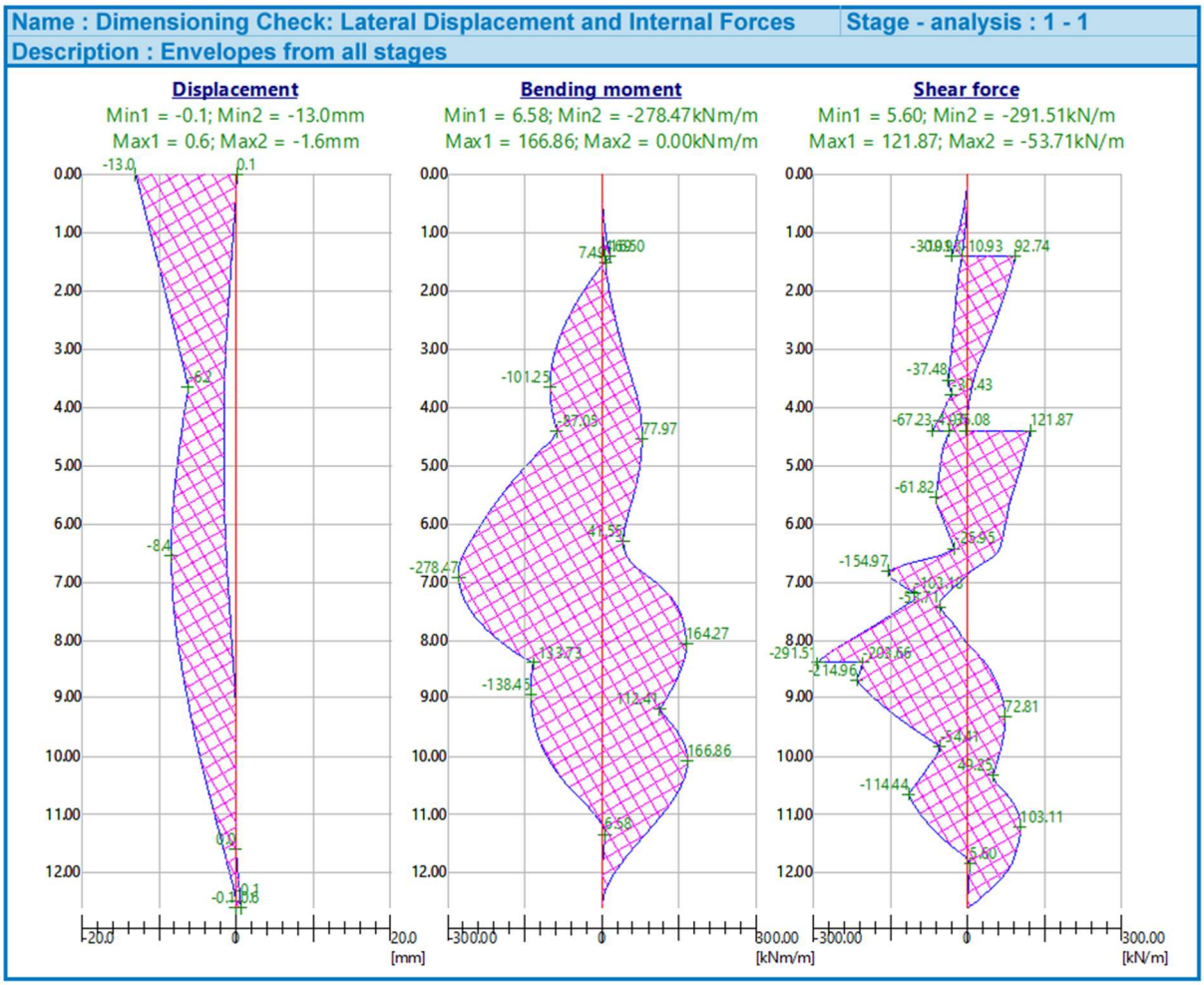

Figure E.1 Envelopes of internal forces and lateral displacement

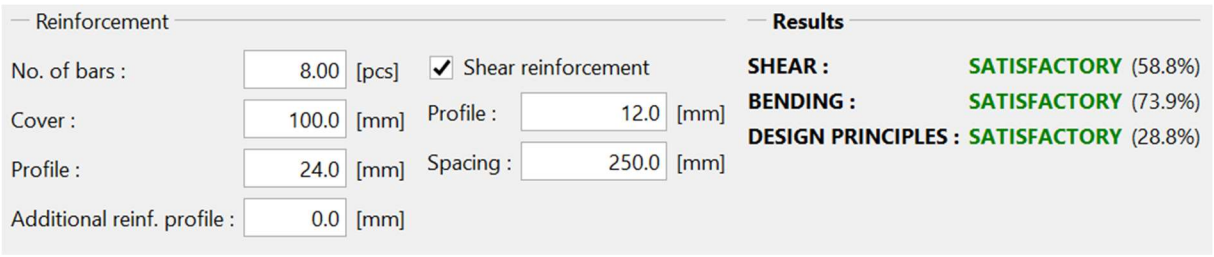

Figure E.2 Designed reinforcement and verification

Appendix F. *Schema of Construction Sequence*

1. Ground grading and guide wall construction

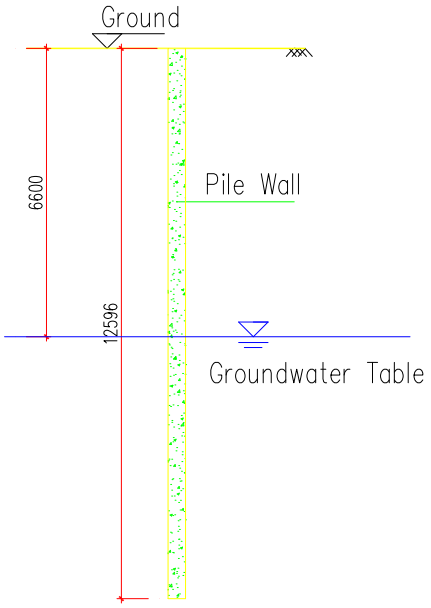

2. Pile wall construction

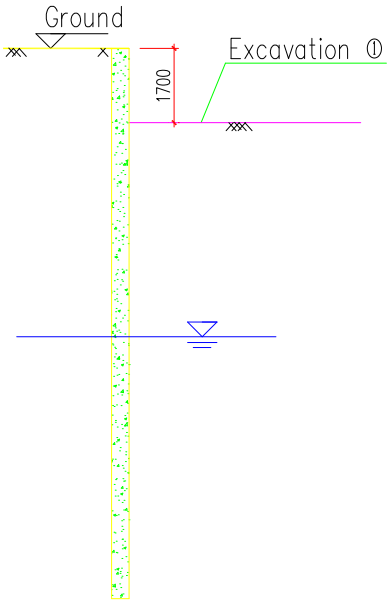

3. Excavation ①

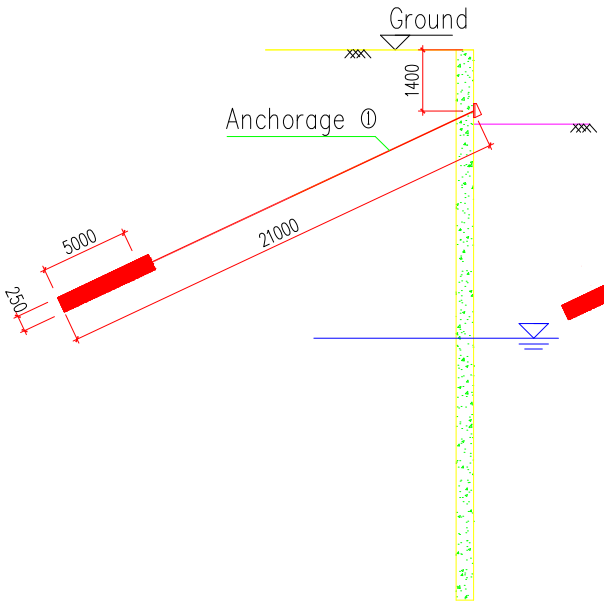

4. Anchorage ①

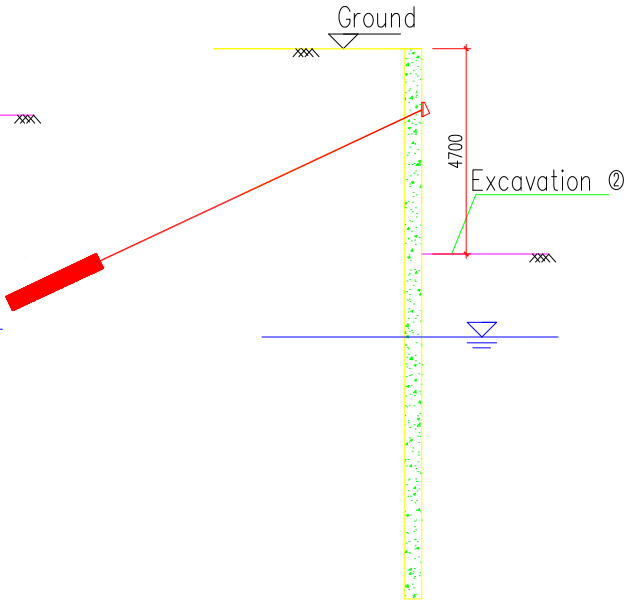

5. Excavation ②

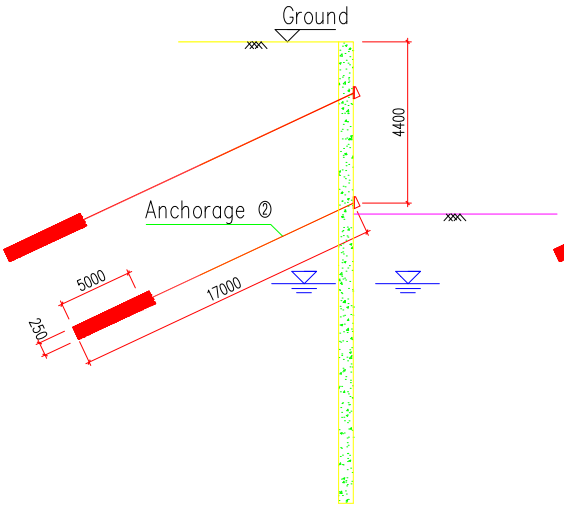

6. Anchorage ②

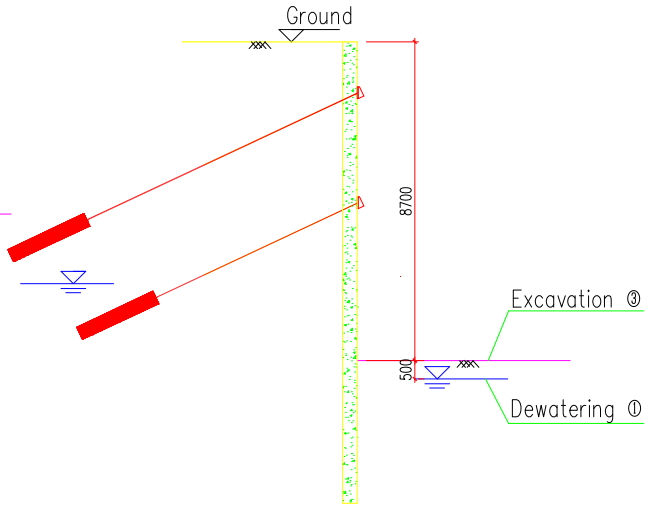

7. Excavation ③ and dewatering

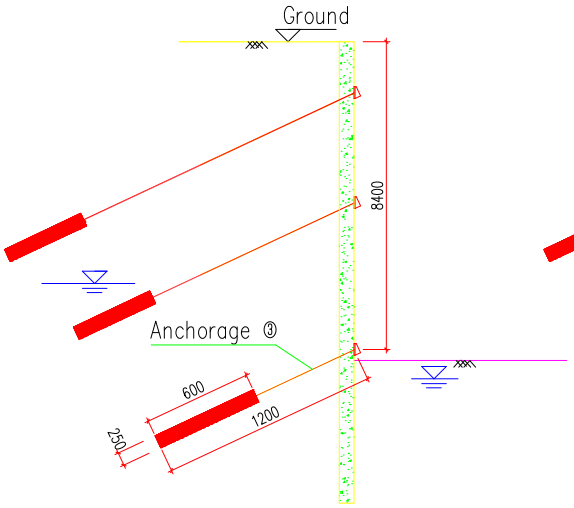

8. Anchorage ③

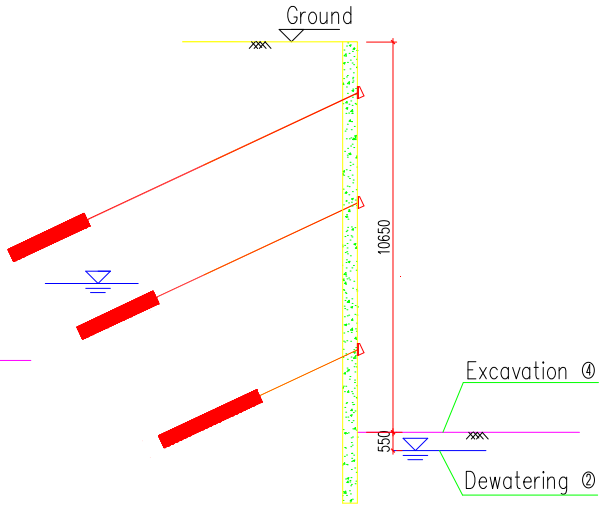

9. Excavation ④ and dewatering

Appendix G. *Schema of the Designed Retaining Wall*

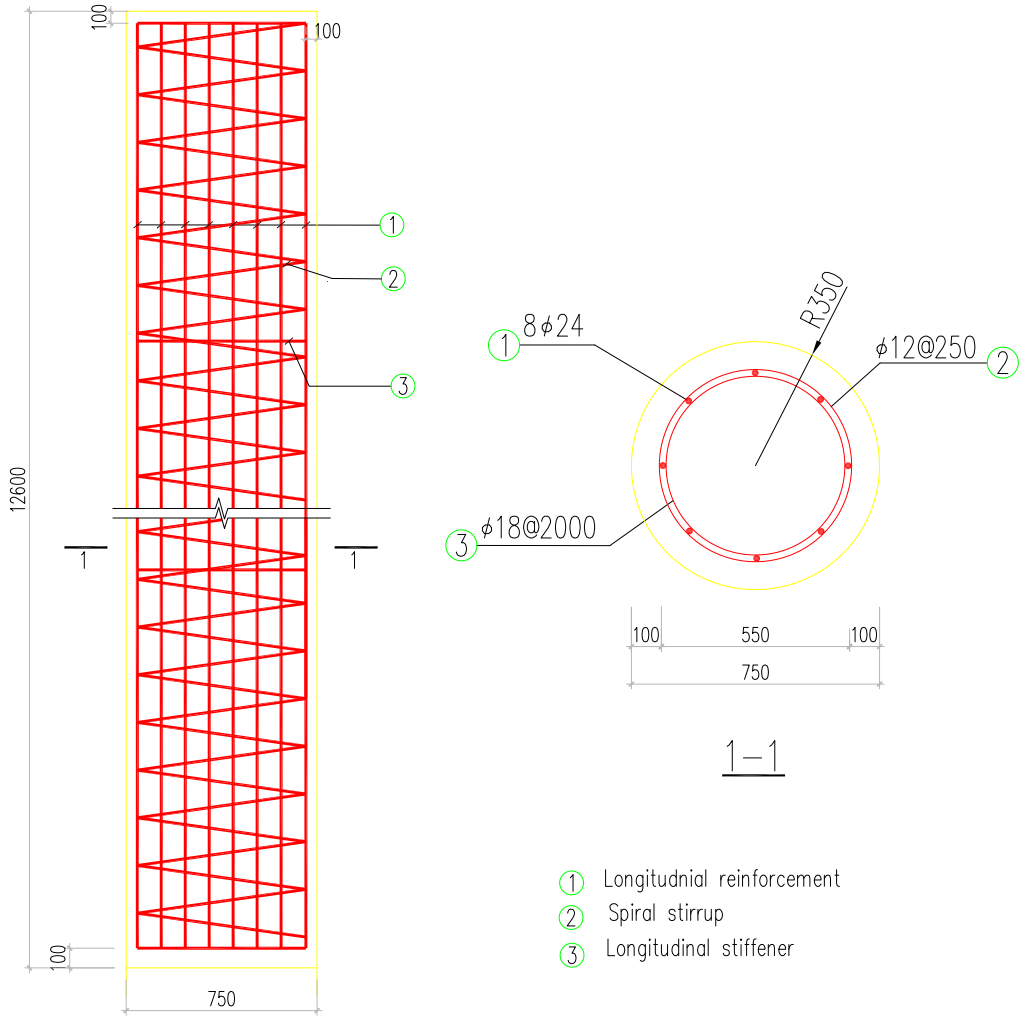

Reinforcements of the secondary piles

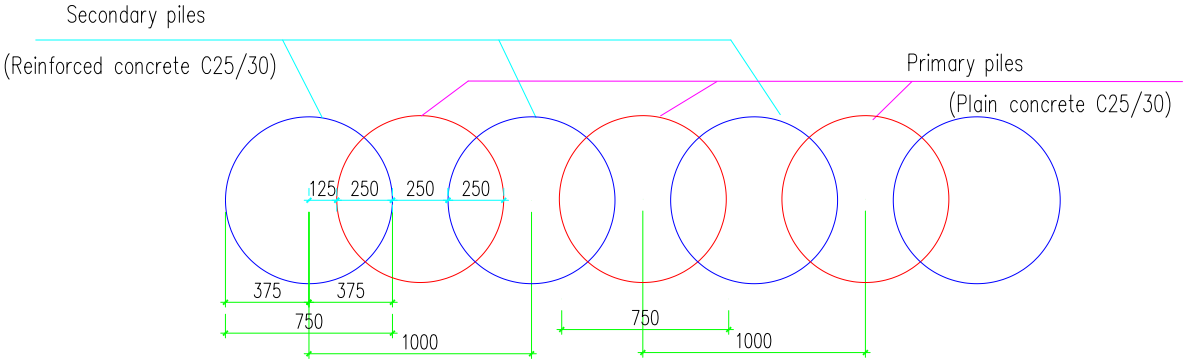

Schema of the secant pile wall